ABSTRACT OF THE Ph.D. THESIS

ENTITLED

RADIATION INDUCED MODIFICATION OF SOME DIELECTRIC SOLIDS

by

Dipak Sinha
Department of Chemistry,
N.E.H.U. Shillong - 793003

Chemical modifications observed in irradiated polymeric materials have imparted the initial motivation for studying their impact on track registration properties of a sensitive detector. In polymeric track detectors, only those charged particles with linear energy transfer (LET) above a critical values can create distinct etchable tracks. Atomic radiations such as UV rays and X-rays, nuclear radiations like gamma rays and beta rays are low LET radiations. They mostly affect the physical and chemical properties of the polymeric films. Though they can not create any tracks but can affect etch rate values of detectors depending upon the absorbed dose. For track detectors exposed to high LET charged particles followed or preceded by low LET radiation exposure, both the bulk-etch rate and track-etch rate are found to vary in accordance with the absorbed doses of low LET radiations. Having a thorough knowledge about these effects is,

therefore, necessary specially when track detectors are used for detecting charged particles in an atmosphere of intense low LET background radiation. Besides, it is useful in evaluating the dosimetric properties of track detectors.

Experimental evidence shows that the track registration characteristics of plastic Solid State Nuclear Track Detectors (SSNTDs) are greatly affected when exposed to high doses of gamma rays. The modifications in characteristics originate from the structural alterations produced by irradiation of polymers. Studies have also been carried out on metal alloys and metallic glasses. The action of electromagnetic radiation is known to be one of the major sources of altering the properties of the materials they pass through. The changes are strongly dependent on the internal structure of the absorbing substances and the radiation gamma doses. It may be expected that the interaction of gamma-rays with solids cause electronic ionisation (or excitation) of the orbital electrons and possibly atomic displacements. Since polymeric solid state nuclear track detectors consist of long chain organic molecules, the net effect on the material is the formation of many broken molecular chains and radicals leading to a reduction in the average molecular weight of the substance. Such radiation induced modifications of polymeric materials may influence their etching characteristics, optical properties and some other properties such as thermal stability, morphology and optical band gap which in turn change the track registration properties of these track detectors.

Gamma exposure of the dielectric solids is not an uncommon phenomenon. In nuclear reactors during the process of fission, a high dose of gamma radiation is produced along with the neutrons. This produces different effects on its physical and chemical properties. Since the track detectors are increasingly used in diverse fields such as radiation dosimetry, cosmic-ray study, heavy ion Physics, microanalysis, uranium prospecting etc., so a proper characterisation of these detectors is necessary. Though the passage of lighter particles and gamma rays through these detectors can not be directly recorded, but the modifications that they produce on these detectors can be quantified.

The foremost application of a knowledge of the physico-chemical changes in matter with radiation dose is in the field of radiation dosimetry. Radiation dosimetry provides the basic knowledge required for quantitative measurements of radiation. In addition to that it can also be used to assess the ambient radiations and thus provide a protection against radiation hazards. Keeping these factors in mind we have attempted to study the modifications that take place in seven polymeric solids viz. **PADC (Homalite)**, **PADC (American Acrylics)**, **Lexan**, **Makrofol-E**, **Polycarbonate**, **Triafol-TN** and **Triafol-BN**, by the passage of gamma rays in the dose range from 10^1 Gy to 10^6 Gy.

In order to characterize the irradiated polymers, five different techniques have been used. They are : (1) Nuclear track technique, (2) IR spectroscopy, (3) UV-VIS spectroscopy, (4) ESR spectroscopy and (5) Thermogravimetric analysis. In track technique some of the important properties related to track parameters like, bulk-etch rate, track-etch rate, activation energy, complete etching time, true track length etc. were quantifically determined with gamma doses for assessing the response of these detector materials towards track registration under intense gamma background region. In order to understand the chemical and structural modifications in these polymers, spectroscopic studies (IR, UV-VIS and ESR) were carried out. For dosimetric applications of these detectors, dose dependent variation in transmittance at different wave lengths in the UV-VIS region were measured. Thermogravimetric studies were also performed to investigate the changes in thermal stability of these polymers caused by gamma radiation of different doses.

The present investigations have revealed that several physico-chemical changes occur in polymers due to gamma exposure. It is found that except some Polycarbonates (Lexan, Makrofol-E, Polycarbonate), all the other detectors gives the higher etch-rate values at the dose of 10^6 Gy. This increase in the etch-rate values is due to the scissioning of the molecular chains of these polymers. Spectroscopic studies have revealed that in the case of PADC (American Acrylics), the linkage of polyallyl chain with diethyleneglycol got raptured at the

dose of 10^6 Gy, leading to a production of oxygen centered radicals. For Triafol-BN, the increase in the etch-rate values is attributed to the destruction of ether/ester group of the polymer. For Polycarbonates (Lexan, Makrofol-E and Polycarbonate), it is the C-H bond of the benzene ring that breaks, which can not reduce the molecular weight of these polymers to an appreciable extent, and hence no increase in the etch-rate values takes place.

For almost all the detectors, it is found that transmittance starts decreasing with increasing dose (> 10^3 Gy) in the UV-VIS region. Moreover, with increasing doses, the transmittance shifts to the higher wave length region. This quantitative change in transmittance is very useful for dosimetric applications.

TGA studies have revealed that thermal resistance has not been modified by different doses of gamma radiation for Lexan, Makrofol-E and PADC (Homalite). However, for PADC (American Acrylics), Triafol-BN and Polycarbonate, thermal stability decreases at higher doses and the materials start losing weight at lower temperatures.

The thesis is laid out in the form of six chapters.

CHAPTER-1 contains the background, nature and importance of the studies related to the modification's induced by radiation in polymeric SSNTD's.

CHAPTER-2 presents a brief review on the interaction of radiation with matter and the subsequent events. Firstly interaction of gamma radiation with matter followed by interaction of radiation with polymers have been discussed. Introduction to nuclear tracks, track registration criteria along with theories used for track formation are also presented briefly. Section 2.5 contains the details about the literature available on radiation induced changes or modifications in polymers. Lastly stabilization against radiation-induced damage are also mentioned in brief.

CHAPTER-3 deals with a detail description of the techniques used to characterize the irradiated polymers. Some important parameters of track studies, like bulk-etch rate, track-etch rate, true track length, activation energy etc. are discussed in details. Several spectroscopic techniques like, IR, UV-VIS, ESR are discussed from section 3.2 to 3.4. Thermogravimetric analysis which has been used to study the thermal behavior of these detectors are also discussed in the end of this chapter.

CHAPTER-4 contains a systematic account of the experimental techniques used to characterize the irradiated polymers. At the very beginning the classification of the detectors and the properties are discussed. There-after, the

preparation of detectors and their irradiations to gamma source and Cf source are described. From section 4.3 to 4.6 contains the details about the experimental procedure of chemical etching, measurement of track parameters, determination of etch rates and determination of activation energies. Section 4.7 to 4.9 deals with the spectroscopic techniques which have been used to characterize the polymers. Lastly a brief experimental procedure about TGA is also mentioned here.

CHAPTER-5 contains results and discussion. It is divided in three parts. Part-1 discusses the details about the modifications in different types of polyallyl diglycol carbonate (PADC). Part-2 consists of the results and discussion on three types of bisphenol-A carbonates viz., Makrofol-E, Lexan and Polycarbonate. Part-3 deals with the work on Triafol-TN and Triafol-BN polymers.

CHAPTER-6 The significant conclusion of the present investigation are highlighted. A brief description on the potentialities and scopes of this work along with some future perspectives is also presented in this chapter.

RADIATION INDUCED MODIFICATION OF SOME DIELECTRIC SOLIDS

BY

DIPAK SINHA

DEPARTMENT OF CHEMISTRY
SCHOOL OF PHYSICAL SCIENCES

SUBMITTED

In fulfilment of the requirement of the degree of

DOCTOR OF PHILOSOPHY

in

CHEMISTRY

of

NORTH-EASTERN HILL UNIVERSITY,
SHILLONG -793003
INDIA

dedicated

to

Sudeshna

Declaration

The North-Eastern Hill University

Month : November, Year : 1997

I Mr. Dipak Sinha, hereby declare that the subject matter of this thesis is the record of work done by me, that contents of this thesis did not form the basis of the award of any previous degree to me or to the best of my knowledge to anybody else, and that the thesis has not been submitted by me for any other research degree in any other University/Institute.

This is being submitted to the North Eastern Hill University for the degree of **DOCTOR OF PHILOSOPHY** in Chemistry.

Dipak Sinha

Mr. Dipak Sinha

M.C. Mahanta 27/11/97

(Head)
Department of Chemistry
North Eastern Hill University
Shillong.

K.K. Dwivedi 27.11.97

Dr. K.K. Dwivedi
Supervisor

Acknowledgements

It is a privilege to express my sincere and heartfelt gratitude to my supervisor **Dr. K.K. Dwivedi** for his caring and dynamic guidance throughout the course of this work

I am also deeply grateful to Dr. A. Mawar, Dr. S. Ghosh, Dr. A. Srivastava, Rosaline Mishra, S. Tripathy for their advice and help during this work.

I wish to thank Dr. V.G. Dedgaonkar, Pune University, for his help in gamma irradiation.

I thank to Dr. A. Lemtur and Dr. Harish Chandra for certain result oriented discussions and suggestions.

I gratefully acknowledge the guidance, help and cooperation I received from the Head, Department of Chemistry, Prof. M.K. Mohanti and the Dean, School of Physical Sciences, Prof. S.N. Bhatt.

I express my sincere thank to the faculty members in the Department of Chemistry for their constant encouragement.

My heartfelt thank goes to Prof. M.K. Choudhuri, IIT, Guwahati, who was a great source of inspiration and Dr. S.N. Rai, for the help I received from him during the tenure of my research work.

A special mention also goes to the non teaching staff of the Dept. of Chemistry for the help and cooperation I got from them.

I am thankful to RSIC, NEHU for allowing me to use all the facilities available there.

A deep note of appreciation is due to my research colleagues and friends : Arun, Khub, Suchandra, Gagan, Thomas, Binda, Jayashree, Guna, Nadeem, Wancy, Akhilesh, Deppa, Sushmita and Upasana (Rolly) who stood by me through all odds to lend a helping hand.

I also thank Dr. S.N. Majumdar, Dr. B. Paul, Dr. S. Choudhury, Mr. P. Mawar, Santush da, Paramita , and all others who helped me during the tenure of my work..

I am grateful to MCST&E, Govt of Mizoram, Department of Chemistry, N.E.H.U. and CSIR, New Delhi for the financial assistance during the course of my work.

My thanks also are due to Mrs. Rekha Dwivedi, Tinu and Vinni for their love and care.

I express my deep sense of gratitude to my parents and family members for their encouragement through out this work.

I could make all my acknowledgements only because of my God who abides with me throughout my life.

Dipak Sinha

Dipak Sinha

CONTENTS

Page No.

LIST OF TABLES

LIST OF FIGURES


CHAPTER-1

CHAPTER-1

INTRODUCTION

Since its inception about 40 years ago, the field of track detection using solid state nuclear track detectors (SSNTDs) has been constantly developed. Track detectors are being increasingly used in various fields like Biomedical [1], Environmental [2], Anthropology [3], Space research [4,5] and Nuclear sciences [6,7]. For newer and more innovative applications of these detectors a systematic study on the effects of external factors on their physical and chemical properties is essential. So the field of radiation chemistry which comprises a study of the physico-chemical variations in matter induced by nuclear radiations is very important. Radiations are produced from both natural and man-made sources and are omni-present. Radiations comprise not only the charged particles like electrons, protons, alpha particles, fission-fragments and accelerated heavy ions, but also the electromagnetic radiations such as X-rays and gamma-rays.

It is well known that unlike charged particles gamma rays are a highly penetrating form of electromagnetic radiation. They do not lose energy at every interaction with the orbital electrons of the atoms constituting the material they pass through. The energy loss of gamma rays occurs either through collisions with atomic electrons or

through scattering as a photon of a longer wave length or through producing electron-positron pairs. Thus gamma ray do not have a specific range in matter as charged particles do. The principal methods of gamma interactions with matter are (a) *Photoelectric effect* (b) *Compton scattering* and (c) *Pair-Production*.

Experimental evidence shows that the track registration characteristics of plastic Solid State Nuclear Track Detectors (SSNTDs) are greatly affected when exposed to high doses of gamma rays [8-16]. The modifications in characteristics originate from the structural alterations produced by irradiation of polymers. Studies have also been carried out on metal alloys [17] and metallic glasses [18]. The action of electromagnetic radiation is known to be one of the major sources of altering the properties of the materials they pass through. The changes are strongly dependent on the internal structure of the absorbing substances and the radiation gamma doses. It may be expected that the interaction of gamma-rays with solids cause electronic ionisation (or excitation) of the orbital electrons and possibly atomic displacements. Since polymeric solid state nuclear track detectors consist of long chain organic molecules, the net effect on the material is the formation of many broken molecular chains, leading to a reduction in the average molecular weight of the substance. Such radiation induced modifications of polymeric materials may influence their etching characteristics [19-22], optical

properties [23] and some other properties such as thermal stability [24] and morphology [25] which inturn change the track registration properties of these track detectors.

Gamma exposure of the dielectric solids is not an uncommon phenomenon. In nuclear reactors during the process of fission, a high dose of gamma radiation is produced along with the neutrons. This produces different effects on bulk and track etch characteristics of detectors. High radiation doses also cause inaccuracy in the determination of the age of geological samples as determined by fission track dating technique. The track detectors are increasingly used in diverse fields such as radiation dosimetry, cosmic-ray study, heavy ion Physics, microanalysis, uranium prospecting etc., so a proper characterisation of these detectors is necessary. Though the passage of lighter particles and gamma rays through these detectors can not be directly recorded, but the modifications that they produce on these detectors can be quantified.

The foremost application of a knowledge of the physico-chemical changes in matter with radiation dose is in the field of radiation dosimetry. Radiation dosimetry provides the basic knowledge required for quantitative measurements of radiation. In addition to that it can also be used to assess the ambient radiations and thus provide a protection against radiation hazards. Keeping these factors in mind we have attempted to characterise the modifications that take place in seven polymeric solids viz. **PADC, (Homalite), PADC**

(American Acrylics), **Lexan**, **Makrofol-E**, **Polycarbonate**, **Triafol-TN** and **Triafol-BN**, by the passes of gamma rays between dose range from 10^1 Gy to 10^6 Gy.

So far a lot of work on polymeric films as well as on track detectors have been done [20-28], but no systematic study concerning the effects of gamma radiation on the physico-chemical properties such as track properties, optical properties, thermal stability, structural alterations etc. has been done extensively.

In this dissertation we present a detailed account of the response of seven polymeric detectors exposed to different doses of gamma rays in terms of –

(a) registration and development of tracks in polymeric detectors

(b) determination of bulk-etch rate, track-etch rate. maximum etchable track length, complete etching time, under different etching conditions

(c) determination of activation energy for bulk - etching

(d) modifications of activation energy for bulk-etching by different doses of gamma radiation

(e) dependence of bulk-etch rate and track-etch rate on gamma doses

(f) change in absorbance of transmittance caused by different doses of gamma radiation in the UV and VIS region

(g) changes in thermal stability due to gamma irradiation

(h) Study of IR, ESR, as well UV & VIS for determining the structural changes that take place in these irradiated samples.

REFERENCES

[1] Raggenkamp H. G., Kiesewetter H., Spohr R., Daur U. and Busch L. C., Production of single-pore membranes for the measurement of red blood cell deformability. Biomedizinische Technik. 26 (1981), 167-169.

[2] Fischer B. E. and Spohr R. Production and use of nuclear tracks: Imprinting structure on solids. Rev. Mod. Phys. 55 (1983), 907-948.

[3] Fleischer R. L; Price P.B.; Walker R. M. and Leakley L.S.B. Fission track dating of Bed I, Olduvai Gorge. Science. 148 (1965), 72-74.

[4] Fleischer R. L; Price P. B; Symes E. M. and Miller D.S. Fission track ages and track annealing behaviour of some micas. Science. 143 (1964b), 349-351.

[5] Krishnaswami S., Lal D., Prabu N. and Mac Dougall D. Charateristics of fission tracks in Zircon: Applications to Geochronology and cosmology. Earth Planet. Sci. Letters. 22 (1973), 51-59.

[6] Perelygin V. P., Shadieva N. H., Tretyakova S. P., Boos A. H. and Brandt R., Ternary fission produced in Au, Bi, Th and U with Ar Ions. Nucl. Phys. A. 127 (1969), 577-585.

[7] Gibson W. M. and Nielson K. O., Direct determination of the life time of excited compound nuclei by angular distribution measurements of fission fragments emitted from single crystals. Phys.Rev. Letters.24 (1970), 114-117.

[8] Khan H.A., Asharf M.A., Yameen S., Haroon M.R. and Hussain A. The effects of high gamma dose on the response of plastic track detectors. Nucl. Instr. Meth. 127 (1975), 105-108.

[9] Zamani M., Sampsonidis D. and Charalambous S. Dose rate effects on CR-39 SSNT Detector. Nuclear Tracks. 12 (1986), 125-128.

[10] Acierno D., La Mantia F. P., Titomanlio G., Calderaro G. and Castiglia F. Gamma-radiation effects on a polycarbonate. Radiat. Phys. Chem. 16 (1980), 95-99.

[11] Frank A. L. and Benton E. V. Dielectric plastic as high exposure gamma-ray detectors. Radiat. Effects. (1970), 269-272

[12] Portwood T. and Henshaw D. L. The Effect of gamma dose on the alpha response of CR-39. Nucl. Tracks. 12 (1986), 105-108.

[13] Varnagy M. Measurement of gamma dose by means of a Cellulose Nitrate Solid State Nuclear Track Detector. Nucl. Instrum. Meth. 152 (1978), 531-533.

[14] Zamani M., Sauvides E., Petrakis J. and Charalambous S. Gamma dose discrimination properties of SSNT-Detectors. Nucl. Tracks. 12 (1986 b), 141-144.

[15] Joseph A. and Varier K. M. Gamma ray dosimetric studies on CR-39 detectors. Indian Journal of Pure and Appplied Physics. 33 (1995), 406-409.

[16] Singh S. and Singh B. The effect of gamma irradiation on etching characteristics of some solid state nuclear track detectors. Nucl. Tracks Radiat. Meas. 15 (1988), 199-202.

[17] Chaki and Li J. Heavy-ion damage of an amorphus mettalic alloy. J. Nucl. Materials. 140 (1986), 180-184.

[18] Dunlop A., Legrund P., Lesueur D., Larenzelli N., Marillo J., Barbu A. and Bouffard S. Phonon soft modes and damage production by high electronic excitations in pure metals. Europhys. Lett. 15 (1991) , 765-770.

[19] Sharma S. L., Pal T., Rao V. V. and Enge W. Effect as gamma irradiation on bulk etching rate of CR-39. Nucl. Tracks Radiat. Meas. 18 (1991), 385-389.

[20] Shweikani R., Durrani S. A. and Tsuruta T. Effects of gamma irradiation on the bulk and track etching properties of Cellulose Nitrate (Daicel 6000) and CR-39 plastics. Nucl. Tracks Radiat. Meas. 22 (1993), 153-156.

[21] Komaki Y., Ishikawa N. and Sakurai T. Effect of Gamma rays on etching of heavy ion tracks in Polyimide. Radiat. Meas. 24 (1995), 193-196.

[22] Abu-Jarad F., Hala A.M., Farhat M. and Islam M. Effect of high gamma dose on the CR-39 properties. Radiat. Meas. 28 (1997). (in press)

[23] Fink D., Muller M., Chadderton L.T., Cannington P.H., Elliman R.G. and McDonald D.C. Optically absorbing layers on ion beam modified polymers : a study of their evolution and properties. Nucl. Instr. Meth. B32 (1988), 125 -130.

[24] Fukuda K. Effect of high gamma ray and electron doses on the annealing behaviour of Natural Mica. Radiat. Effects. 45 (1979), 123-124.

[25] Akber R. A., Nadeem K., Majid C. A., Hussain A., Zaman N., Chaudhary M. A. and Khan H. A. Studies of structural changes

produced by high doses of gamma-rays in some plastic track detectors. Nucl. Instr. Meth. 173 (1980), 217-221.

[26] Tidjani A. and Watanabe Y. Gamma-oxidation of linear low density polyethylene: the dose effect of irradiation on chemical and physical modifications. J. Polym. Sci. A, Polym. Chem. 33 (1995), 1455-1460.

[27] Tidjani A. and Watanabe Y. Study of the effect of gamma-dose rate on the oxidation of polypropylene. J. Appl. Polym. Sci. 60 (1996), 1839-1845.

[28] Mayaki S., Dasilva A. O. and Tidjani A. Effects of Gamma irradiation on Cellulose Nitrate LR-115 Type 11. Radiat. Meas. 26 (1996), 657-661.

CHAPTER-2

CHAPTER-2

TYPES OF RADIATION AND THEIR INTERACTION WITH MATTER

2.1. TYPES OF RADIATION :-

Radiations are broadly classified into two categories:

(a) Charged particles

(b) Neutral radiations

The charged particle radiations include heavy charged particles like heavy ions, fission fragments , α-particles and protons and light charged particles like the electrons and positrons. Neutral radiations consist of neutrons and electromagnetic radiations namely gamma rays and X-rays.

(a) Charged particles

Electrons and Positrons :- energy is in the range of 10 eV to few MeV and velocity is in the range of 10^9 to 10^{10} cm/s.

Alpha and Protons : energy is in the range of 1 MeV to few MeV and velocity is in the range of 10^8 to 10^9 cm/s.

Fission fragments : energy is in the range of 60 MeV to 100 MeV, velocity is in the range of 10^7 to 10^8 cm/s and the charge state of +20 to +22 .

Accelerated Particles : Accelerators are the most versatile heavy ion sources which provide monoenergetic, monoisotopic and highly parallel beams of practically all ions. An extremely wide range of areal flux of 10^0-10^{12} cm^{-2} and ion energies of 10^0-10^3 MeV/u is attainable depending on the type and size of the accelerator.

(b) Neutral and uncharged radiations

Electromagnetic radiations :- X-rays have energy upto 100 keV and gamma rays have energy ranging from 20 keV to 10 MeV.

Neutrons :- energy is in the range of 0.025 eV to a few MeV.

2.2. INTERACTION OF RADIATION WITH MATTER :-Charged particles interact with matter through coulombic forces. On the other hand, interaction of radiation that do not have charge, is a two step process. First they undergo a reaction/interaction to produce charged particles to which kinetic energy is transferred and these particles then interact through coulombic forces.

(a) Heavy charged particles :- Heavy charged particles interact with matter through a series of binary collisions with the electrons of the atoms and molecules via coulombic interaction and produce ionisation and excitation in the medium (or absorber). According to the law of conservation of momentum, the maximum kinetic energy (T_e) which can be imparted to the electron by a charged particle of mass M and energy E in a single collision is given as

$$(T_e)_{max} = 4m_0(E/M) \qquad (2.1)$$

A proton of energy 5 MeV can transfer a maximum of 10 keV energy to the electron. Due to small loss in energy per collision, heavy charged particles generally travel in a straight path in a medium. At the end of the path, the charged particles become neutral and free unable to lose energy electronically.

(b) Electrons :- Like heavy charged particles, electrons also lose their energy in a stopping medium by collisional losses through coulombic interactions. In electron electron collisions, the incident electron can lose up to one half of its energy in a single collision. The mean deflection of an incident electron as a result of an ionisation or radiation collision is also large compared to a heavy particle. In addition the electron also suffers scattering by elastic collision with the nuclei and electrons of the target atoms, resulting in further deflection from their direction of incidence.

Electrons also lose their energy by emission of Bremsstrahlung. High speed charged particles passing close to the nucleus of an atom may be decelerated and radiate electromagnetic radiation. The energy loss due to emission of Bremsstrahlung will be greatest for light particles and stopping materials of higher atomic number.

(c) Electromagnetic Radiation :- Electromagnetic radiations like X-rays and gamma rays lose their energy in a stopping material through the following three processes –

(1) Photoelectric Effect:- In this process a photon is absorbed in the medium and the energy is transferred to the atom. This energy if transferred to one of the electrons (normally tightly bound electrons), then the velocity of that electron will be too high to remain in the orbital resulting in its emission. The difference between the incident photon energy (E_γ) and the ionization energy of the electron (E_b) appears as the kinetic energy (E_e) of the ejected electron.

$$E_e = (E_\gamma - E_b) \qquad (2.2)$$

The probability of emission of K electron is higher than the other electrons provided the energy of the photon is higher than the threshold energy required for its ejection.

(2) Compton Scattering :- In this process the photon interacts with an electron which may be loosely bound or free. The incoming photon is deflected through an angle θ, with respect to its original direction and a fraction of its energy is transferred to the electron (Fig.2.1).

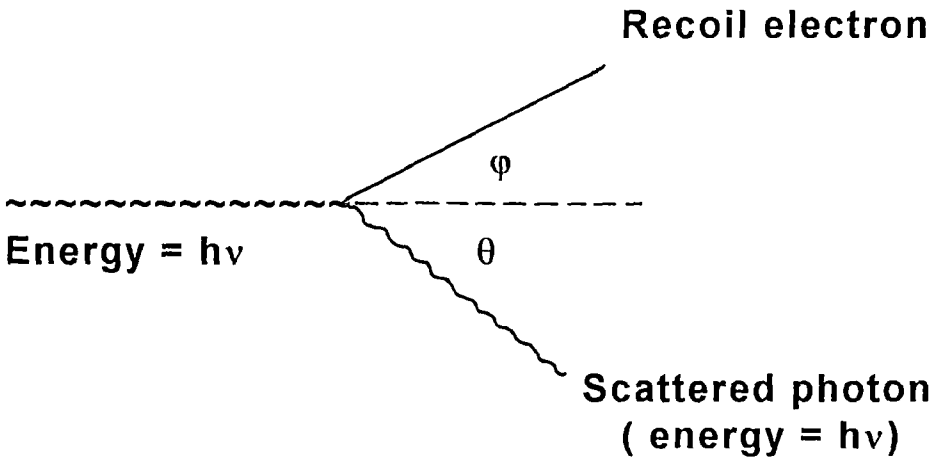

Fig. 2.1 The Compton effect

The outgoing photon energy is given by,

$$h\nu' = h\nu / [1+\{(h\nu/m_oc^2)\ (1-\cos\theta)\}] \qquad (2.3)$$

The electron energy (E_a = hν–hν') is zero at θ = 0 and maximum (≥ $h\nu-m_oc^2/2$) at θ =180. Since electrons in the entire energy region between E = 0 and ≥ $h\nu - m_oc^2/2$ are produced, a continuous response of the detector is obtained. Therefore, this interaction is not very useful for detection. Compton Scattering predominates for photon energies between 1 and 5 MeV in high Z materials and over a wide range of energies in low Z materials.

(3) Pair production :- This process involves the complete absorption of a photon in the vicinity of an atomic nucleus with the formation of an electron- positron pair. This interaction occurs mainly in the coulomb field of the nucleus of the absorbing material. The conservation of energy is given by the equation

$$h\nu - 2m_oc^2 = E_{e+} + E_{e-} \qquad (2.4)$$

where E_{e+} and E_{e-} are kinetic energies of positron and electron and m_o is the rest mass of positron or electron.

(d) Neutrons :- Neutrons do not directly produce ionisation in matter. However they interact with nuclei of atoms of the absorbing medium by different nuclear reactions. Neutrons interact with matter by elastic and inelastic scattering and nuclear reactions.

2.3. INTERACTION OF RADIATION WITH POLYMERS :-The interaction of radiation with a polymer and the subsequent events can be chronologically divided into three distinct periods : energy absorption, establishment of thermal equilibrium, and the establishment of chemical equilibrium [1].

(a) Energy absorption :- There are three modes of energy absorption : viz., electron displacement (ionisation and excitation), atomic displacement, and generation of impurity atoms as a result of

nuclear reactions. For non-relativistic particles, the probability of energy transfer through a nuclear reaction is small compared to other modes of energy transfer[1]. Even if such an event does occur, it is quite discrete and obvious. Thus it need not be discussed with the other, more nearly continuous energy loss mechanisms. Except at very low velocities of the incident charged particle, the energy transfer via atomic displacement can also be neglected. However, the possibility of a 'displacement' spike occurring in last few microns of a heavy particle path can not be discounted at this time. Thus, the primary mechanism for energy absorption in polymeric system is electronic displacement. This takes place in the time period of less than 10^{-15} second.

(b) Thermal equilibrium :- The second phase, lasting for approximately from 10^{-12} to 10^{-9} second, involves the transport and disposition of absorbed energy by molecular motion the thermal equilibrium within the solid is established. Again there are three alternatives : energy can be emitted as luminescence, it can be dissipated as heat, or energy can be stored as potential energy in the form of chemically reactive species. The exact path followed depends strongly on the structure of the molecule and the environmental conditions. A fraction of the energy emitted during luminescence can be in the form of short ultraviolet light which will be locally reabsorbed by the plastic. However, since the amount of energy involved in luminescence is generally of the order of only a few

percent of the total, the photochemistry arising from this effect can be neglected. The great bulk of the energy ends up as heat. In case of slow, massive, very heavily ionising particles, such as fission fragments, the sudden deposition of a large amount of energy in a highly restricted space may for a period of 10^{-11} second, raise the local temperature in excess of several hundred degrees centigrade - the so-called 'thermal' spike concept [2]. Temperature in this range can activate certain atomic and electronic processes resulting in extensive atomic rearrangements and local chemical changes. Other damage spikes such as "plasticity", "displacement electron", [2] and "ion explosion" [3] have also been proposed.

(c) Chemical equilibrium :- The duration of the third and final stage may be extended by diffusion processes and reaction rate may vary from a minimum of about 10^{-2} second upto years in certain solids. It involves the reduction of the small fraction of the energy which ended up as potential energy of the reactive species to a thermally stable level[1]. These species include electrons, excited molecules, ions and radicals. While the life time of excited molecules is short (10^{-9} to 10^{-8} s), measurable populations of the other species may persist almost indefinitely. This is because electrons are held in traps while ions and radicals are stabilized by the cage effect. The cage effect greatly enhances the probability of immediate recombination of the chemically reactive species

inside the cage, while at the same time impending reactions with molecules on the out side.

2.4. NUCLEAR TRACKS :- One of the important, versatile and widely applicable technique of radiation detection by visual devices is based on solid state nuclear track detectors. It is already a known phenomenon that the energetic charged particles create submicroscopic damage trails in solid dielectrics such as glasses, plastics and inorganic crystals. These trails are of the order of 5 – 10 nm in diameter and are visible only at high magnification under an electron microscope. Due to the rapid fading characteristics of such latent tracks under the influence of high electron flux, it becomes difficult to make accurate measurement of any desired track parameter. With the help of suitable etching processes it is possible to enlarge and fix these trails into permanent tracks which could be easily observed under an optical microscope. Out of several track developing techniques, chemical etching is by far the most simple, accurate and widely used technique. The principle of chemical etching of nuclear tracks is based on the fact that the damage- trails are associated with large free energy, leading to a preferential etching along the track as compared to normal material when the detector is immersed in any suitable chemical etchant. The speed with which the undamaged material of the detector is dissolved away by the etchant solution is known as bulk-etch rate (V_G). On the other hand, the rate of increase of track length

with respect to etching time is defined as track-etch rate (V_T). The shapes of the etched tracks depend on the relative magnitude of the etch rates. In most plastic track detectors, one observes narrow conical tracks where as in glass detectors, shallow etch-pits are generally observed.

In the past, three decades an aura of excitement and fascination has been created in the field of nuclear tracks in solid dielectrics [4-15] partly because of its simple methodology but primarily because of the great diversity of its usefulness in scientific and technological domains which range from Anthropology [16], Geochronology[17,18] to Space research [17,18], from Geophysics [19], Superfluidity [20], Lithography[21] and Dosimetry [22] to Biomedical research [23] and from Gem diamond manufacture [24] to the Cancer therapy [25]. In addition to the broad range of applications of Solid State Nuclear Track Detectors (SSNTDs), the usefulness of these detectors in Nuclear Physics is particularly becoming more and more important. The study of heavy ion nuclear reactions [26,27], high resolution particle identification [28,29], ternary fission [30,31], measurement of reaction cross-section and life time [32-34], detection of short lived heavy nuclei [35], discovery of super heavy elements [36], exotic decay [37,38], range and energy loss measurement in elemental and complex media [39-50], Preparation of microfilters [51-52] involve extensive use of SSNTDs.

Experience shows that the track registration characteristics of polymeric Solid State Nuclear Track Detectors (SSNTDs) are greatly affected when exposed to high doses of gamma rays [53-58]. The modification in characteristics originates from the structural alterations by irradiation of polymers. Since polymeric solid state nuclear track detectors consist of long chain molecules, the net effect on the matrix due to irradiations is the production of many broken molecular chains, leading to a reduction in the average molecular weight of the substance. All these modifications change the track properties like bulk-etch rate, track-etch rate, etching efficiency, activation energy for bulk- and track-etching.

In polymeric track detectors, only those charged particles with linear energy transfer (LET) above a critical values can create distinct etchable tracks. Atomic radiations such as UV rays and X-rays, nuclear radiations like gamma rays and beta rays are low LET radiations. They mostly affect the physical and chemical properties of the polymeric films. Though they can not create any tracks but can affect etch rate values of detectors depending upon the absorbed dose [53]. For track detectors exposed to high LET charged particles followed or preceded by low LET radiation exposure, both the bulk-etch rate and track-etch rate are found to vary in accordance with the absorbed doses of low LET radiations [54,55]. Having a thorough knowledge about these effects is, therefore, necessary when track detectors are used for detecting charged particles in an atmosphere

of intense low LET background radiation. Besides, it is useful in evaluating the dosimetric properties of track detectors.

2.4.1. Track registration criteria :- The ability to predict which particle will produce latent (etchable) tracks in a given polymeric system is the basic requirement in the understanding and purposeful utilisation of detectors. In the past few years, several track registration criteria have been proposed. We will consider these criteria both in terms of their utility as well as the physical track formation mechanisms that are implied. What distinguishes the latent track region from the unaffected bulk material ? Also, the exact chemical and physical properties of the preferentially etchable region depends very strongly on the mass, charge and velocity of the track forming particles, on the chemical structure and physical state of the dielectric material used during irradiation and the environmental conditions. However, in general it is expected that this region will have the properties listed in Table–2.1

Table–2.1

Properties of the latent track region in the irradiated polymers

---

(1) Reduced molecular weight

(2) Increased number of polymeric chain ends

(3) Increased solubility

(4) Presence of new chemical species such as

a. free radicals

b. trapped gases (CO, CO_2, H_2, O_2 etc.)

c. increased unsaturation

(5) Reduced physical density

(6) increased optical absorption, particularly in the UV region.

The parameters which influence track etching can be separated into five broad categories : (1) The material parameters (which will include the chemical composition, molecular weight, the extent of Crystallinity, solvent content, etc.); (2) the particle parameters (charge : Z, mass :M, velocity : V) ; (3) the irradiation environmental parameter (temperature, atmosphere, etc.); (4) the pre-etch storage parameters (atmosphere, temperature, etc.); and (5) the etching parameters (including type of etching solution, concentration, temperature, time etc.). The question considered here is, given a particular track detecting material, how the track registration depend upon the particle parameters when all other

etch-influencing parameters remain fixed ? In other words which function Z, M, or V best predicts the condition $V_T/V_G > 1$?

2.4.2. Theories used for track formation :- Various authors have suggested that track formation should be related to a number of different parameters, such as total energy loss rate, primary ionisation, restricted energy loss, etc. Once they sets up a track formation criteria, which takes the form of a statement that tracks are formed in a medium when and only when, the chosen parameters exceed some critical value whatever be the bombarding particle. For a valid track formation, parameters, (say) X, should be possible to draw a unique threshold value, X_c, separating the region of track etchability from that corresponding to non-etchability. In recent years, this view of track formation criteria has been modified somewhat in that, less emphasis is now placed on the threshold value of X. This is because experimental data have accrued [59,60] to show that the track etching rate (V_T) is a smoothly varying function of incident particle parameters. It is now usual to seek a parameter X such that V_T (X) always has the same value (for a given combination of detector and etching conditions) at a given value of X, regardless of the combination of ionic charge and velocity that may lead to the X value in question.

The concept of the thermal spike was introduced as a mechanism by which energetic particles could produce considerable disruption of a crystal lattice. In this model the passage of an energetic particle is

assumed to produce intense heating of a localised region (thermal spike concept) of the lattice. The region is therefore raised to a high temperature[2], from which it cools rapidly via heat conduction. As a result of this heating episode various atomic processes are activated, and damage to the lattice is produce.

Chadderton et al.[61] and Chadderton and Torrens [62] have presented more detailed considerations of the manner in which the electronic excitation produced by the fission fragment is transferred to the lattice atoms. They found that, in metals, energy is lost by δ-rays primarily via electron-electron collisions down to very low electron energies-because the energy loss per collision is greater, and the relaxation time is shorter, than the electron-phonon interactions. Thus the excitation is spread through out a large volume by the electrons before significant energy transfer to the lattice occurs; and therefore the peak temperature to which the lattice is raised in a metal is low.

In insulators, on the other hand, electrons can interact readily with polar and acoustic modes of lattice vibration; and, indeed once the δ-ray energy falls below that equal to the band-gap width-i.e. several electron-volts release by the δ-rays of further electrons into the crystal's conduction band becomes impossible. Therefore, electron-phonon collisions are expected to be the predominant energy loss process in insulators, and the excitation is communicated to the lattice more efficiently in such materials.

The nature of track formation appears to be distinctly different in polymers from what it is in inorganic solids. The damage along tracks in inorganic solids consists mainly of displaced atoms. which can be explained by "ion explosion spike" model [3], is the use of burst of ionisation along the path of a charged particle to create an electronically unstable array of adjacent ions which eject one another from their normal sites into interstitial positions.

2.5. RADIATION INDUCED CHANGES OR MODIFICATIONS OF POLYMERS :- Irradiation of polymeric material induces irreversible changes in their macromolecular structure and, like in case of electrons or gamma irradiation, it can be used to change in a controlled way the physical properties of thin films or to modify the near surface characteristics of a bulk polymer [63,64]. Significant effects of ion irradiation are observed at a fluence as low as 10^{11} ions/cm^2, where chemical modifications take place. Primary phenomena associated with radiation interaction are chain scission, chain aggregation, formation of double bonds and molecular emission [65]. All these effects depend on target parameters (composition, molecular weight, temperature, etc.) and on ion beam parameters (energy, mass, charge and fluence). Molecular emission from polymers always occurs with the release of neutral hydrogen and carbon-hydrogen groups and with a significant change of the polymer stoichiometry. If present in the polymer chain, other atomic species (O, F, Cl, N) are also ejected [66]. After irradiation, most of the

properties of polymers (optical, electrical, mechanical, thermal etc.) are modified together with its chemical behaviour as shown by solubility and molecular weight distribution measurements (67, 68).

At high fluence (10^{14} - 10^{17} ions/cm^2) an enrichment of carbon generally occurs, leading to more or less complete carbonisation such that the final sample composition may have little memory of the original chain structure. Properties of such materials are similar to amorphous carbon in terms of optical absorbance, electrical properties, hardness and chemical inertness are similar to those of amorphous carbon, but they may eventually contain heteroatoms like N,O, S, if these are present in the original polymer structure [67,69,70]. Application of radiation on polymers leads to a change in the electrical conductivity, which has been studied by Forrest et al.[71] and Wnek et al.[72], who have characterised the temperature and some doping effects induced in polymers by different ions. Marletta et al.[73] have found a correlation between chemical structure modifications and electrical change of some polymers like polystyrene, polyimide and polyestersulphane and Aleshin et al.[74] have reported the electrical behaviour of the ion irradiated polyimide. Optical properties of ion beam irradiated polymers have been characterised by Elman et al.[75] , Davenas et al.[76] and Fink et al.[77] correlated the changes in the optical properties with the mechanism of energy deposition. Ion beam effects on PMMA have been studied by Mladenov and Emmoth [78]

and its applications on fabricating light guides by Kulish et al.[79]. Phase transition during irradiation of ferroelectric polymers has been reported by Legrad et al.[80]. Improvements in surface smoothness, hardness and wear resistance of polymers by multiple ion implantation has been studied by Lee et al. [81].

When radiation is absorbed by matter, ions and free radicals are formed, which are the precursors of all subsequent chemical transformations. Free radicals arise as a result of bond scissions. In liquids the lifetime of these species is extremely short. They combine, as a result of very rapid radical-radical coupling and positive ion interactions, with either electrons or negative ions. The same situation is met in a polymer above its glass transition temperature, where the high mobility of the polymer favours encounters of the various reactive species. In contrast, if the polymer is irradiated in a vitreous state, mobility is considerably reduced and trapped radicals and ions are always present. The life times of these species may become extremely long (weeks or months) and are essentially determined by the temperature : the farther away the system from its glass transition temperature, the longer the life time of trapped species. Free radicals are detected by ESR signals [82,83,84] which can be used to determine their concentration, their nature and the kinetics of their decay. Ionic species also often give ESR signals. They can be characterised by radiation induced conductivity or by post

irradiation thermoluminescence which is caused by positive negative charge combination. Trapped ions or radicals absorb light and may be responsible for more or less transient discolouration. Crystallinity of polymer is also responsible for the trapping of transient species, particularly radicals. If, however, the system is above T_g (glass transition temperature) the mobility of the polymeric segments is large enough for the valencies to "move out" of the crystalline zones, usually by inter and intramolecular atom (hydrogen) transfer. The most obvious changes in the bulk properties of irradiated polymers are brought about by modification of their molecular weight due to cross-linking or degradation. Cross-linking increases the modulus and hardness of the polymer, but this effect become apparent only for very high cross-link densities. If, however, the polymer is partially crystalline, such as polyethylene, moderate cross linking imparts to the material a nonmelting behaviour. Above its crystalline melting point a cross linked polymer does not flow, but exhibits rubber elasticity. This modification is of great commercial importance for numerous products such as insulators, hot-water pipes and others, and this accounts for the fairly large scale manufacture of radiation cross-linked polymers in industry. Radiation degradation is a random chain scission process which gradually reduces the molecular weight of the polymer. Low molecular weight products are produced statistically and they may plasticize the material. As a

result of this the polymer weakens and loses most of its valuable properties after high radiation doses.

Some of the degradation products may be useful. Thus, wastes of perfluorinated polymer (Teflon) are reclaimed by irradiation in air which converts a useless material into lower molecular weight polymers which find specific uses in sprays. Polyisobutylene (butyl rubber) is degraded by irradiation to yield lubricating oils, cellulose degrades to glucose. It has been observed by Biersack et al. [85] that refractive index of a polymer can be altered by ion irradiation, which is again commercially important for optical device fabrication. Differential scanning calorimetry (DSC) performed on an ion irradiated polyvinylidene film [86] shows a decrease of the melting point and of the enthalpy with irradiation dose. This behaviour is characteristic of a loss of Crystallinity due to the internal organisation of the polymer. Track registration properties of a polymeric detector is greatly influenced by exposing to gamma radiation. It has been observed that gamma exposure changes the bulk-etch rate, track-etch rate and also the detector efficiency. A lot of work has been done on gamma effect on etching characteristics [87,88,89].

So far we have discussed the changes or modifications caused by the radiation. Basically all types of physical or chemical changes take place in the polymer because of the bond cleavages, giving rise to nonsaturated fragments called "free radicals". The most

interesting phenomenon about this type of bond cleavage is that, in this radiation interaction, which particular bond will be broken can not be predicted, on the basis of energy consideration alone. Because the energy spent in ionisation (20 eV or more) is much larger than the bond energies of simple organic molecules which are

$$H\text{-}CH = 4.3 \text{ eV};$$

$$CH_3\text{-}CH_3 = 3.7 \text{ eV};$$

$$F\text{-}CH_3 = 4.6 \text{ eV}$$

These value are merely presented here to illustrate the differences in orders of magnitude between the energy deposited and the strengths of the chemical bonds present in the system. It follows that the energy available largely exceeds the amount required to cleave any bond. In spite of this, all the bonds are not broken in random. Experimental evidence shows that selectivity rules apply, which do not follow bond energy considerations alone.

2.6. STABILIZATION AGAINST RADIATION-INDUCED DAMAGE :-

Polymers can be stabilized against radiation damage by the addition of substances which either divert the absorbed energy towards other chemical processes or stabilise the free radicals produced, thereby preventing them from causing further damage. The first group of substances includes aromatic compounds which are known to act as "energy sinks". Thus, benzene protects

cyclohexane and other saturated hydrocarbons from radiolysis by taking up their energy. An excited or ionised cyclohexane molecule transfers its excess energy to the aromatic compound. The latter being much more stable against radiation damage, (owing to the delocalization of the excited energy) most of the energy are lost and ends up as heat. This sequence of reactions can be represented as :

$$M^* + Ar = M + Ar^* \qquad (2.5)$$

$$Ar^* = Ar + Heat \qquad (2.6)$$

Here M is the molecule of interest and Ar the aromatic additive. In reaction (2.5) the excited species M* is deactivated which prevents its break down. The presence of aromatic groups in repeating units in a polymer also accounts for the radiation stability of such polymers as Polystyrene, Polyaryletherketones, Polyarylimides etc. The second group of substances comprises so called "free radical scavengers" which readily react with free radicals and prevent them initiating degradation processes. This group includes well-known "stabilisers", "anti-oxidant" and other additions which are present in most commercial polymers.

REFERENCES

[1] Benton E.V. On the latent track formation in organic nuclear charged particle track detectors. Radiat. Effects. 2 (1970), 273-280.

[2] Billington D. S. and Crawford H. Jr. Radiation damage in solids. Princeton University Press (1961), Princenton, N.J.

[3] Fleischer R. L; Price P. B. and Walker R. M. The ion explosion spike mechanism for formation of charged particle tracks in solids. J. Appl. Phys. 36 (1965a), 3645-3652.

[4] Young D. A. Etching of Radiation damage in Lithium Fluoride. Nature. 182 (1958), 375-377.

[5] Silk E. C. H. and Branes R. S. Examination of fission fragments tracks with an electron microscope. Phil. Mag. 4 (1959), 970-971.

[6] Fleischer R. L; Price P. B. and Walker R. M. Tracks of charged particles in solids. Science. 149 (1965b) , 383-393.

[7] Fleischer R. L; Price P. B. and Walker R. M. Solid state track detectors, Applications to nuclear science and geophysics. Ann. Rev. Nucl. Sci. 15 (1965), 1-28.

[8] Fleischer R. L; Price P. B. and Walker R. M. "Nucl .Tracks in Solids, Principles and applications" Univ. of California Press, (1975).

[9] Proceedings of the 13th Int. Conf. on SSNTD, Rome, Sept. 23-27, Nucl. Tracks. Radiat. Meas. 12 (1986) ,5-988.

[10] Proceedings of the 14th Int. Conf. on SSNTD, Lahore, April, 2-6, Nucl. Tracks. Radiat. Meas. 15 (1988) ,11-802 .

[11] Proceedings of the 15th Int. Conf. on SSNTD, Marburg, Sept. 3-7, Nucl. Tracks. Radiat. Meas. 19 (1991) ,11-974.

[12] Proceedings of the 16th Int. Conf. on SSNTD, Beijing, Sept. 7-11, Nucl. Tracks. Radiat. Meas. 22 (1993) ,9-945.

[13] Proceedings of the 17th Int. Conf. on SSNTD, Dubna, August, 24-28, Nucl. Tracks. Radiat. Meas. 25 (1995) ,11-776.

[14] Dwivedi K.K. and Mukherji S. Bulk-etching and track-etching rates of some Solid Dielectric Track Detectors. Nucl. Instr. Meth. 159 (1979), 433-438.

[15] Dwivedi K.K. and Mukherji S. Heavy ion track lengths in Solid Dielectric Track Detectors. Nucl. Instr. Meth. 161 (1979), 317-326.

[16] Fleischer R. L., Price P.B., Walker R. M. and Leakley L.S.B. Fission track dating of Bed I, Olduvai Gorge. Science. 148 (1965), 72-74.

[17] Fleischer R. L; Price P. B; Symes E. M. and Miller D.S. Fission track ages and track annealing behaviour of some micas. Science. 143 (1964b) , 349-351.

[18] Krishnaswami S., Lal D., Prabu N. and Mac Dougall D. Charateristics of fission tracks in Zircon: Applications to Geochronology and cosmology. Earth Planet. Sci. Letters. 22 (1973), 51-59.

[19] Fleischer R. L., Price P. B., Walker R. M. and Maurette M. Origin of fossil charged particle tracks in meteorite. J. Geophys. Res. 72 (1967a), 331-353.

[20] Gamota G. Creation of quantized vortex rings in superfluid Helium. Phys. Rev. Letters. 31 (1973), 517-520.

[21] Fischer B.E. and Spohr R. Heavy ion Microlithography - a new tool to generate and investigate submicroscopic structures. Nucl. Instr. and Meth., 168 (1980), 241-246.

[22] Fleischer R. L., Alter H. W., Furman S. C., Price P. B. and Walker R. M. Technological applications of Science : the case of particle track etching. Science. 178 (1972), 255-263.

[23] Raggenkamp H. G., Kiesewetter H., Spohr R., Daur U. and Busch L. C. Production of single-pore membranes for the measurement of red blood cell deformability. Biomedizinische Technik. 26 (1981), 167-169.

[24] Chrenko R. M. Boron content and frofiles in large laboratory diamonds. Nature. 229 (1971), 165-167.

[25] Seal S. A sieve for the isolation of cancer cells and other large cells from the blood. Cancer. 17 (1964) , 637-643.

[26] Vater P., Beker H. J., Brandt R. and Freiesleben H. Multi-fragment decay relations induced by heavy ions and studied with mica track detectors. Nucl. Instr. Meth. 147 (1977), 271-278.

[27] Hagg R., Fiedler G., Ulbrich R., Breitbach G. and Gottschalk P. A. Fragment correlations in the reaction 9.03 MeV/u $^{238}U + ^{nat}U$. Z. Physik. A. 316 (1984) , 183-193.

[28] O'Sullivan D., Price P. B., Shirk E. K., Flower P. H., Kidd J. M., Kodetich E. J. and Thorne R. High resolution measurements of slowing cosmic rays from Fe to U. Phys. Rev. Letters. 26 (1971), 463-466.

[29] Beaujean R. and Enge W. Isotopenanalyse on neiderenargetischen teilchen der elemente bor, kohlenstoff, stickstoff und sauerstoff aus der kosmischein strahlung in plastik-detektoren. Z. Physik. 256 (1972), 416-440.

[30] Perelygin V. P., Shadieva N. H., Tretyakova S. P., Boos A. H. and Brandt R. Ternary fission produced in Au, Bi, Th and U with Ar Ions. Nucl. Phys. A. 127 (1969), 577-585.

[31] Medeczky L. and Somogyi G. Investigations on ternary photofission with track recorders of different sensitivity. Rad. Effects. 5 (1970), 51-59.

[32] Szabo J., Csikai J. and Varnagy M. Low-energy cross sections for $^{10}B(p,\alpha)^{7}Be$. Nucl. Phys. A. 195 (1972), 527-533.

[33] Zvara I., Belov V. Z., Chelnokov L. P., Domanov V. P., Hussonois M., Korotkin Yu. S., Schegolev V. A. and Shalayevsky M. R. Chemical separation of Khurchatovium. Inorg. Nucl. Chem. Letters. 7 (1971), 1109-1116.

[34] Gibson W. M. and Nielson K. O. Direct determination of the life time of excited compound nuclei by angular distribution measurements of fission fragments emitted from single crystals. Phys.Rev. Letters. 24 (1970), 114-117.

[35] Flerov G. N., Oganesyam Yu. Ts., Lobanov Yu. V., Kuznetsov V. I., Druin V. A., Perelygin V. P., Gavrilov K. A., Tretyakova S. P. and Plotko V. M. Synthesis and physical identification of the isotope of element 104 with mass number 260. Phys. Letters. 13 (1964), 73-75.

[36] Geisler F. H., Phillips P. R. and Walker R. M. Search for super heavy elements in natural and proton induced materials. Nature. 244 (1973), 428-429.

[37] Barwick S. W., Price P. B. and Stevenson J. D. Radioactive decay of ^{232}U by ^{24}Ne emission. Phys. Rev. C 31 (1985), 1984-1986.

[38] Price P. B., Stevenson J. D., Barwick S. W. and Bavan H. L. Phys. Rev. Letters. 54 (1985), 158-161.

[39] Dwivedi K. K., Raju J., Vater P. and Brandt R. Studies on the fission of heavy ions and particle evaporation using Nuclear Track Detectors. Nucl. Track Radiat. Meas. 22 (1993), 577-582.

[40] Northcliffe L. C. Energy loss and effective charge of heavy ions in Al. Phys. Rev. (1960), 120, 1744-1749.

[41] Bimbot R., Della Negra S., Gardes D., Gauvin H., Fleury A. and Hubert F. (1978) Stopping power measurements for 4-5 meV/nucleon ^{16}O, ^{40}Ar, ^{63}Cu and ^{84}Kr in C, Al, Ni, Ag and Au. Nucl. Instr. Meth. 153, 161-169.

[42] Bimbot R., Gardes D., Geissel H., Kitahara T., Armbruster P., Fleury A. and Hubert F. Stopping power measurements for 3-5 MeV/nucleon ^{86}Kr, ^{132}Xe, ^{206}Pb and ^{238}U in solids. Nucl. Instr. Meth. 174 (1980), 231-236.

[43] Saxena A. and Dwivedi K. K. Energy loss and mean ranges of ^{93}Nb in Nickel and Tantalum. J. Phys. D: Appl. Phys. 23 (1990), 476-480.

[44] Saxena A., Ghosh S. and Dwivedi K. K. Mean ranges of ^{132}Xe in Lead. Nucl. Sci. J. 32 (1995), 203-208.

[45] Dwivedi K. K., Srivastava A., Ghosh S., Sinha D., Saxena A. and Brandt R. Energy loss and mean ranges of ^{86}Kr and ^{197}Au in Tantulam. Radiat. Meas. 26 (1996), 561-563.

[46] Saxena A. and Dwivedi K. K. Mean ranges and energy-loss of ^{86}Kr in Aluminium and ^{238}U in Hostaphan Polymer by Nuclear Track Technique. Nucl. Tracks Radiat. Meas. 17 (1990) , 447-452.

[47] Dwivedi K. K., Kocsis Zs., Vater P. and Rrandt R. Mean Ranges of ^{209}Bi ions in ZnP-Glass Detector. Nucl. Track Radiat. Meas. 22 (1993), 47-49.

[48] Ghosh S., Saxena A. and Dwivedi K. K. Range and energy loss of 16.34 MeV/u ^{238}U in Kapton Polyimide. Rad. Effect. Defects in Solids. 112 (1990), 149-153.

[49] Srivastava A., Laldawngliana C., Sinha D., Ghosh S., Dwivedi K. K. and Brandt R. Measurement of range and energy-loss of energetic ^{58}Ni and ^{197}Au Ions in Kapton. Nucl. Sci. J. 33 (1996), 85-93.

[50] Ghosh S., Sinha D., Mawar A., Singh S., Srivastava A., Dwivedi K. K. and Brandt. R. Mean ranges of ^{161}Dy in Hostaphan and Kapton. Nucl. Tracks Radiat. Meas. 28 (1997) (in press)

[51] Dey M., Raju J., Ghosh S. and Dwivedi K.K. Development and characterization of polycarbonate microfilters. Nucl. Tracks Radiat. Meas. 22 (1993), 907-908.

[52] Heise S., Vater P., Brandt R. Dwivedi K.K. and Dankmeyer C. On the development of polypropylene (PP) microfilters. Nucl. Tracks Radiat. Meas. 22 (1993), 909-910.

[53] Frank A.L. and Benton E.V. Dielectric plastics as high-exposure gamma-ray detectors. Radiation Effects. 2 (1970), 269-272.

[54] Shweikani R., Durrani S.A. and Tsuruta T. Effects of gamma irradiation on the bulk and track etching properties of Cellulose Nitrate (Daicel 6000) and CR-39 Plastics. Nucl. Tracks Radiat. Meas. 22 (1993), 153-156.

[55] Portwood T. and Henshaw D. L. The Effect of gamma dose on the alpha response of CR-39. Nucl. Tracks. 12 (1986), 105-108.

[56] Abu-Jarad F., Hala A.M., Farhat M. and Islam M. Effect of high gamma dose on the CR-39 properties. Radiat. Meas., 28 (1997) , (in print)

[57] Akber R.A., Nadeem K., Majid C.A., Hussain A., Zaman N., Chaudhary M. A. and Khan H.A. Studies of structural changes produced by high doses of gamma rays in some plastic track detectors. Nucl. Instr. Meth. 173 (1980) , 217-221.

[58] Joseph A. and Varier K.M. Gamma ray dosimetric studies on CR-39 detector. Indian Journal of Pure & Applied Physics. 33 (1995), 406-409.

[59] Katz R. Track structure theoty in radiobiology and in radiation detection. Nucl. Track. Detection. 2 (1978) , 1-28.

[60] Hashemi-Nezhad S. R., Bull R. K. and Durrani S. A. Electron and alpha-particle damage in biotite mica : Implications of track formation mechanisms. 11th Int. Conf. Solid State Nuclear Track Detectors, Bristol. Nucl. Tracks. 3 (1981), 23-6.

[61] Chadderton L.T., Morgan D.V., Torrens I. McC., and Van Vliet D. On the electron microscopy of fission fragment damage. Phil. Mag. 13 (1966), 185-195.

[62] Chadderton L.T. and Torrens I. McC. Fission damage in crystals. Methuen, London, 1969.

[63] Tidjani A. and Watanabe. Study of the effect of ν-dose rate on the oxidation of polypropylene. J. Appl. Polymer Science, 60 (1996), 1839-1845.

[64] Mazzoldi P. and Arnold G. W. Ion beam modifications of Insulators. (eds) 2, Elsevier, Amsterdam (1987).

[65] Venkatesan T. High energy ion beam modification of polymer films. Nucl. Instr. and Meth. B 7/8 (1985), 461-467.

[66] Venkatesan T., Bworn W. L., Murray C. A. Marcantonio K. J. and Wilkens B. J. Polymer. Eng. Sci. 40 (1984), 681-684.

[67] Venkatesan T., Caleagno L., Elman B. S. and Foti C. Ion beam modifications of insulators. (eds) 2, P. Mazzoldi and G. W. Arnold (Elsevier, Amsterdamn) 301 (1987).

[68] Puglisi O., Liccialdello A., Calcagno L. and Foti G. Molecular weight distribution and solubility changes in ion bombarded polystyrene. Nucl. Instr and Meth. B 19/20 (1987), 865-871.

[69] Lovinger A.J., Forrest S. R., Kaplon M. L., Schmidt P. H. and Venkatasen T. Structural and morphological investigation of the developement of electrical conductivity in ion-irradiated thin films of an organic material. J. Appl. Phys. 55 (1984), 476-482.

[70] Marletta G. Chemical reactions and physical property modifications induced by keV ion beams in polymers. Nucl. Instr. and Meth. B 46 (1990), 295-305.

[71] Forrest S. R., Kaplon M. L., Schmidt P. H. Venkatesan T. and Lovinger A. Large conductivity changes in ion-beam-irradiated organic thin films J. appl. Phys. Letters. 41 (1982), 706-710.

[72] Wnek G. E., Dresselhaus M. S. and Wasserman B. Matter. Res. Soc. 27 (1984), 413.

[73] Marletta G., Pignataro S. and Oliveri C. Reflection electron energy loss (REELS) of conductive polymers obtained by keV/bombardment. Nucl. Instr. Meth. B 39 (1989), 773-777.

[74] Aleshin A. N., Gribanov A. V., Dobrodunov A. V., Suvoronov A. V. and Shlimak I. S. Sov. Phys. Solid State. 31 (1989), 6.

[75] Elman B. S., Thakur M. K., Sandman D. J. and Newkirk M. A. Ino implantation studies of polydiacetylene crystals. J. Appl. Phys. 57 (1985), 4996-4999.

[76] Davenas J., Xu X. L., Boiteaux G. and Sage D. Relation between structure and electron properties of ion irradiated polymers. Nucl. Instr. and Meth. B 39 (1989), 754-763.

[77] Fink D., Muller M., Chadderton L. T., Cannington P. H., Elliman R. G. and Mc Donald D. C. Optically absorbing layers on ion beam modified polymers : A study of their evolution and properties. Nucl Instr. and Meth. B 32 (1988), 125-130.

[78] Mladenov G. M. and Emmoth B. Poly (methyl methacrylate) sensitivity variation versus the electronic stopping power at ion lithography exposure. Appl. Phys. lett. (1960), 38, 1000-1004.

[79] Kulish J. R., Franke H., Singh A., Lessard R. A. and Knystautas E. J. Ion implantation, a method for fabricating light guides in polymers. J. Appl. Phys. 63 (1988), 2517-2521.

[80] Macchi F., Daudin B., Hillairet J., Lauzier J., N'Goma J.B., Cavaille J.Y. and Legrand J. F. Micromechanical properties of electron irradiated PVDF-TrFE copolymers. Nucl Instr. and Meth. B 46 (1990), 334-337.

[81] Lee E. H. Lewis M. B., Blan B. J. and Mansur L. K. Improved surface properties of polymer materials by multiple ion treatment. J. Mater. Res. 6 (1991), 610-628.

[82] Komaki Y., Ishikawa N., Morishita N. and Takumara S. Radicals in heavy ion irradiated polyvinylidine fluoride. Radiat. Meas. 26 (1996), 123-129.

[83] Koul S.L., Champbell I. D., Chadderton L. T., Langroo M., Fink D..and Biersack J. P. ESR and track-etch studies of irradiated polymers. Nucl Instr. and Meth. B 32 (1986), 383-388.

[84] Edmonds E.A. and Durrani S.A. Relationship between Thermoluminescence, Radiation-Induced Electron Spin Resonance and track etchability of Lexan Polycarbonate. Nucl. Tracks. 3 (1979), 3-11.

[85] Biersack J. P. and Kallweit R. Ion beam induced changes of the refractive index of PMMA. Nucl. Instr. and Meth. B 46 (1990) 309-312.

[86] Le Moel A., Duraud J. P., Lecomte C., Valin M. T., Henriot M., Le Gressus C., Darnez C., Balanzat E. and Demanet C. M. Modifications induced in Polyvinylidene Fluoride by energetic ions. Nucl. Instr. and Meth. B 32 (1988), 115-119.

[87] Sharma S. L., Pal T., Rao V. V. and Enge W. Effect of gamma irradiation on bulk-etch rate of CR-39. Nucl. Tracks Radiat. Meas. 18 (1991), 385-389.

[88] Komaki Y., Ishikawa N. and Sakurai T. Effects of gamma rays on etching of heavy ion tracks in Polyimide. Radiat. Meas. 24 (1995), 193-196.

[89] Singh S. and Singh B. The effect of gamma irradiations on etching characteristics of some Solid State Nuclear Track recorders. Nucl. Tracks Radiat. Meas. 15 (1988), 199-202.


CHAPTER-3

CHAPTER-3

TECHNIQUES OF CHARACTERIZATION OF IRRADIATED POLYMERS

It has already been discussed in Chapter 2 about chemical and physical changes which take place in irradiated polymers. Keeping these in mind, here we describe some techniques which have been used to characterize the irradiated and pristine polymers. The techniques used are as follows :-

(a) **Track technique**

(b) **IR spectroscopy**

(c) **UV - VIS spectroscopy**

(d) **ESR spectroscopy**

(e) **Thermogravimetric analysis**

3.1. TRACK TECHNIQUE:- Chemical modifications observed in irradiated polymeric materials have imparted the initial motivation for its use as a track detector. In polymeric track detectors, only those charged particles with linear energy transfer (LET) above a critical values can create distinct etchable tracks. Atomic radiations such as UV rays and X-rays, nuclear radiations such as gamma rays and nuclear particles like electrons are low LET radiations. They mostly effect the

bulk-etch rate of the detector depending upon the absorbed dose. For track detectors exposed to high LET charged particles followed or proceeded by low LET radiation exposure, both the track-etch rate and bulk-etch rate are found to vary in accordance with the absorbed dose of low LET radiation.

It is an already known phenomenon that, when a heavy charged particle passes through a di-electric medium, it creates tracks. So the basic requirement for track study is the heavy ion source as well as dielectric solids (track detectors). The details of heavy ion sources are given below.

3.1.1. Heavy ion sources

(a) Alpha particle sources :- Usually heavy nuclei (A>200) are energetically unstable towards the spontaneous emission of α-particles. The probability of α - decay is governed by the mechanism of 'barrier penetration' and the half-life of most of the useful sources vary from a few days to many thousands of years. Most alpha-particle energies range from 4 to 6 MeV/U. Also, there exists a very strong correlation between alpha-particle energy and the half-life of the present nucleus. Isotope (^{253}Es) with shortest half-life emits alpha-particles of highest energies (E = 6.5 MeV). Alpha particles lose their energy rapidly in materials therefore the sources must be prepared in very thin layers in order to obtain more energetic ions. High energy alpha-particles can be obtained from accelerators which are

described in section (C). In all our experiments, 252-Cf was used as the alpha particle source.

(b) Spontaneous Fission Sources :- Theoretically all heavy nuclei are unstable and undergo spontaneous fission forming lighter fragments. Spontaneous fission from transuranic nucleides is a very simple and useful way of obtaining heavy ions of about 1 MeV/u specific energy. The penetration depth of these fragments in solids is of the order of 10μm. The most widely used source is ^{252}Cf which undergoes spontaneous fission with a half-life of 2.65 years. The median light and median heavy fragments have masses 108.55 and 143.55 [1], kinetic energies 106.2 ± 0.7 MeV and 80.3 MeV [1] and the most probable charges obtained from Mukherji's prescription [2] are 42.55 and 55.45 respectively. The fragments have initial positive charge of +20, but as they interact with matter, additional electrons are picked up by the ions thus reducing their effective charges. Nuclear reactors are being routinely used to produce high flux (10^{10} cm^{-2}) of induced fission fragments by exposing ^{235}U foils at neutron outlet ports. The energy and mass distribution of the reactor generated fission fragments are nearly same as those obtained from radio-active sources. However better beam collimination could be achieved for induced fission fragments.

(c) Heavy ion accelerators :- Accelerators are the most versatile heavy ion sources which provide monoenergetic, monoisotopic and highly

parallel beams of practically all ions. An extremely wide range areal flux (10^0-10^{12} cm $^{-2}$) and ion energies (10^0-10^3 MeV/u)) is attainable depending on the type and size of accelerator. Accelerated heavy ion beams are quite useful for various nuclear experiments in elemental and complex media. In last two decades or so, particle accelerators have initiated research activities in the fields of heavy ion interactions with matter [3-4].

3.1.2. Methods and formulations associated with track study

3.1.2.1. Bulk-etch rate (V_G) :- The bulk-etch rate (V_G) is defined as the speed with which the undamaged material of the detector is dissolved away by the etchant solution under a given etching condition. There are three different methods of determining V_G.

(a) Track diameter method :- The initial damage formed in the detector is very small and is about 5-10 nm. When this is etched in a suitable etchant, the etch rate along the surface is normal while along the track it is too fast. Thus, for a detector irradiated perpendicular to the surface, the etching rate will be very fast along the track while it will be normal along the surface. Thus we can find out the rate of increase of track diameter with etching time. If D is the track diameter (μm) at a etching time t (h), the bulk etch rate (in μm/h) is given by

$$V_G = (D/2t)(\tan\theta + \sec\theta) \qquad (3.1)$$

where θ is the cone angle. For any cone angle less than 5°, the term ($\tan\theta + \sec\theta$) may be approximated as unity. Therefore, we can write,

$$V_G = D/2t \qquad (3.2)$$

(b) Thickness method :- This method is based on the rate of decrease of thickness of the material with etching, assuming same rate of etching for both the surfaces of the detector. If X_i be the initial thickness, and X_f the thickness after a certain interval of time t, then V_G is given by

$$V_G = (X_i - X_f) / 2t \qquad (3.3)$$

(c) Gravimetric Technique :- This method is based on the measurement of the weight lost by a sample foil of known area after it is etched by the ehchant solution of known concentration for a given period of time at a given temperature. If m grams is the loss in weight of the detector after an etching time t (in hours), then the bulk-etch rate(in μm/h) is given as

$$V_G = \Delta m/2s\rho t \ X\ 10^4 \qquad (3.4)$$

where ρ is the density of the detector foil in g/cm^3, and 's' is the surface area of the foil in cm^2.

3.1.2.2. Track-etch rate (V_T) :- The rate of increase of track length with respect to etching time is defined as track etch rate (V_T). Assuming that , over a small portion of the track, V_T remains almost constant, the track etch rate (V_T) may be determined by measuring the small increase in track length Δl (in μm) in short etching time Δt (in h) from the equation

$$V_T \approx \Delta l / \Delta t \quad (\mu m/h) \qquad (3.5)$$

3.1.3. Determination of the true track length from the observed track lengths :- The track length 'l' observed under the microscope is the projected length of the track inside the dielectric on its surface plane of the platform of the microscope. Since the fission fragments enter at a known angle ϕ , with respect to the surface plane of the dielectric, the observed length of the track L' , is given by

$$L' = l / \cos \phi \qquad (3.6)$$

Fig.3.1 shows the geometry of the track. The true track length L in plastic is different from L′ owing to two reasons : (a) bulk-etching and (b) over-etching corrections.

(a) Bulk-etching correction (ΔS) :- As has been mentioned earlier, the etchant attacks both the radiation affected as well as the unaffected areas. At a particular temperature and concentration of the etchant, the general or bulk-etch rate V_G is constant, while the track-etch rate, V_T, is always greater than V_G, but varies at different points on the track owing to the variation in the energy-deposition rate at these points. Since a finite etching time t is required for enlarging track diameter to the lower limit of visibility, the etchant has time to dissolve out some amount of the dielectric from the surface [5,6]. As shown in Fig.3.1, $V_G t_1$ is the thickness of the surface layer removed in time t_1 of etching, the length of the track which is consequently removed is equal to $V_G t_1/\sin\phi$. Assuming that at time 't_c' is the time just necessary to reveal upto the end of the track, the true track length is given by,

$$L = l/\cos\phi + V_G t_c / \sin\phi \qquad (3.7)$$

where 'l' is the observed projected track length on the surface plane. However, in order to determine the time for complete etching t_c, it is necessary to etch the sample for some more time, thus some correction has to be made for over etching.

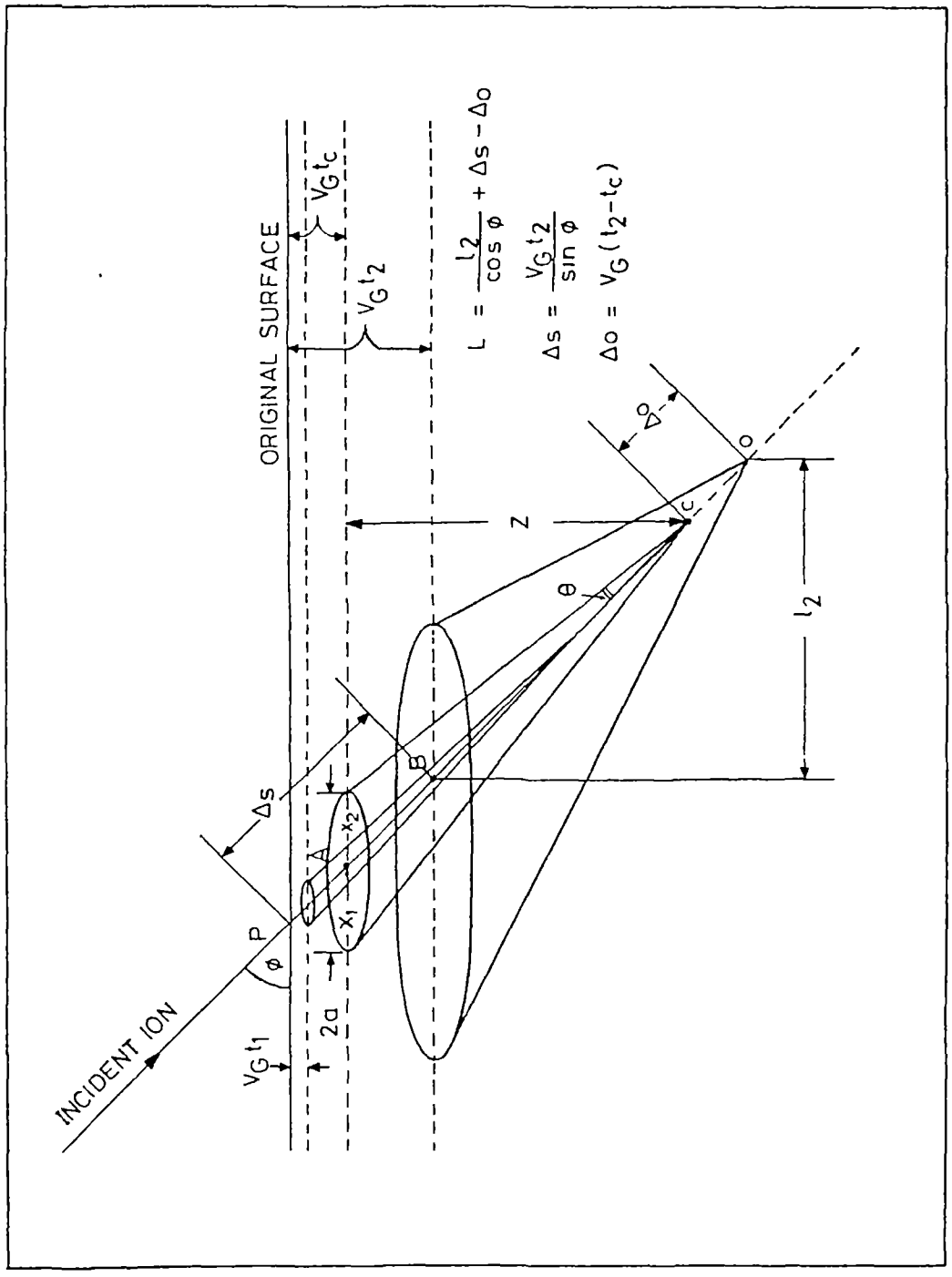

Fig. 3.1. Schematic representation of the geometry of track-etching in plastics

(b) Over-etching correction (Δ_0) :- If the total time of etching is t and the time for complete etching is t_c, then during the period $(t-t_c)$ the track would get extended inside the dielectric along the track direction by an amount $V_G(t-t_c)$. Thus, the projected track length (l) would be related to the true length (L) by [7] ,

$$L = l/\cos\phi + V_G t/\sin\phi - V_G (t-t_c) \qquad (3.8)$$

From the above equation it is clear that for the determination of the true track length, it is necessary to determine experimentally l, V_G and t_c. If $t > t_c$ then, since L is constant, a plot of L versus time would give t_c.

3.1.4. Determination of Activation energy (E_a) : A few scientists have tried to correlate the variation of bulk-etch rate with temperature in analogy with the variation of the rate of a chemical reaction with temperature. If V_G is the bulk-etch rate at a temperature T(K) for a particular solid state nuclear track detector (SSNTD) then the dependence of V_G on T is given as

$$V_G = A\, e^{-Ea/kT} \qquad (3.9)$$

where A = a constant.

E_a = Activation energy for bulk-etching

k = Boltzman's constant

T = Temperature in absolute unit

Thus, $$\text{Log } V_G = -E_a / 2.303\,kT + \log A \qquad (3.10)$$

A plot of Log V_G versus 1/T usually gives a straight line and from its slope one can determine the activation energy (E_a). If 'm' is the numerical value of the slope of such a plot, then we can get activation energy in unit of KJ mol^{-1} from the relation which is given below,

$$E_a = 19.165\ m \qquad (3.11)$$

3.2. INFRARED STUDY :- Irradiation of polymers results in chemical changes which lead to an alteration of their properties. From the IR peak assignment, clues for radiochemical destruction processes are derived [8]. For these results it is favourable to use polymers having functional groups which exhibit strong absorption lines such as C=C, C=O, or aromatic groups.

There exists some thumb rules in polymer radiation chemistry. For example, molecules with long side chains or heavily branched ones are known to be especially radiation sensitive. On the other hand, the back-bone structure frequently preserved. Further, aromatic groups are known to reduce the polymer irradiation sensitivity, due to the delocalization of the excited energy. IR spectroscopy is one of the most powerful analytical techniques which offers the possibility of chemical

identification. The technique is based upon the simple fact that a chemical substance shows marked selective absorption in the infra-red region. After absorption of IR-radiation, the molecules start vibrating in different modes giving rise to absorption bands, so called IR-absorption spectrum.

It is obvious that a complex molecule is likely to have an infra-red spectrum exhibiting a large number of normal vibrations. Each normal mode involves some displacement of all, or nearly all, the atoms in the molecule, but while in some of the modes all atom may undergo approximately the same displacement, in others the displacements of a small group of atoms in the molecule may be much more vigorous. Thus we may divide the normal modes into two classes : the skeletal vibrations, which involves all the atoms to almost the same extent, and the characteristic group vibrations, which involve only small portions of the molecule, the remainder being more or less stationary. Skeletal frequencies usually fall in the range of 1400 - 700 cm^{-1} and arise from linear or branched chain structure of the molecule. It is seldom possible to assign particular bands to specific vibrational modes, but the whole complex of bands observed is highly typical of the molecular structure under examination. Further , changing a substituent (on the chain, or on the ring) usually results in a marked change in the pattern of the absorption bands. Thus, these bands are referred to as the "fingerprint" bands, because a molecule or functional group structure moiety may often be recognised merely

from the appearance of this part of the spectrum. Group frequencies on the other hand, are usually almost independent of the structure of the molecule as a whole and, with a few exceptions ,fall in ranges above and well below that of the skeletal modes. We should at this point consider very briefly the intensities of infra-red bands. It is a known phenomenon that infra-red spectrum appears only if the vibration produces a change in the permanent electric dipole of a molecule. It is reasonable to suppose, then, that the more polar a bond, the more intense will be the infrared spectrum arising from vibrations of that bond.

3.3. UV-VIS SPECTROSCOPY :- Although rotational, and sometimes vibrational, fine structure do not appear in the liquid or solid state, but the position and intensity of the rather broad absorption band is due to an electronic transition which is characteristic of the molecular group involved. In this branch of spectroscopy the position of an absorption is almost invariably given as the wavelength at the point of maxium absorption, λ_{max}, quoted either in Angstrom unit ($1A^{\circ}=10^{-10}m$) or in nanometers ($1nm= 10^{-9}m$), the later being more commonly used. It should be noted that a large energy change, corresponding to a high frequency or wave-number, is represented by a small wavelength. For practical reasons the electronic spectrum is divided into three regions : (1) the visible region, between 4000 A° and 7500 A° (400 - 750 nm or 25000 - 13300 cm^{-1}), (2) the near ultra-violet region, between 2000 A° and 4000 A° (200 - 400 nm, or 50000 - 25000

cm^{-1}), and (3) the far ultra-violet region, below 2000 A° (below 200 nm or above 50000 cm^{-1}).

Electrons in a vast majority of molecules fall into one of the three classes : π-electrons, σ-electrons, and non-bonding electrons (called n-electrons). In chemical terms a single bonds between atoms, such as C-C, C-H, O-H, etc. contains only sigma electrons, a multiple bond, C=C, C=C, C=N etc., contains π-electrons in addition to σ-electrons, while atoms to the right of carbon in the periodic table, notably nitrogen, oxygen, and halogens, possess n-electrons. In general sigma electrons are most firmly bound to the nuclei and hence require a great deal of energy to undergo transitions, while the π and n-electrons require less energy, the n-electrons usually (but not invariably) requiring less than the π electrons.

In any material, exposure to γ-radiation causes alteration of the physical and chemical properties. The changes are strongly dependent on the internal structure of the absorbing substances and the intensity of gamma radiation. It may be expected that the interaction of gamma-rays with solids can cause electronic ionisation (or excitation) of the orbital electrons and possibly atomic displacements. The photoconduction electrons produced will go back and forth and become freely or loosely bound to trapping centres somewhere in the material structure. These new electronic configurations, in addition to the possible displacement of atoms would cause a change in the molecular structure

and possibly a change in the number and nature of double bonds. These structural changes would cause a change in the optical properties of the absorbed substances [9,10].

3.4. ESR SPECTROSCOPY :- Many researchers have studied the radiation damage of polymeric materials subjected to γ-rays or electrons through the use of [11] electron spin resonance spectroscopy for polyethylene(PE) [12], polypropylene (PP), polyvinyl chloride (PVC) [13], and polyvinylidene fluoride (PVDF) [14]. Edmonds and Durrani [15] examined the relation between ESR and tracks in polycarbonate (Lexan). Le Moel et al. [16,17] studied radicals in PVDF irradiated with 800 MeV oxygen ions. Koul et al. [18,19] examined the relation between ESR and the gamma-ray irradiated CR-39 and track etching properties of Polyimide (Kapton) irradiated with He, Al, and Xe ions. Chipara et al.,[20] Barb et al., [21] and Komaki et al. [22] investigated the high energy ion induced defects in polymers using ESR technique. ESR basically depends on the nature of unpaired electrons or radicals. These radicals may be formed by interactions of radiations with polymers. If the life time of such radicals is greater than about 10^{-6}s, they may be studied by ESR methods. Shorter lived species may also be studied if they are produced at low temperature in the solid state.

3.5. THERMOGRAVIMETRIC STUDY :- Usually the most important property of organic polymers is their thermal stability, because their

physical and physico-chemical properties can be easily altered by heat treatments. Measurement of weight loss as a function of temperature is called thermogravimetry or thermogravimetric analysis (TGA). Weight losses that takes place during polymer decomposition, follows a definite pattern and this is also useful in characterising polymer structure, particularly where decomposition occurs.

There are basically two types of TGA - isothermal and nonisothermal. In the former, weight loss is recorded as a function of time at a constant temperature. In the nonisothermal TGA, sample temperature is increased at constant rate and weight loss is recorded as a function of upheat temperature. This provides more useful information, since it directly indicates the upper limits of thermal stability.

It has been observed by Fakuda [23] that physical strength of natural mica increases because of gamma exposure. He also proposed that a correlation exists between radiation exposure and point defects. The gamma-ray irradiation is known to induce point defects and defect clusters [24]. The specific defects and defect clusters might be responsible for hardening of ionic crystals.

REFERENCES

[1] Schmit H. W., Neiler J. H. and Walter F. J. Fragment energy correlation measures for ^{252}Cf spontaneous fission and ^{235}U thermal-neutron fission. Phys. Rev. (1966), 14, 146-152.

[2] Mukherji S. Nuclear charge distribution in fission. Nucl. Phys. A, (1969), 129, 297.

[3] Geissel H., Laichter Y., Schneider W.F.W. and Armbruster P. Energyloss and energy loss straggling of fast heavy ions in matter. Nucl.Instr. Meth. 194 (1982), 21-29.

[4] Dwivedi K.K., Srivastava A., Ghosh S., Sinha D., Saxena A. and Brandt R. Energy loss and mean ranges of ^{86}Kr and ^{197}Au in Tantalum. Radiat. Meas. 26 (1996), 561-563.

[5] Price P. B., Fleischer R. L., Peterson D. D., O'Ceallaigh C., O'Sullivan D. and Thomson A. High resolution study of low energy cosmic rays with lexan track detectors. Phys. Rev. 21 (1968), 630-633.

[6] Blok H., Kiely F. M. and Pate B. D. Track lengths of heavy ions in mica. Nucl. Instr. and Meth. (1972), 100, 403-407.

[7] Dwivedi K.K. and Mukherji S. Heavy ion track lengths in Solid Dielectric Track Detectors. Nucl. Instr. Meth. 161 (1979), 317-326.

[8] Fink D., Hosoi F., Omichi H., Sasuga T. and Amaral L. Infrared transmission of Ion irradiated polymers. Radiation Effects and Defects in Solids. 132 (1994), 313-328.

[9] Higazy A. A. and Hussein A. Optical absorption studies of gamma-irradiated magnesium phosphate glasses. Radiation Effects and Defects in Solids. 133 (1995), 225-235.

[10] Joseph A. and Varier K. M. Gamma ray dosimetric studies on CR-39 detectors. Indian Journal of Pure and Applied Physics. 33 (1995), 406.

[11] Ranby B. and Babeck J. F. ESR spectroscopy in polymer research. (1977) Springer, Berlin.

[12] Ohnishi S., Sugimoto S. and Nitta I. Temperture dependence of the ESR spectrum of irradiated oriented polyethylene. J. Chem. Phys. 37 (1962), 1283-1288.

[13] Ohnishi S., Sugimoto S. and Nitta I. Electron spin resonance study of radiation oxidation of polymers. Polypropylene and Poly (Vinyl Chloride). J. Poly. Sci. A 1 (1963) , 625-637.

[14] Seguchi T., Makuuchi K., Suwa T., Tamura N., Abe T. and Takehisa M. Electron spin resonance studies on irradiated poly-(vinylidene fluoride). Nippon Kagaku Kaishi (1974). 1309-1314.

[15] Edmonds E. A. and Durrani S. A. Relationship between thermoluminescence, radiation induced electron spin resonance and track etchability of Lexan Polycarbonate. Nucl. Tracks. 3 (1979), 3-11.

[16] Le Moel A., Duraud J. P., Lemaire I., Balanzat E., Ramillon J. M. and Dasmez C. Electronic and structural modification of polyvinylidene fluoride under high energy Oxygen ion irradiation. Nucl. Instrum. Meth. B 17 (1987), 891-894.

[17] Le Moel A., Duraud L. P., Lecomte C., Valin M. T., Henroit M., Le Gressus C., Darnez C., Balnzat E. and Demanet C. M. Modifications induced in polyvinyllidene fluoride by energetic ions. Nucl. Instrum. Meth. B 32 (1988), 115-119.

[18] Koul S. L., Campbell I. D., Mc Donald D. C., Chadderton L. T., Fink D., Biersack J. P. and Muller M. Energy transfer mechanisms

and the radiation chemistry of noble gas irradiated polymers. Nucl.Instrum. Meth. B 32 (1988 a), 186-193.

[19] Koul S. L., Campbell I. P. Chadderton L T., Langroo M., Fink D. and Biersack J. P. ESR and track-etch studies of irradiated polymers. Nucl. Instrum. Meth. B 32 (1988 b), 186-193.

[20] Chipara M. I., Bunget I., Georgescu R., Georgescu E. and Vilcov I. ESR studies on PET irradiated with high energy ions.. Nucl. Instrum. Meth. B 209/210 (1983), 395-400.

[21] Borb D., Chipara M. I., Velter S., Apel P. Yu. and Rogalski M. ESR studies on Melinex irradiated with oxygen ions. Nucl. Tracks Radiat. Meas. 16 (1989)

[22] Komaki Y., Ishikawa N., Morishita N. and Takamura S. Radicals in heavy ion-irradiated polyvinylidene fluoride. Radiat. Meas. 26, 1 (1996), 123-129.

[23] Fakuda K. Effects of High gamma-ray and electron doses on the annealing behaviour of Natural Mica. Radiation Effects. 45 (1979) 123-124.

[24] Varley J. H. O. A mechanism for the displacement of ions in an ionic lattice. Nature. 174 (1954), 886-887.

CHAPTER-4

CHAPTER-4

EXPERIMENTAL TECHNIQUES

4.1. PREPARATION OF DETECTORS : In the present investigation seven different of track detectors have been used, viz. **PADC (Homalite)**, **PADC (American Acrylics)**, **Makrofol-E**, **Lexan**, **Polycarbonate**, **Triafol-TN** and **Triafol-BN**. Some of the important properties and chemical structures of these detector have been listed in Tables 4.1, 4.2 and 4.3. These detectors are classified into three different broad categories namely (a) polyallyldiethyleneglycol dicarbonate [PADC(Homalite) and PADC (American-Acrylics)], (b) bisphenol-A polycarbonate (Lexan, Makrofol-E, polycarbonate) and (c) Cellulose derivatives (Triafol-TN and Triafol-BN). Brief description about these detector materials are given below.

(a) <u>The PADC Detectors</u> :- PADC is a highly cross-linked thermoset polymer prepared by the polymerisation of a liquid monomer diethyleneglycol bis (allyl carbonate) [1].

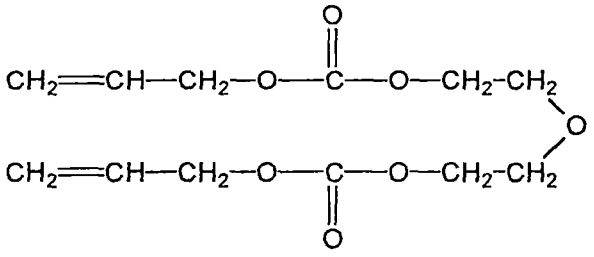

Polymerisation of PADC represents a transformation from the unsaturated monomers to the saturated polymer. However, in the process of the formation of a three-dimensional network, various closed zones are formed and these may contain unused monomer molecules which characterise the residual unsaturation left in the polymer sample. Isolation and random trapping of the unused monomers leads to structural inhomogeneities which are responsible for the non-uniformity and non-reproducibility of etching response observed in a large number of PADC samples. To eliminate the above problems, curing, a process to ensure a uniform polymerisation, is needed. Because of the exothermic nature of the polymerisation of PADC [2] specifically controlled temperature time cycles which are derived assuming a constant rate of polymerisation [3], are employed during polymerisation. Despite the utmost care during manufacturing, there is always the possibility of little unsaturation. The network structure of PADC polymer is,

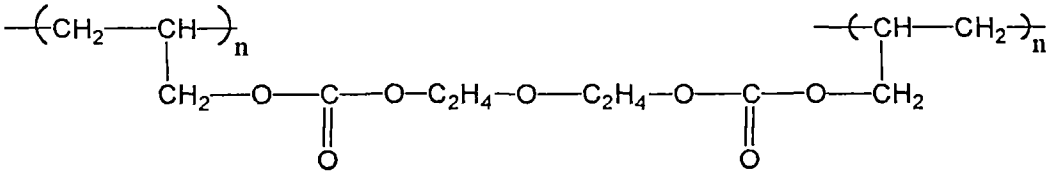

(b) <u>Polycarbonate</u> :- Polycarbonates [4-6] are polyesters of carbonic acid. Although carbonic acid itself is not a stable

compound, its derivative (Phosgene, urea, carbonates) are commercially available. The reaction of phosgene with bisphenol A was developed into commercial production by Farbenfabriken Bayer in Germany. The product is known by the trade names of Lexan and Merlon.

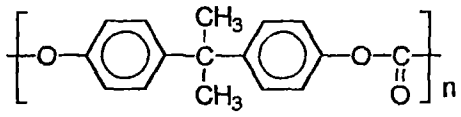

Bisphenol A polycarbonate

While any dihydroxy compound, in principle, form a polycarbonate with phosgene, only bisphenol-A has gained commercial importance. This is due to a combination of low monomer cost and usually good polymer properties.

(c) Cellulose derivatives :- Cellulose esters are much more important at the present time. Cellulose acetate of varying degree of substitution is prepared by first treating with acetic acid, then with acetic anhydride and a mineral acid catalyst. The fully acetylated product is subsequently reacted with water to achieve the desired degree of substitution. Mild hydrolysis gives an almost completely acetylated cellulose known as triacetate (Triafol-TN).

Cellulose acetate-butyrate mixture, is the other commercially important ester. The mixed ester is generally more soluble and have

better impact resistance than cellulose acetate. This is made by the esterification of cellulose with the mixture of acetic anhydride and butyric anhydride. Polymer contains 26%-29% acetyl group and 17%-48% butyl group.

Two sets of seven samples of each polymer were cut from the commercially available sheets. Several pieces of size 2 X 2 cm^2 for one set and 3X3 cm^2 for other set were made. They were then washed thoroughly with soap solution and then with deionised water. The clean samples were dried inside vacuum desiccator and then kept in covered plastic boxes.

4.2. IRRADIATION OF DETECTORS :- In the present experiment, a ^{252}Cf source having half-life of 2.65 years and activities 5.7 $X10^3$ fission/minute and 1.84 X 10^5 alpha particles/minute was used as a source of fission fragments and alpha particles. Two kinds of gamma exposure were made. One is known as pre-gamma exposure and other one is known as post-gamma exposure. In the case of pre-gamma exposure, the detectors were first exposed to gamma source followed by fission fragments and alpha source (^{252}Cf). But for post-gamma exposure, the detectors were first exposed to fission fragments and alpha source followed by gamma exposure. Seven samples of first set of each material were exposed at normal incidence to the fission fragments from a ^{252}Cf source for about 7-10 mins and then together with the unexposed second set were subjected to various doses of

TABLE - 4.1

Properties of PADC(Homalite) and PADC(American Acrylics)

Properties	PADC(Homalite)	PADC(American Acrylics)
1. Composition	$C_{12}H_{18}O_7$	$C_{12}H_{18}O_7$
2. Density (g/ml)	1.32	1.32
3. Thickness(μm)	1500	650
4. Uniformity	Good	Good
5. Clarity	Good	Good
6. Surface view	Optical Grade	Optical Grade
7. Chemical etchant	6N NaOH	6N NaOH
8. Colour	Colourless	Colourless
9. Molecular weight	274	274
10. Manufactures	Homalite Corporation	American Acrylics Corporation
11. Chemical name	Allyldiglycol carbonate	Allyldiglycol carbonate

TABLE-4.2

Properties of Lexan, Makrofol-E and Polycarbonate

Properties	Lexan	Makrofol-E	Polycarbonate
1. Composition	$C_6H_{14}O_3$	$C_6H_{14}O_3$	$C_6H_{14}O_3$
2. Density(g/ml)	1.20	1.14	1.20
3. Thickness(μm)	500	300	300
4. Uniformity	Good	Good	Good
5. Clarity	Good	Poor	Good
6. Surface view	Optical Grade	Optical Grade	Optical Grade
7.Chemical etchant	6N NaOH	6N NaOH	6N NaOH
8.Colour	Colourless	Colourless	Colourless
9. Molecular weight	254.0	254.0	254.0
10. Manufactures	GEC, USA	Bayer AG.FRG	Bayer AG. FRG
11. Chemical name	Polycarbonate	Polycarbonate	Polycarbonate

TABLE - 4.3

Properties of Triafol-TN and Triafol-BN

Properties	Triafol-TN	Triafol-BN
1. Composition	$C_{12}H_{16}O_8$	$C_{20}H_{32}O_5$
2. Density(g/ml)	1.30	1.20
3. Thickness(μm)	100.0	200.0
4. Uniformity	Good	Good
5. Clarity	Fair	Fair
6. Surface view	One side smooth	One side smooth
7. Chemical etchant	3N NaOH	6N NaOH
8. Colour	Blue	Violet
9. Molecular weight	288	385
10. Manufactures	Bayer AG, FRG	Bayer AG, FRG
11. Chemical name	Cellulose Triacetate	Cellulose acetate butyrate

gamma rays. The gamma exposures were done from a ^{60}Co gamma source, having a dose rate of 3.0 kGy/h. The gamma exposures were done at room temperature in the dose range of $10^1 - 10^6$ Gy. There was about 8% error associated with 10 Gy of gamma dose where as higher doses are accurate within 1%. The second sets were subsequently cut into small pieces (0.5 X 0.5 cm^2) and exposed to fission fragments and alpha particles at normal incidence for track study. Two samples of pre-gamma exposed set (10^3 Gy and 10^6 Gy) of Polycarbonate, Lexan, Makrofol-E, along with a pristine sample were then cut into small pieces (0.5 X 0.5 cm^2) and then exposed to fission fragments at an angle of 45° in vacuum for 30 minutes.

The experimental arrangement for 45° angle irradiation is shown in Fig.4.1. For 90° irradiation, the samples were nicely fixed to the one side of the collimator and were placed the other side of the collimator at a distance of 1 cm away from the Cf-source. Then the exposures were done for around seven to ten minutes. The irradiations were done inside a desiccator in air. For irradiation at 45°, triangular perspex block having angles of 45° between the base and the hypotenuse were used. Detectors were fixed on the largest face on the triangular perspex block. The mounted perspex block was attached to the collimator platform. A circular ^{252}Cf source on stain less steel backing was placed at distance of 1 cm from one face of the collimator while the SSNTD placed on the perspex block was infront of the other side. The source, collimator

and SSNTD were properly aligned. The whole set-up was then placed inside a desiccator and the irradiation were done in vacuum. The irradiation was continued for 30 minutes. After irradiation's each of the irradiated samples was taken out and preserved in plastic boxes.

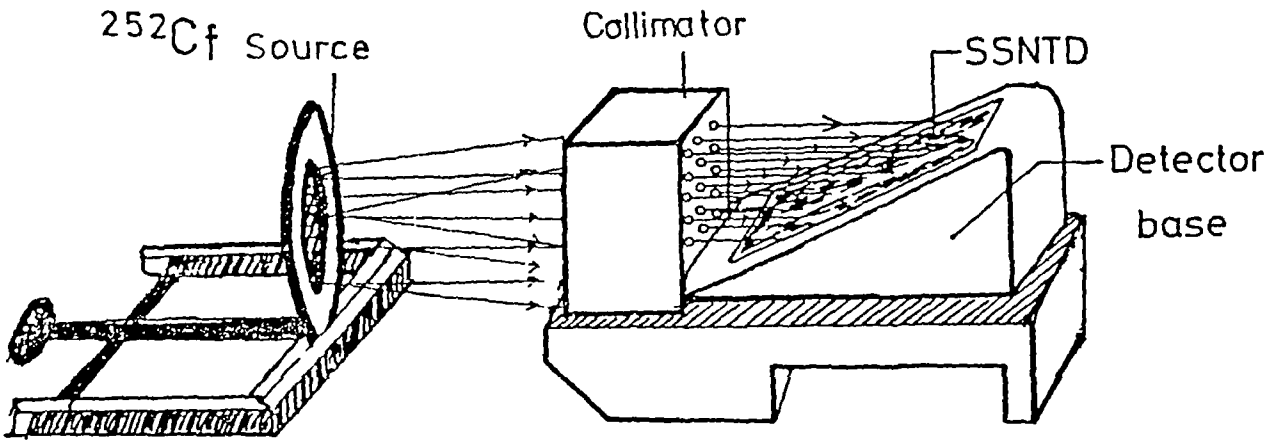

Fig. 4.1. Diagram of the irradiated assembly showing the positions of the source, collimator and detector foil

4.3. CHEMICAL ETCHING FOR TRACK DEVELOPMENT :- The chemical etching of these detectors was done for one set at a time. Before etching, the detectors were washed with soap solution to remove all the greasy substances and the contamination from the surface and dried between the layers of soft filter paper and later dried in a vacuum desiccator. The detectors (except Triafol-TN) were then etched with 6N NaOH solution at four different temperatures

(viz. 55°, 60°, 65°, 70°C). For Triafol-TN detector, 3N NaOH solution was used as the etchant. One pristine sample was also etched each time for comparative study. Etching was carried out for different time periods ranging from 1.5 h to 10 h depending on the material. The accuracy in the maintenance of temperature was ± 1°C. Since the bulk-etch rates of PADC (Homalite), PADC (American Acrylics) and Triafol-BN were very high at 10^6Gy, they were etched for shorter duration (5 - 40 minutes). After every etching the detectors were washed in running water followed by 2-3 washing in distilled water. For the detectors Lexan, Makrofol-E and Polycarbonate, the track-length measurements were done for pre-gamma exposed set at 60°C etching temperature. Maximum etchable track lengths were obtained by etching the detectors in successive manner and the etching was terminated when round track tips were formed. Track length measurements were done for pristine and at two different doses (10^3Gy and 10^6Gy).

4.4. MEASUREMENT OF TRACK PARAMETERS :- Etched track lengths and diameters in each of the detectors were measured with the help of a "Leitz" optical microscope fitted with a special objectives of 40X and 100X (water immersion). After every etching, washing and drying, the samples were mounted on a special holder and viewed under microscope. About 20-25 tracks were measured for each detector to find out the most probable track diameters and it was found to increase linearly with etching time. The error involved in the

measurement of track diameter was ±0.43 μm. In all measurements we have considered the systematic errors only (i.e. ±0.43 μm). Similarly measurements were carried out for each identified track after every etching. The samples were exposed to fission fragments and alpha particles from a ^{252}Cf source. Alpha tracks and fission fragment tracks were distinguished from the size of the tracks. Fission fragments tracks are larger in diameter as compared to alpha tracks. Alpha-tracks could not be measured for Makrofol-E, Lexan, polycarbonate, Triafol-TN , Triafol-BN detectors as alpha particles do not create etchable tracks in these solids.

4.5. DETERMINATION OF BULK-ETCH RATE AND TRACK-ETCH RATE :- Bulk-etch rates were determined by track diameter method. The rate of increase of track diameter with etching time was determined by plotting etching time versus track diameter. Bulk-etch rate (V_G) was then derived from the slope of the curve. The track-etch rate (V_T) was obtained by measuring both fission fragment track diameters and the alpha track diameters and using the standard relation given by Durrani (7].

$$V_T = V_G \left[(1+x^2)/(1-x^2)\right] \qquad (4.1)$$

Where V_G is the bulk-etching rate (μm/h), $x = D_f/D_\alpha$, is the ratio of the diameter D_α (μm) of the alpha particles track to D_f (μm) diameter of the fission fragments track.

4.6. DETERMINATION OF ACTIVATION ENERGY :- Activation energy for bulk etching of these detectors was determined by plotting Log (V_G) against the reciprocal of etching temperature in absolute units. Activation energy for all the detectors exposed to different doses of gamma radiation were determined.

4.7. IR SPECTRA :- For IR study, irradiated samples along with the pristine were cut into small pieces of 1.0X1.0 cm^2 . The spectra were then recorded by a Nicolet (Impact 410) Fourier-transforming instrument (FTIR) keeping air as the reference. The samples were put vertically on a sample holder having a hole size 9 mm diameter and the spectra were taken in the range between 4000-500 cm^{-1} . All the samples were taken in the solid state. But in the case of both PADC (Homalite) and PADC (American Acrylics), because of the high thickness of these detectors, spectra could not be taken in the solid state. Here all the absorption peaks went beyond the base line. So in case of these two detectors, the samples were ground properly with KBr and made a thin film and the spectra were taken by the conventional PERKIN ELMER IR spectrometer.

The IR measurements took place typically a few months after the gamma irradiation, so that the results reported here reflects the stationary state of the irradiated foils.

4.8. UV - VIS SPECTRA :- UV - VIS spectra of the pristine and irradiated samples were taken for these materials by Beckman DU-650

spectrophotometer. For such measurements the samples were cut into small pieces of 0.5X1.5 cm^2. For each set of detectors there were seven samples including the Pristine one. The samples were then put vertically inside a quartz-shell and the absorption spectra were recorded in the range 200-800 nm keeping air as the reference. The scan speed was 1200 nm/min.

For a better understanding of dose dependent variation of transmission(%) in these detectors in the UV - VIS region, some particular wavelengths were chosen. It was then at these particular wavelengths, transmittance (%) were recorded for all doses of gamma radiation. This may be useful for gamma dosimetric studies.

4.9. ESR SPECTRA :- First derivative ESR measurements were done using a Varion (E-109, X-band) spectrometer with 100 kHz field modulation. For these studies samples of sizes 0.5 x 0.5 cm^2 each were put inside a quartz tube (one at a time) and the spectra were recorded at room temperature. A 9.6 GHz microwave frequency was used for this instrument. The instrumental set up for ESR studies are as follows - field set : 3380 $\pm$ 800 Hz, time constant : 0.250 s, scan time : 8 min, amplitude : 0.5 Gauss, receiver gain : 1.25 X 10^5 , microwave power : 5 mW.

The ESR measurements were done after few months of gamma irradiation. So the results reported here reflects the stationary state of

the detectors. The radicals formed might go so many transformations and ultimately comes to a stable state. So our results gives the information about the stable state of the transformation.

4.10. THERMOGRAVIMETRIC STUDY :- TGA study were performed by using PERKIN-ELMER instrument. Here the detectors were cut into small pieces(0.25 X 0.25 cm^2) and were kept on a thermobalance. The samples were then heated upto the required temperature at a constant heating rate. This heating rate was 20°C/min for all the detectors. The detectors were heated upto a very high temperature, so that in the process of heating, they lost most of its weight. Heating temperature varied from one detector to other detector. For example, PADC (both Homalite and American Acrylics) were heated upto a temperature of 560°C-580°C. For Polycarbonates it goes to 680°C - 710°C. Triafol-TN and Triafol-BN were heated upto the range of 600°C - 650°C. This heating results in TG-curve, in which the weight loss is recorded as a function of temperature.

REFERENCES

[1] Stejny J. The polymer physics on CR-39 - the state of understanding. Radiat. Prot. Dosim. 20 (1987), 31-36.

[2] Turner T.W., Clapham V.M., Fews A.P. and Henshaw D.L. On the quantitative analysis and effects of internal temperature fluctuations during cure of the polycarbonate CR-39. Proc. 11th Int. Conf. SSNTD'S (1981), 141-144, Bristol, Pergamon Press, Oxford.

[3] Somogyi G. Status of development in the field of CR-39 track detectors. Proc. 11th Conf. SSNTD'S (1981), 101-113, Bristol, Pregamon Press, Oxford.

[4] Christopher W.F. and Fox D.W. "Polycarbonates", Reinhold, New York, 1962.

[5] Schrell H. "Chemistry and Physics of Polycarbonates" Wiley-Interscience, New York, 1964.

[6] Vernaleken H. in "Interfacial Synthesis" (F. Millic) and C.E. Carreher, Jr.,Eds.), Marcel Dekker, New York, 1975.

[7] Shweikani R., Durrani S.A. and Tsuruta T. Effects of Gamma Irradiation on the bulk and track etching properties of Cellulose Nitrate (Daicel 6000) and CR-39 plastics. Nucl. Tracks Radiat.Meas. 22 (1993), 153-156.


CHAPTER-5

CHAPTER-5

RESULTS AND DISCUSSION

This chapter is divided in three parts. Part-1 discusses the details about the modifications in different types of polyallyl diglycol carbonate (PADC). Part-2 Consists of the results and discussion on three types of bisphenol-A carbonates viz. Makrofol-E, Lexan and Polycarbonate. Part-3 deals with the work on Triafol-TN and Triafol-BN polymers.

PART-1

5.1.1 PHYSICALLY OBSERVABLE CHANGES :- In the case of PADC (Homalite), upto a dose of 10^5 Gy, there was no change in the colour of the detector. At 10^6 Gy, it became light yellow. But for PADC (American Acrylics), the detector remained colourless upto a dose of 10^4 Gy,. At 10^5 Gy, it became light yellow and at further higher dose that is at 10^6 Gy, the detector turned into red colour. This change in the colour is attributed to the formation of radicals.

5.1.2 TRACK STUDIES :- The effect of gamma rays on bulk and track-etch rates of PADC (Homalite) are shown in Figs. 5.1.1 & 5.1.2. By examining these graphs, it is clear that bulk-etch rate (V_G) and track-etch rate (V_T) remains almost invariant upto gamma dose of 10^4 Gy. Then they start increasing slowly till 10^5 Gy. Between 10^5 Gy and

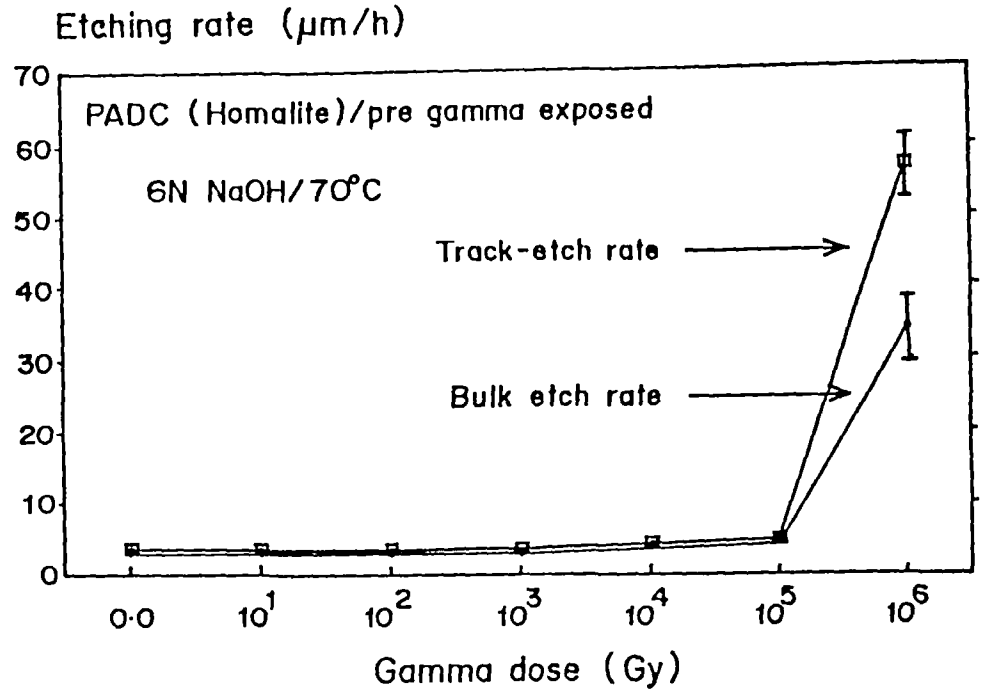

Fig. 5.1.1. Bulk - and Track-etch rate of pre-gamma irradiated PADC (Homalite).

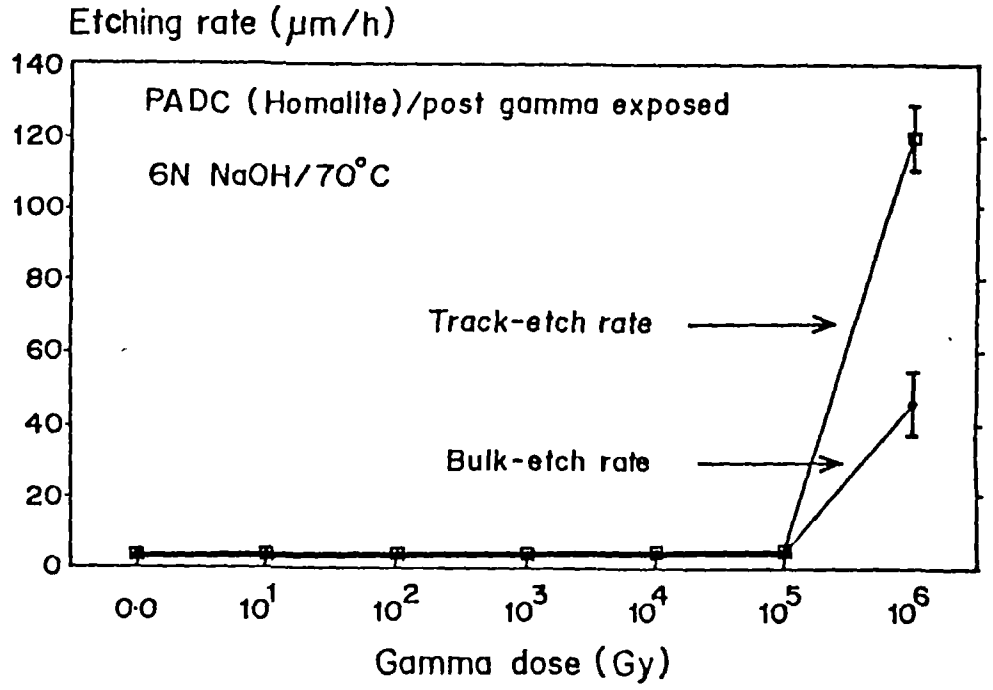

Fig. 5.1.2. Bulk - and Track-etch rate of post-gamma irradiated PADC (Homalite).

10^6 Gy, there is a certain increase in V_G and V_T. This sudden increase is observed both in pre- and post-gamma exposure sets. Tables 5.1.1 to 5.1.4 list the values of etch rates for different doses of gamma rays and at different etching temperatures for PADC (Homalite). It is interesting to observe that both the bulk and track-etch rates are higher in the case of post gamma exposure. These results are showing the similar trends as observed by some earlier workers [1-7].

A possible explanation for the increase in etch-rates can be attributed to the decrease in the average molecular weight [8] by scissions of the molecular chains caused by gamma rays [9,10]. On the other hand, in the case of post-gamma irradiation, the existing latent tracks produced by the charged particles are presumably enhanced by deposition of additional energy at the latent damage trails created by fission fragments. It is clear by comparing the Figs. 5.1.1 & 5.1.2 that V_G and V_T values for post-gamma dose are higher than those of pre-gamma dose.

It is also noted that an increase in the normalized (the ratio of etch rates for irradiated and pristine materials) etch-rate takes place both for bulk-etch rate and track-etch rates at the dose of 10^6 Gy and are given in Table 5.1.5 to Table 5.1.8. At 70°C, an increase of 11.28 folds for V_G and 15.60 fold for V_T for pre -gamma exposure and an increase of 15.65 folds for V_G and 32.95 fold for V_T for post-gamma

TABLE - 5.1.1 BULK- ETCH RATE (V_G) IN μm/h FOR PRE-GAMMA EXPOSED PADC (Homalite)

Temperature	No Dose	10^1 Gy	10^2 Gy	10^3 Gy	10^4 Gy	10^5 Gy	10^6 Gy
55°C	0.40 ± .02	0.39 ±.02	0.40±.02	0.41±.02	0.42±.02	0.43±.02	4.34±.60
60°C	0.69 ± .03	0.72 ±.03	0.72±.03	0.72±.03	0.78±.03	0.78±.03	9.33±1.2
65°C	1.61 ± .05	1.63 ±.05	1.63±.05	1.65±.05	1.86±.05	1.95±.05	17.3±3.5
70°C	2.98 ±.11	3.02±.11	3.02±.11	3.01±.11	3.35±.11	3.74±.11	33.63±4.5

TABLE - 5.1.2. BULK-ETCH RATE (V_G) IN μm/h FOR POST-GAMMA EXPOSED PADC (Homalite)

Temperature	No Dose	10^1 Gy	10^2 Gy	10^3 Gy	10^4 Gy	10^5 Gy	10^6 Gy
55°C	0.40±.02	0.40±.02	0.40±.02	0.41±.02	0.42±.02	0.43±.02	5.70±.60
60°C	0.69 ±.03	0.69±.03	0.68±.03	0.72±.03	0.70±.03	0.76±.03	11.20±1.2
65°C	1.61±.05	1.61±.05	1.64±.05	1.65±.05	1.72±.05	2.07±.05	20.70± 3.5
70°C	2.98±.11	3.08±.11	3.08±.11	3.18±.11	3.38±.11	3.98±.11	46.50± 4.5

TABLE - 5.1.3. TRACK-ETCH RATE (V_T) IN μm/h FOR PRE-GAMMA EXPOSED PADC (Homalite)

Temperature	No Dose	10^1 Gy	10^2 Gy	10^3 Gy	10^4 Gy	10^5 Gy	10^6 Gy
55°C	0.55±.02	0.48±.02	0.48±.02	0.50±.02	0.65±.02	0.85±.02	8.18±.60
60°C	0.92±.03	0.95±.03	0.95±.03	0.97±.03	0.96±.03	0.96±.03	15.80±1.2
65°C	2.42 ±.05	2.06±.05	2.11±.05	2.10±.05	2.23±.05	2.59±.05	28.87±3.5
70°C	3.64 ±.11	3.50±.11	3.53±.11	3.63±.11	4.18±.11	4.95±.11	56.99±4.5

TABLE - 5.1.4. TRACK-ETCH RATE (V_T) IN μm/h FOR POST-GAMMA EXPOSED PADC (Homalite)

Temperature	No Dose	10^1 Gy	10^2 Gy	10^3 Gy	10^4 Gy	10^5 Gy	10^6 Gy
55°C	0.55±.02	0.55±.02	0.55±.02	0.56±.02	0.68±.02	0.90±.02	16.8±.60
60°C	0.92±.03	0.95±.03	0.95±.03	0.94±.03	0.99±.03	1.12±.03	31.6±1.2
65°C	2.42±.05	2.43±.05	2.46±.05	2.49±.05	2.49±.05	3.74±.05	61.9±3.5
70°C	3.64±.11	3.80±.11	3.81±.11	3.77±.11	4.46±.11	5.26±.11	119.9±4.

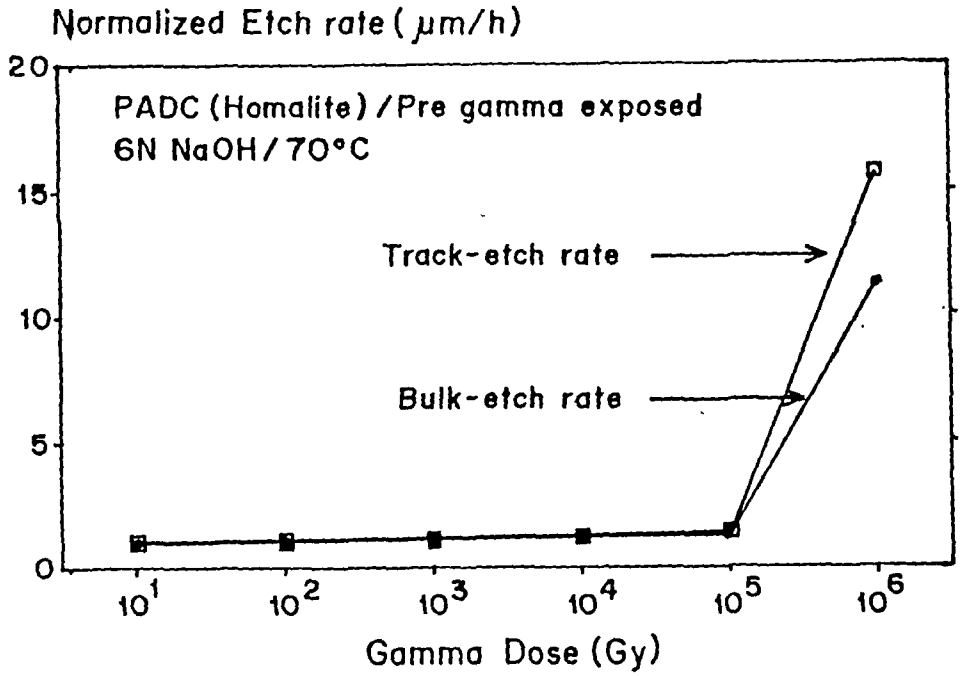

Fig. 5.1.3. Normalized etch-rate of pre-gamma irradiated PADC (Homalite) at the etching temperature of 70°C.

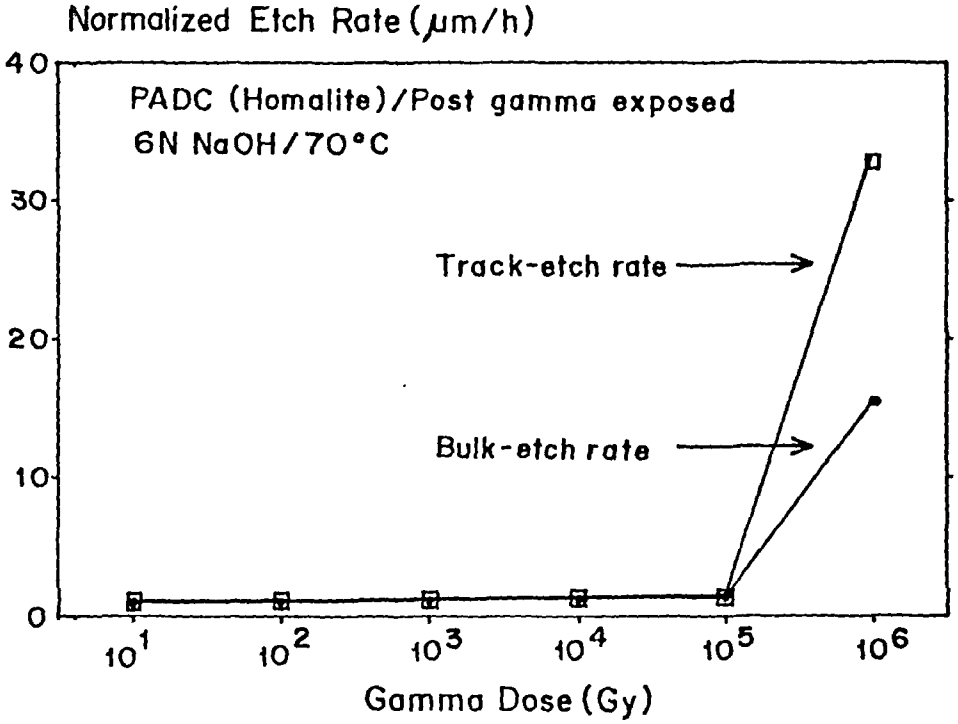

Fig. 5.1.4. Normalized etch-rate of post-gamma irradiated PADC (Homalite) at the etching temperature of 70°C.

exposure has been reflected from the results as shown in Figs.5.1.3 & 5.1.4.

In order to find out the activation energy for bulk-etching at different doses of gamma radiation, the data of $\log(V_G)$ versus 1/T are plotted for both pre- and post-gamma exposure and are dipicted in Figs.5.1.5 & 5.1.6. From the graph it is clear that all the fitted straight lines are parallel to each other, revealing the fact that activation energy for bulk-etching remains unaltered by different doses of gamma radiation. Though the etch-rate increases at 10^6 Gy, the activation energy remains the same. Table 5.1.9 gives the value of activation energy for bulk-etching at different doses of gamma rays.

PADC (American Acrylics) also behaves in the similar fashion. Table 5.1.10 to Table 5.1.13 lists the bulk-etch rate and track-etch rate values of this detector at different temperature and for both pre- and post-exposure sets. Figs.5.1.7 & 5.1.8 gives the bulk-etch rate and track-etch rate values at different doses of gamma radiation for both pre- and post-gamma exposure. It shows that both V_G and V_T remains almost invariant upto the gamma dose of 10^5 Gy. However, there is a steep increase in both V_G and V_T at a dose of 10^6 Gy. This enhanced response of this detector at 10^6 Gy is observed in both the cases of pre and post-gamma exposure. Similar increase in etch rates at the dose of 10^6 Gy, for PADC (Homalite) is also observed (Table 5.1.1 - Table 5.1.4). It is found for PADC (Homalite) that post-gamma exposure have higher etch rate values than the pre-gamma exposure.

TABLE - 5.1.5. NORMALIZED BULK-ETCH RATE OF PADC (Homalite) FOR PRE-GAMMA SET

Etching Temperature	Gamma Doses					
	10^1 Gy	10^2 Gy	10^3 Gy	10^4 Gy	10^5 Gy	10^6 Gy
55°C	1.0	1.0	1.02	1.05	1.07	10.85
60°C	1.0	1.04	1.04	1.13	1.13	13.52
65°C	1 01	1.01	1.02	1.15	1.21	10.75
70°C	1.01	1.01	1 01	1.12	1.25	11.28

TABLE - 5.1.6. NORMALIZED BULK-ETCH RATE OF PADC (Homalite) FOR POST-GAMMA SET

Etching Temperature	Gamma Doses					
	10^1 Gy	10^2 Gy	10^3 Gy	10^4 Gy	10^5 Gy	10^6 Gy
55°C	1.0	1.0	1.02	1.05	1.07	14.25
60°C	1.0	1.00	1 04	1.01	1.10	16.23
65°C	1.0	1.01	1.01	1.06	1.28	12.9
70°C	1.03	1.03	1.06	1.13	1.33	15.6

TABLE - 5.1.7. NORMALIZED TRACK-ETCH RATE OF PADC (Homalite) FOR PRE- GAMMA SET

Etching Temperature	Gamma Doses					
	10^1 Gy	10^2 Gy	10^3 Gy	10^4 Gy	10^5 Gy	10^6 Gy
55°C	0.87	0.87	0.91	1.18	1.54	14.87
60°C	1.03	1.03	1.05	1.04	1.05	17.17
65°C	0.85	0.87	0.86	0.92	1.07	11.93
70°C	0.96	0.97	0.99	1.14	1.36	15.65

TABLE - 5.1.8. NORMALIZED TRACK-ETCH RATE OF PADC (Homalite) FOR POST- GAMMA SET

Etching Temperature	Gamma Doses					
	10^1 Gy	10^2 Gy	10^3 Gy	10^4 Gy	10^5 Gy	10^6 Gy
55°C	1.0	1.0	1.01	1.23	1.63	30.56
60°C	1.03	1.03	1.03	1.07	1.21	34.34
65°C	1.0	1.01	1.03	1.03	1.54	25.58
70°C	1.04	1.04	1.03	1.22	1.44	32.94

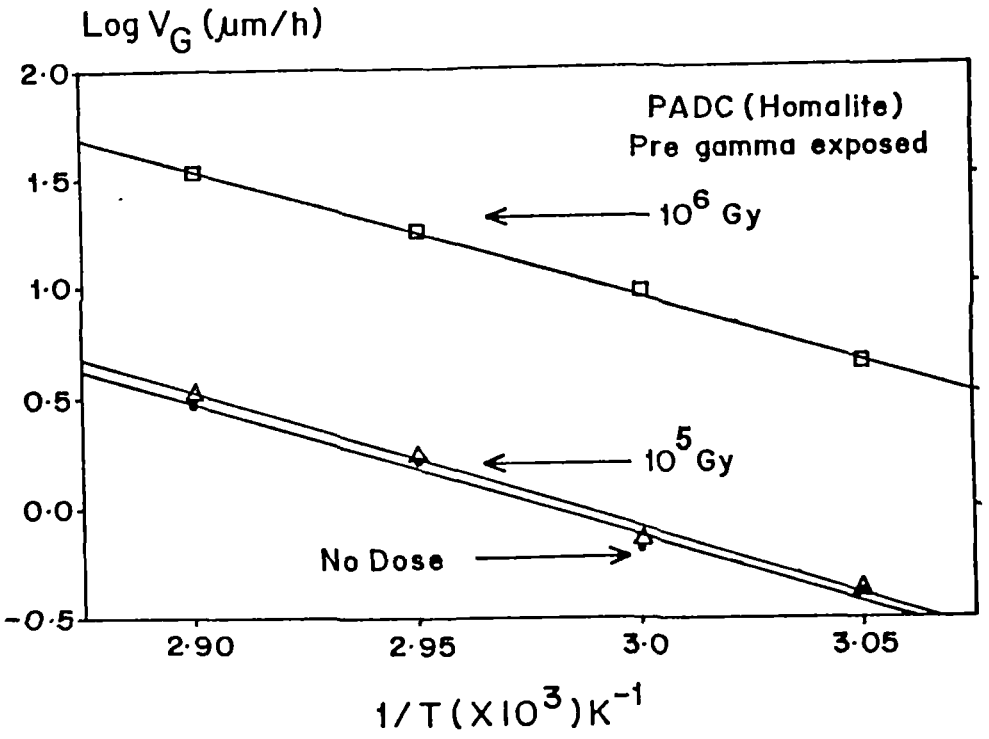

Fig. 5.1.5. Plot of Log V_G versus 1/T for determination of Activation Energy for bulk-etching of pre-gamma irradiated PADC (Homalite).

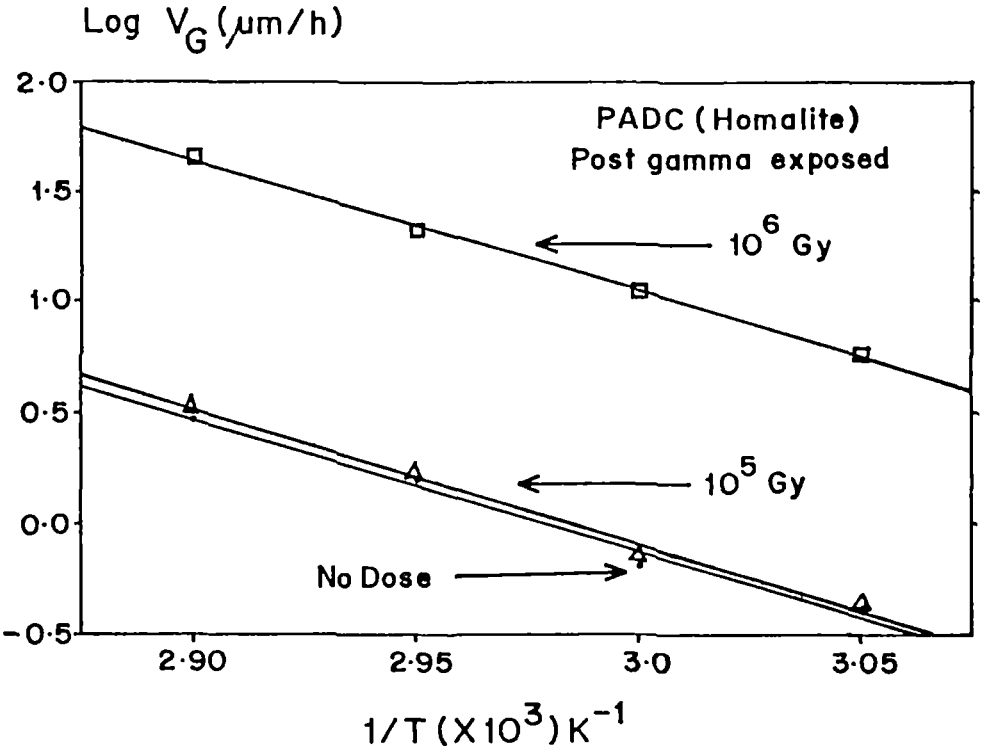

Fig. 5.1.6. Plot of Log V_G versus 1/T for determination of Activation Energy for bulk-etching of post-gamma irradiated PADC (Homalite).

TABLE- 5.1.9. ACTIVATION ENERGY IN kJmol $^{-1}$ FOR BULK-ETCHING OF PADC (Homalite) AT DIFFERENT GAMMA DOSES

Gamma Dose (Gy)	Activation Energy (kJ mol^{-1})	
	Pre gamma Exposure	Post gamma Exposure
No Dose	117.1 ± 4.5	117.1 ± 4.5
10^1 Gy	118.7 ± 4.5	117.8 ± 4.5
10^2 Gy	119.7 ± 4.5	118.2 ± 4.5
10^3 Gy	118.1 ± 4.5	116.6 ± 4.5
10^4 Gy	124.0 ± 4.5	123.9 ± 4.5
10^5 Gy	117.5 ± 8.0	125.2 ± 4.5
10^6 Gy	113.6 ± 6.5	121.4 ± 6.9

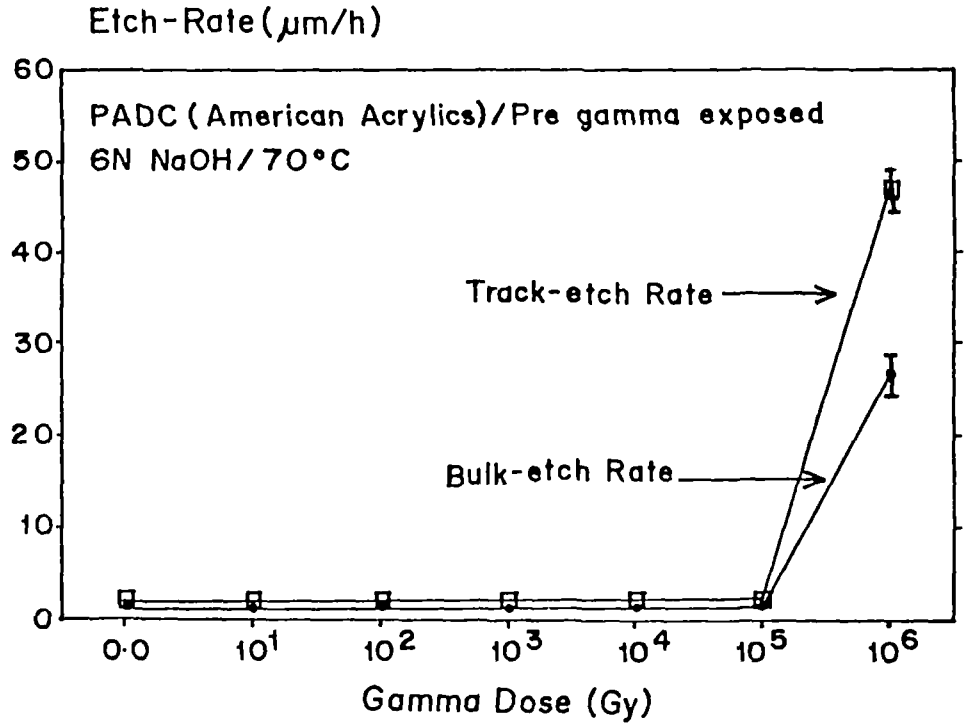

Fig. 5.1.7. Bulk and Track-etch rate of pre-gamma irradiated PADC (American Acrylics).

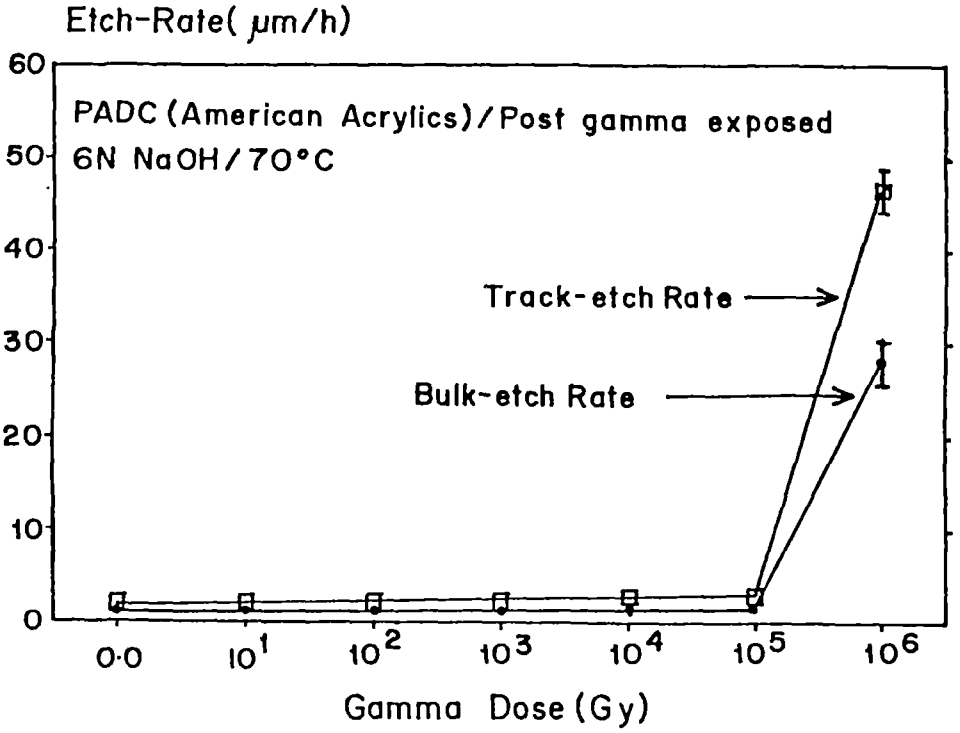

Fig. 5.1.8. Bulk and Track-etch rate of post-gamma irradiated PADC (American Acrylics).

TABLE - 5.1.10. BULK-ETCH RATE (V_G) IN μm/h FOR PRE-GAMMA EXPOSED PADC (American Acrylics)

Temperature	No Dose	10^1 Gy	10^2 Gy	10^3 Gy	10^4 Gy	10^5 Gy	10^6 Gy
55°C	0.35±.05	0.34 ±.05	0.34±.05	0.38±.05	0.39±.05	0.47±.05	7.70±1.1
60°C	0.59±.06	0.58±.06	0.57±.06	0.59±.06	0.73±.06	0.82±.06	11.48±1.2
65°C	0.85±.10	0.87±.10	0.88±.10	0.89±.10	1.16±.10	1.22±.10	18.9±1.3
70°C	1.15±.11	1.15±.11	1.15±.11	1.22±.11	1.19±.11	1.58±.11	26.95±1.8

TABLE - 5.1.11. BULK-ETCH RATE (V_G) IN μm/h FOR POST-GAMMA EXPOSED PADC (American Acrylics)

Temperature	No Dose	10^1 Gy	10^2 Gy	10^3 Gy	10^4 Gy	10^5 Gy	10^6 Gy
55°C	0.35±.05	0.35±.05	0.36±.05	0.38±.05	0.44±.05	0.50±.02	8.15±.10
60°C	0.59±.06	0.59±.06	0.59±.06	0.60±.06	0.82±.06	0.90±.06	12.58±1.2
65°C	0.85±.10	0.86±.10	0.86±.10	0.90±.10	1.21±.10	1.35±.10	21.27±1.3
70°C	1.15±.11	1.14±.11	1.15±.11	1.15±.11	1.47±.11	1.66±.11	28.04±1.8

TABLE - 5.1.12. TRACK - ETCH RATE (V_T) IN μm/h FOR PRE-GAMMA EXPOSED PADC (American Acrylics)

Temperature	No Dose	10^1 Gy	10^2 Gy	10^3 Gy	10^4 Gy	10^5 Gy	10^6 Gy
55°C	0.54±.05	0.53±.05	0.52±.05	0.57±.05	0.55±.05	0.69±.05	14.27±1.1
60°C	0.87±.06	0.89±.06	0.88±.06	0.91±.06	1.05±.06	1.26±.06	19.95±1.2
65°C	1.11±.10	1.15±.10	1.07±.10	1.09±.10	1.51±.10	1.73±.10	29.29±1.3
70°C	1.86±.11	1.86±.11	1.96±.11	1.95±.11	2.17±.11	2.49±.11	46.54±1.8

TABLE - 5.1.13. TRACK -ETCH RATE (V_T) IN μm/h FOR POST-GAMMA EXPOSED PADC (American Acrylics)

Temperature	No Dose	10^1 Gy	10^2 Gy	10^3 Gy	10^4 Gy	10^5 Gy	10^6 Gy
55°C	0.54±.05	0.54 ±.05	0.54±.05	0.55±.05	0.72±.05	0.76±.05	14.32±1.1
60°C	0.87±.06	0.90±.06	0.91±.06	0.89±.06	1.22±.06	1.36±.06	20.18±1.2
65°C	1.11±.10	1.12±.10	1.12±.10	1.23±.10	1.55±.10	1.87±.10	29.45±1.3
70°C	1.86±.11	1.85±.11	1.99±.11	1.99±.11	2.77±.11	2.90±.11	46.70±1.8

But in the present case there are no significant changes both in bulk-etch rates as well as in track-etch rates for post-gamma exposure.

Though the chemical constituents are same for both the detectors, it is quite surprising to observe that in case of PADC (American Acrylics), there is no pre-gamma and post-gamma discrimination. Bulk-etch rates and track-etch rates are same for both pre- and post-gamma exposure. This clearly indicates that the damage created by fission-fragments and alpha particles was not enhanced by post gamma mode of exposure.

Table 5.1.14. to Table 5.1.17. gives the normalized etch rates for PADC (American Acrylics) detector at different doses and at different etching temperatures for pre- and post-gamma exposure. Normalised etch rates are again very much high for this detector at higher dose. Till the dose of 10^4 Gy, no significant change is observed. At 10^5 Gy, there is little increase in the etch rate value. When the dose reaches to 10^6 Gy, it increases abruptly for both pre and post-gamma exposure.

Activation energies for bulk-etching of PADC (American Acrylics) are listed in Table 5.1.18. Though the etch-rate increases, activation energy remains almost constant as in the case of PADC (Homalite). This indicates that activation energy is independent of gamma doses. Fig.5.1.9 & Fig.5.1.10 show the plot of Log V_G versus 1/T for both

TABLE - 5.1.14. NORMALIZED BULK - ETCH RATE OF PADC (American Acrylics) FOR PRE-GAMMA SET

Etching Temperature	Gamma Doses					
	10^1 Gy	10^2 Gy	10^3 Gy	10^4 Gy	10^5 Gy	10^6 Gy
55°C	1.0	1.0	1.08	1.11	1.34	22.0
60°C	1.0	1.0	1.0	1.23	1.24	19.45
65°C	1.02	1.03	1.04	1.36	1.43	22.34
70°C	1.0	1.0	1.06	1.20	1.37	23.43

TABLE - 5.1.15. NORMALIZED BULK - ETCH RATE OF PADC (American Acrylics) FOR POST-GAMMA SET

Etching Temperature	Gamma Doses					
	10^1 Gy	10^2 Gy	10^3 Gy	10^4 Gy	10^5 Gy	10^6 Gy
55°C	1.0	1.02	1.08	1.25	1.43	23.38
60°C	1.0	1.0	1.01	1.39	1.52	21.32
65°C	1.01	1.01	1.05	1.42	1.58	25.02
70°C	1.0	1.01	1.01	1.29	1.46	24.46

TABLE - 5.1.16. NORMALIZED TRACK - ETCH RATE OF PADC (American Acrylics) FOR PRE-GAMMA SET

Etching Temperature	Gamma Doses					
	10^1 Gy	10^2 Gy	10^3 Gy	10^4 Gy	10^5 Gy	10^6 Gy
55°C	0.98	0.96	1.05	1.02	1.27	26.42
60°C	1.02	1.01	1.04	1.20	1.44	22.93
65°C	1.03	0.96	0.98	1.36	1.55	26.38
70°C	1.0	1.05	1.04	1.16	1.34	25.02

TABLE - 5.1.17. NORMALIZED TRACK - ETCH RATE OF PADC (American Acrylics) FOR POST-GAMMA SET

Etching Temperature	Gamma Doses					
	10^1 Gy	10^2 Gy	10^3 Gy	10^4 Gy	10^5 Gy	10^6 Gy
55°C	1.0	1.0	1.01	1.33	1.40	26.51
60°C	1.03	1.04	1.02	1.40	1.56	23.91
65°C	1.0	1.0	1.10	1.39	1.68	26.53
70°C	0.99	1.07	1.07	1.49	1.56	25.10

TABLE-5.1.18. ACTIVATION ENERGY IN kJmol $^{-1}$ FOR BULK-ETCHING OF PADC (American Acrylics) AT DIFFERENT GAMMA DOSES

Gamma Dose (Gy)	Activation Energy (kJ mol^{-1})	
	Pre - gamma Set	Post- gamma Set
No Dose	63.9 ± 4.3	63.9 ± 4.3
10^1 Gy	65.6 ± 4.7	63.3 ± 4.3
10^2 Gy	66.0 ± 3.8	62.3 ± 4.3
10^3 Gy	67.9 ± 4.6	61.3 ± 4.3
10^4 Gy	65.4 ± 4.6	63.5 ± 4.3
10^5 Gy	67.1 ± 3.6	64.1 ± 4.3
10^6 Gy	69.3 ± 4.6	68.5 ± 4.6

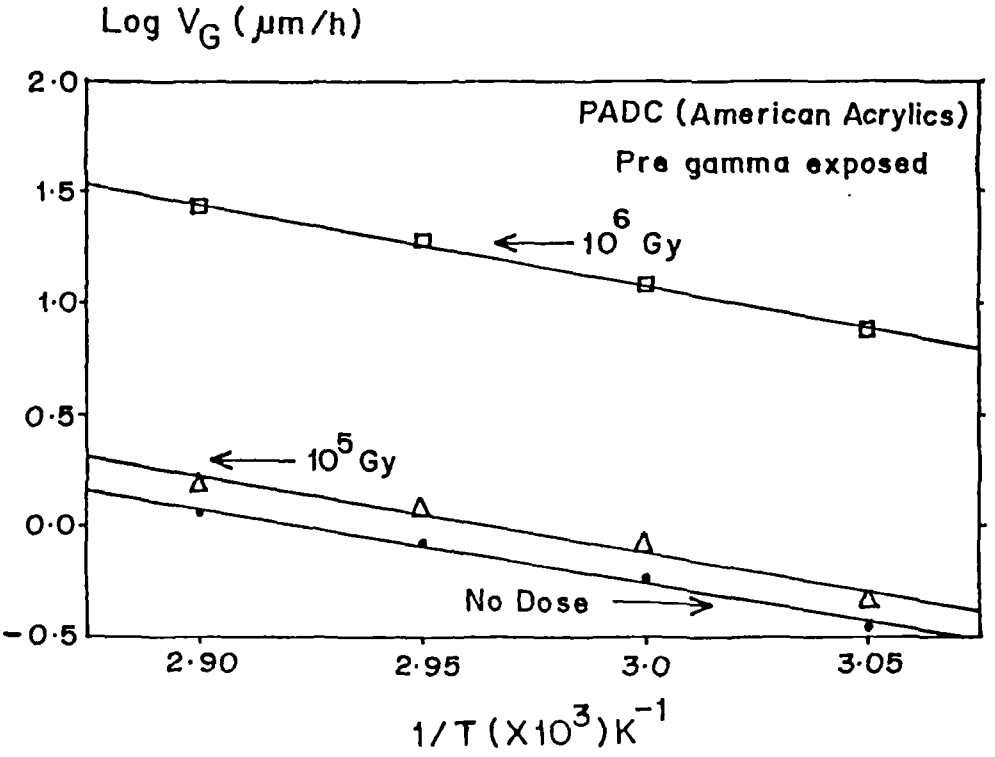

Fig. 5.1.9. Plot of Log V_G versus 1/T gives the parallel straight lines reveals the constancy of Activation Energy for bulk-etching of pre-gamma irradiated PADC (American Acrylics).

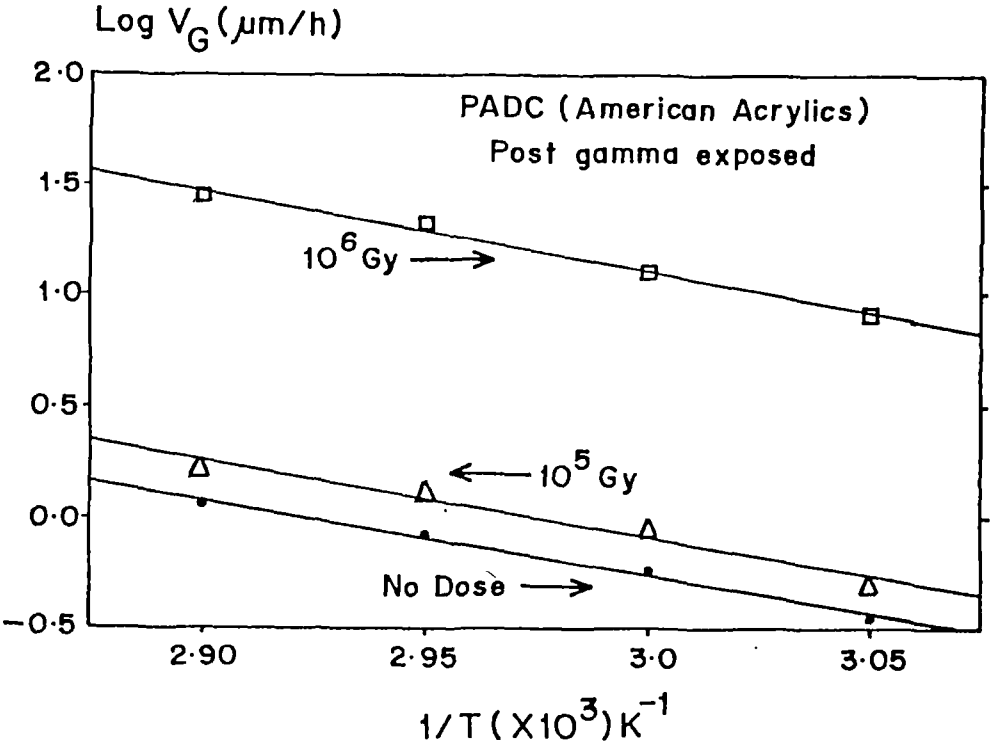

Fig. 5.1.10. Plot of Log V_G versus 1/T gives the parallel straight lines reveals the constancy of Activation Energy for bulk-etching of post-gamma irradiated PADC (American Acrylics).

modes of gamma exposure. The parallel straight lines support the constancy of activation - energy.

5.1.3 SPECTRAL STUDIES :- Track studies for both PADC (Homalite) and PADC (American Acrylics) give clear indications of bond scissioning. Since only at the dose of 10^6 Gy, etch-rate increases for both the detectors, it is understood that upto the dose of 10^5 Gy, neither cross-linking nor appreciable bond cleavage has taken place. So spectroscopic studies were carried out to understand the bond transformations. Details of the experimental (spectroscopic) methods have been presented in chapter-4.

UV - VIS study of PADC (Homalite) is done in the range between 200 nm - 800 nm. Of course there is no absorption peak observed because of the high thickness of the detector. The UV-VIS transmittance spectra of PADC (Homalite) detectors exposed to different gamma doses are shown in Fig.5.1.11. It can be seen that upto the gamma dose of 10^4 Gy there is practically no change in the transmittance. But at 10^5 Gy and 10^6 Gy transmittance starts decreasing and this change is significant in the wave length region between 340 nm - 500 nm. We can see that at lower wave length region (below 427nm) transmittance is more for gamma dose of 10^6 Gy, but at higher wave length region transmittance is more for 10^5 Gy of gamma exposed detector. So it is understood from this study that at higher doses ($>10^4$Gy), transmittance towards UV

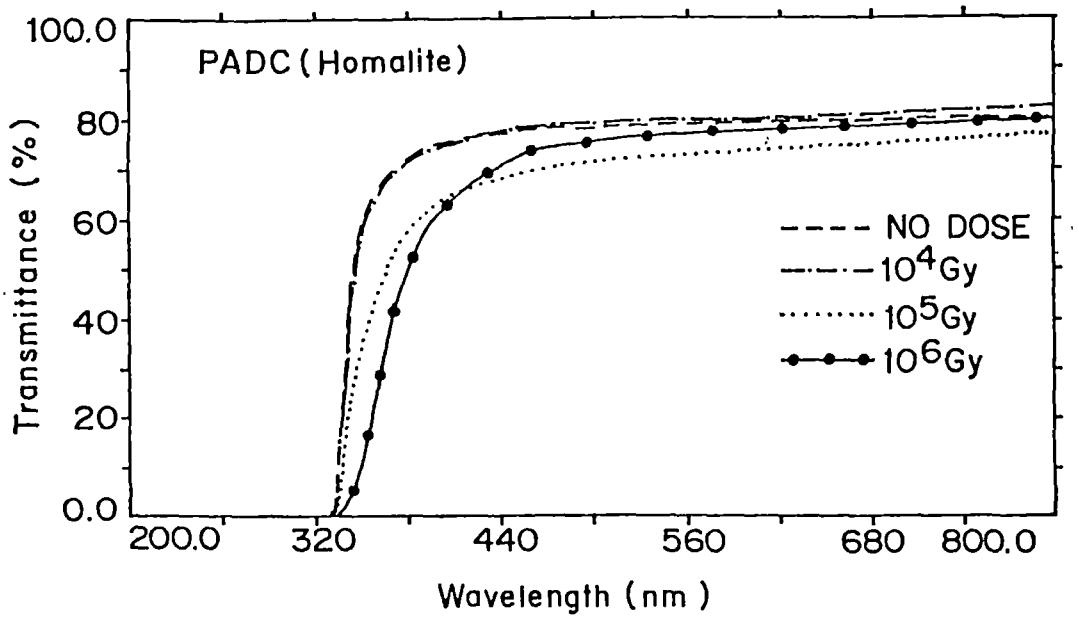

Fig. 5.1.11. UV - VIS transmittance (%) spectra of gamma irradiated PADC (Homalite).

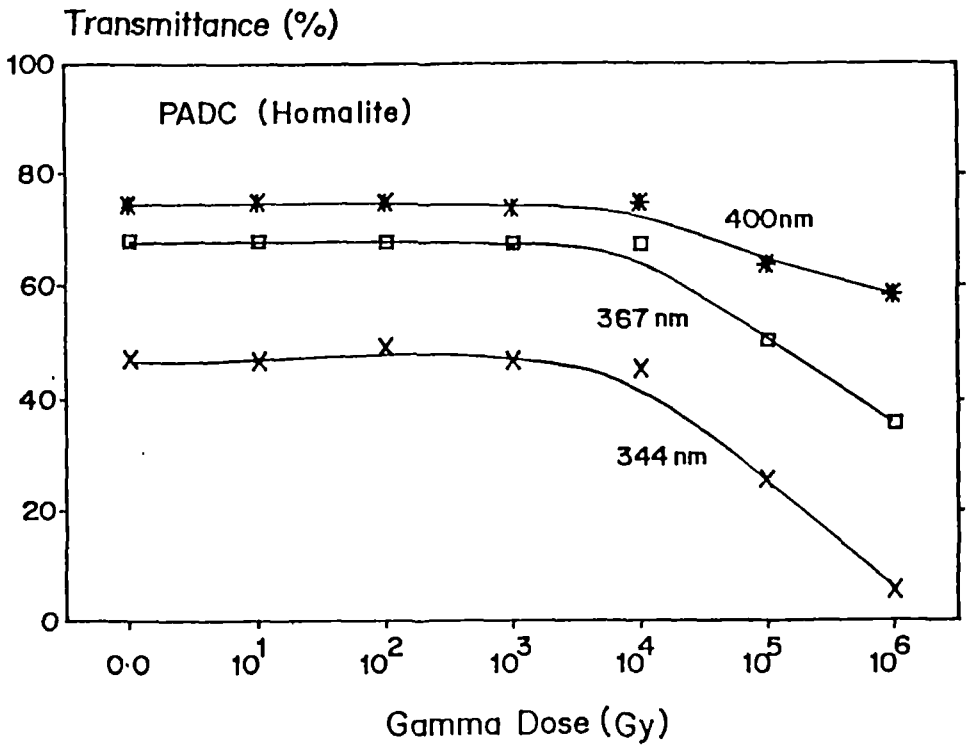

Fig. 5.1.12. Dose dependence change in transmittance (%) of gamma irradiated PADC (Homalite) at different wave lengths.

region significantly decreases with increasing dose. Therefore, dosimetric applications are more feasible for higher doses of gamma radiation in the UV region. For this purpose transmittance(%) values are plotted against gamma dose at different wave lengths and are shown in Fig.5.1.12. Table 5.1.19 gives the values of transmittance at different doses and at different wave lengths for PADC (Homalite).

Fig.5.1.13 gives the UV-VIS transmittance spectra of PADC (American Acrylics) exposed to different doses of gamma radiation. Though the spectra does not give any peak, it is interesting to observe that above the dose of 10^3 Gy, the pattern of the spectra changes with increasing gamma dose. Moreover, with increasing gamma dose the transmittance shifts towards higher wave length region. The UV - VIS spectra taken from the powdered material have not revealed any specific chemical change as the peak positions are not altered by exposing the samples to different doses of gamma radiation.

Table 5.1.20 gives the values of transmittance measured at different doses of gamma radiation for different wave lengths for PADC (American Acrylics). In order to employ this study in dosimetric applications, transmittance are plotted at different wave lengths for samples exposed to different gamma doses. Fig.5.1.14 shows the plots of transmittance as a function of gamma doses. From these plots one may estimate the radiation dose absorbed in PADC (American Acrylics) by measuring the transmittance.

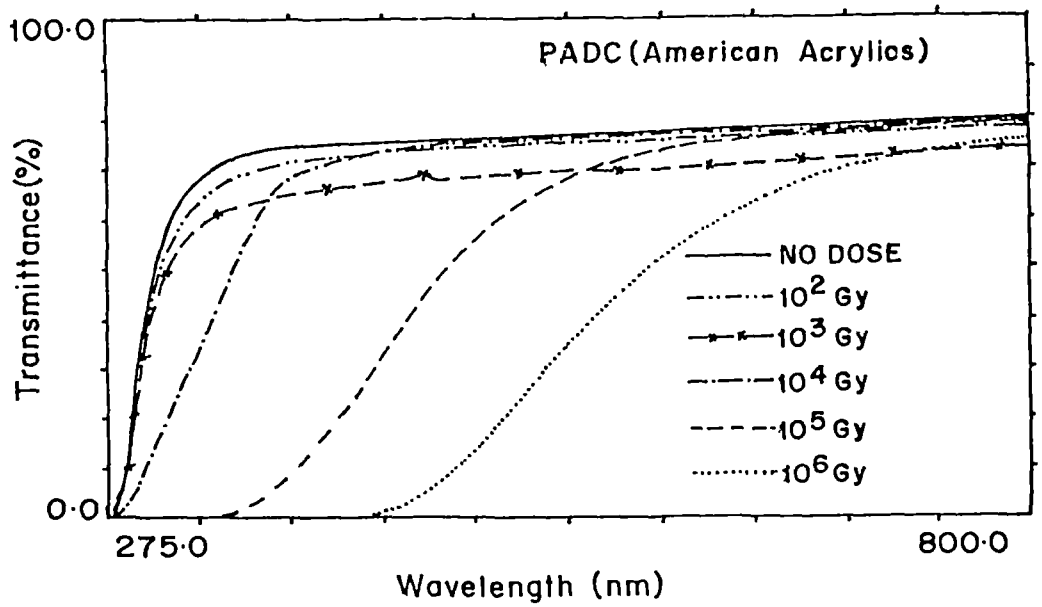

Fig. 5.1.13. UV - VIS transmittance spectra of gamma irradiated PADC (American Acrylics).

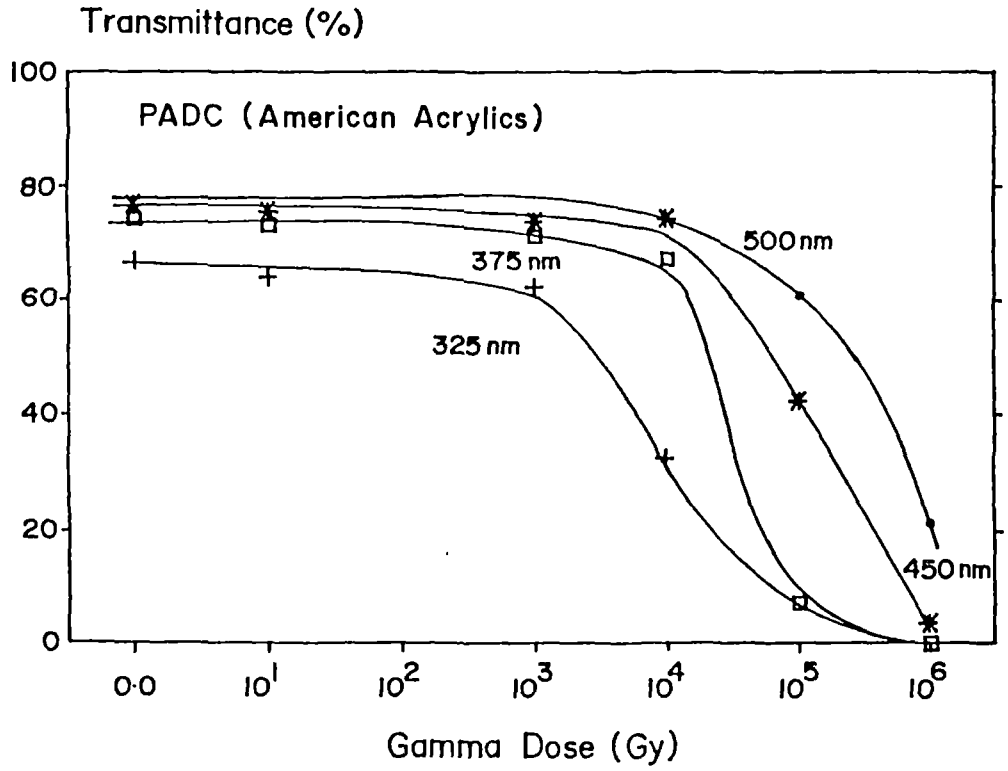

Fig. 5.1.14. Dose dependence variation in transmittance (%) of gamma irradiated PADC (American Acrylics) at different wave lengths.

TABLE - 5. 1.19. TRANSMITTANCE (%) VERSUS WAVE LENGTH OF GAMMA IRRADIATED PADC (Homalite)

Wavelength	No Dose	10^1 Gy	10^2 Gy	10^3 Gy	10^4 Gy	10^5 Gy	10^6 Gy
344 nm	46.73	46.26	47.95	46.80	45.10	25.64	5.60
367 nm	68.03	68.04	68.03	67.51	67.44	50.11	35.78
400 nm	74.53	74.85	74.99	73.80	74.71	63.95	58.55
450nm	77.66	77.82	78.00	76.66	77.80	69.01	71.67
500 nm	78.42	79.06	79.32	79.99	79.21	71.48	75.32

TABLE - 5. 1.20. TRANSMITTANCE (%) VERSUS WAVE LENGTH OF GAMMA IRRADIATED PADC (American Acrylics)

Wavelength	No Dose	10^1 Gy	10^2 Gy	10^3 Gy	10^4 Gy	10^5 Gy	10^6 Gy
310 nm	59.16	56.21	50.17	53.82	21.61	0.13	–
325 nm	66.97	64.35	57.15	62.25	32.93	0.09	0.008
350 nm	72.50	70.69	62.93	68.86	53.26	1.43	0.008
375 nm	74.40	73.33	64.97	71.42	67.36	7.26	0.008
400 nm	75.24	74.42	66.04	72.56	71.23	16.84	0.056
450 nm	76.34	75.83	68.69	74.04	74.58	42.03	3.91
500 nm	77.63	77.63	69.73	75.00	76.30	61.18	21.71

IR study could not provide any information about the bond cleavage or transformations. Both PADC (Homalite) and PADC (American Acrylics) show the same IR peak positions for different gamma doses. Fig.5.1.15 shows one typical IR spectra of PADC (American Acrylics) detector. Here spectra are taken by using the pellets with KBr. Some of the important peak positions are mentioned below.

Peak position (cm^{-1})	Corresponding group/bond
2954	ν_{C-H}
1742	$\nu_{C=O}$
1260	ν_{C-O}
1136	ν_{C-C}
788	δ-(CH_2)-

ESR study of PADC (Homalite) does not show any radical signal. Though the etch-rates clearly shows indication of bond cleavage but there is no spectroscopical proof about the bonds modifications. So we are not able to identify where exactly the bond rapture has taken place or what type of chemical transformations have occurred due to gamma radiation for PADC (Homalite) detector.

For PADC (American Acrylics), ESR study gives a clear picture about the bond cleavage. The track study has indicated that the increase in etch rate is due to the cleavage of polymeric chain, but there is no

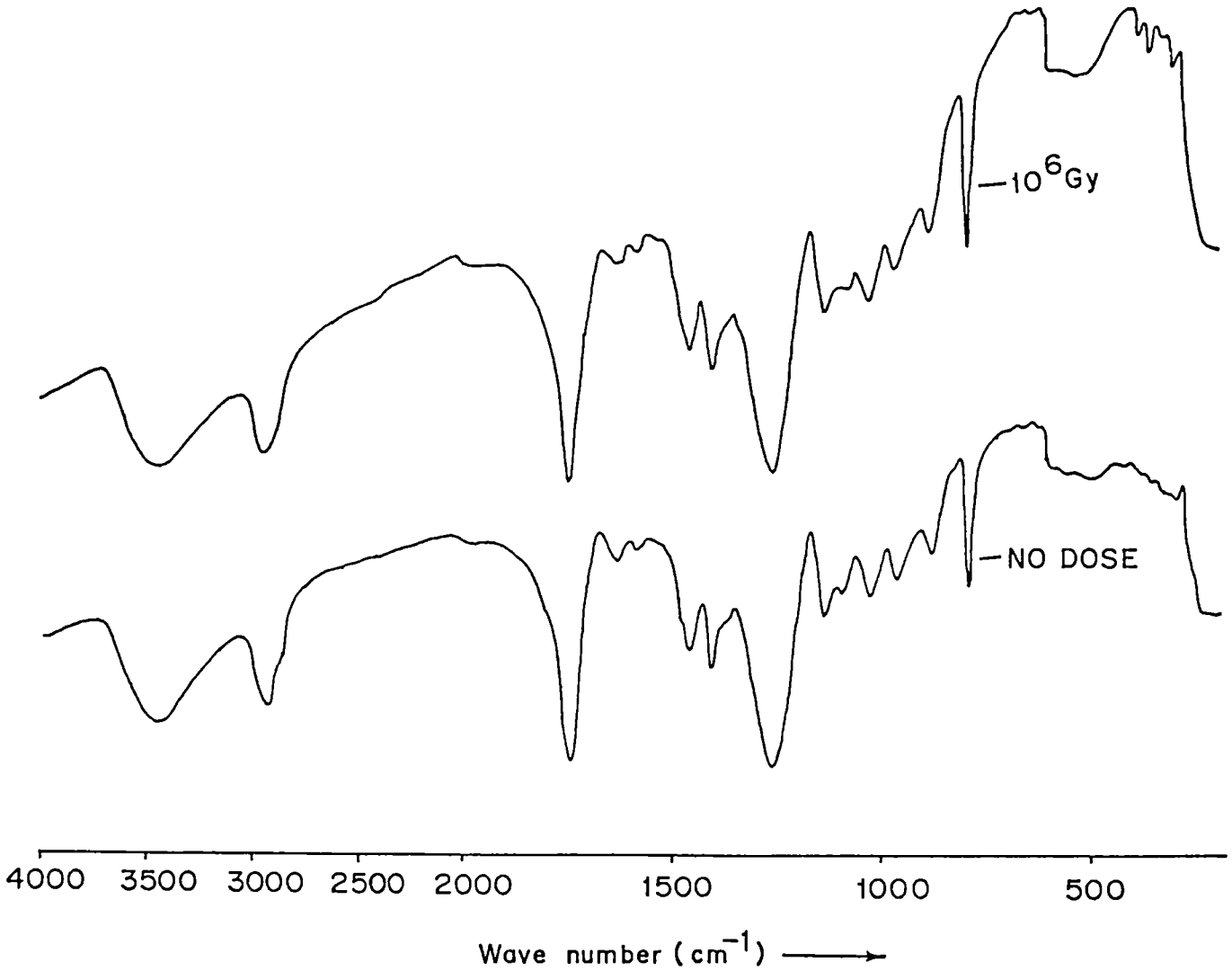

Fig. 5.1.15. IR spectra of gamma irradiated PADC (American Acrylics).

supporting evidence found from IR & UV-VIS study. The ESR study shows that upto a dose of 10^5 Gy, no signal corresponding to radical formation is observed. This means the intensity of scissioning below 10^5 Gy is low and is not reflected as ESR signal. But at the dose of 10^6 Gy, one gets a clear broad radical signal as shown in Fig.5.1.16. This sort of broad radical signal is the characteristic of oxygen radical. It can be possible only if polyallyl chain breaks and forms the radicals.

PADC polymer network consist of polyallyl chains joined by diethyleneglycol links which must have been hit by radiation, so that the destruction of the chains may take place more likely by the following mechanism :

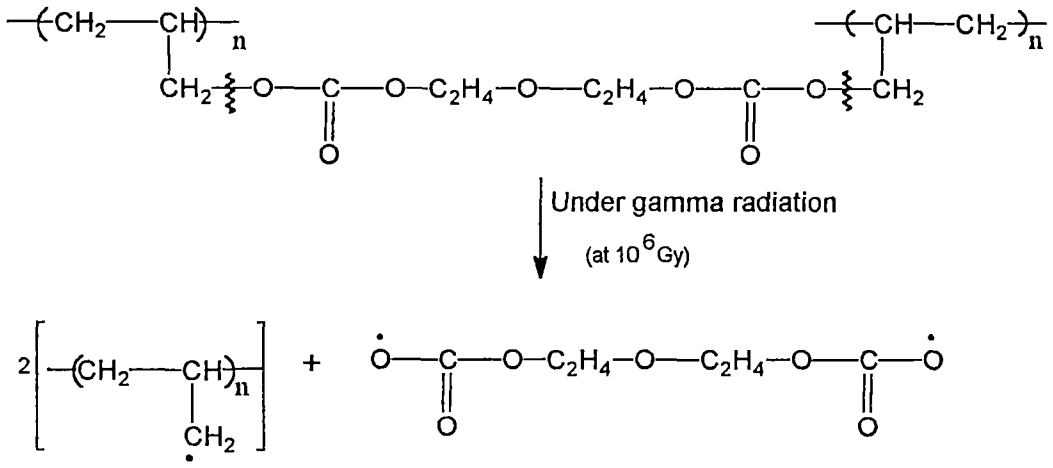

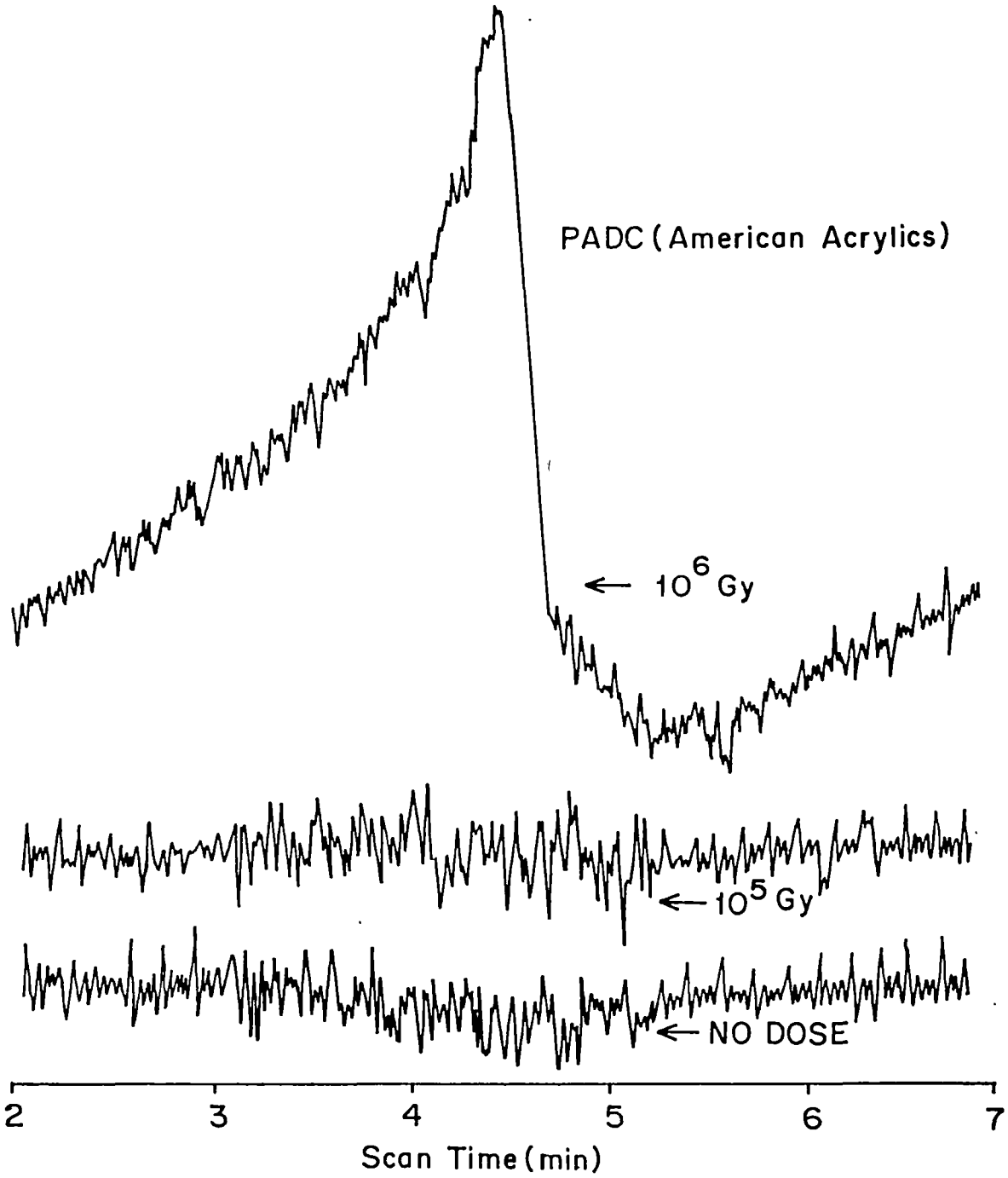

Fig. 5.1.16. ESR spectra of gamma irradiated (American Acrylics) shows the broad signal signifying the presence of Oxygen radical.

Two of the radicals with carbon end thus formed may combine with each other and re-establish the polymeric linkage. That is why we get the signal only for oxygen radical.

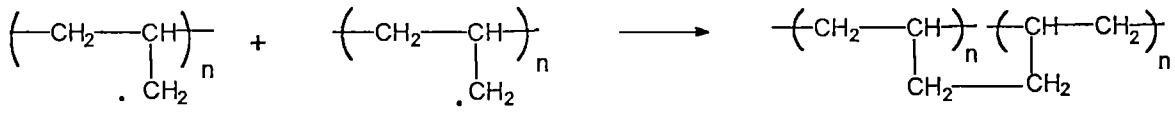

5.1.4. THERMOGRAVIMETRIC ANALYSIS :- TGA study of PADC (Homalite) does not show any appreciable change in the thermal stability of this material because of gamma irradiation. Here the weight loss takes place in a single step. Fig.5.1.17 shows the thermogram which clearly indicates that in all cases the weight loss starts around 270°C and finishes around 490°C. Only there is an observable change at the dose of 10^4 Gy and that is the detector loses its complete weight at around 465°C. From this study no quantitative conclusion could be drawn.

Thermogravimetric analysis of pristine and gamma irradiated (upto 10^5 Gy) PADC (American Acrylics) polymer shows double step decomposition pattern. First step of decomposition starts around 300°C and finishes around 430°C. In this range of temperature about 70% of the total weight is lost. Again the second step of decomposition starts at 430°C and continues upto around 475°C -

485°C as shown in Fig.5.1.18. But at the dose of 10^6 Gy, only single step decomposition is observed. In this case the weight loss starts around 260°C and 100% weight loss takes place around 380°C. Upto the dose of 10^5 Gy, the detector is stable till the temperature range of 475°C - 485°C. But when the dose becomes 10^6 Gy, the thermal resistance comes down and the detector decomposes at lower temperature.

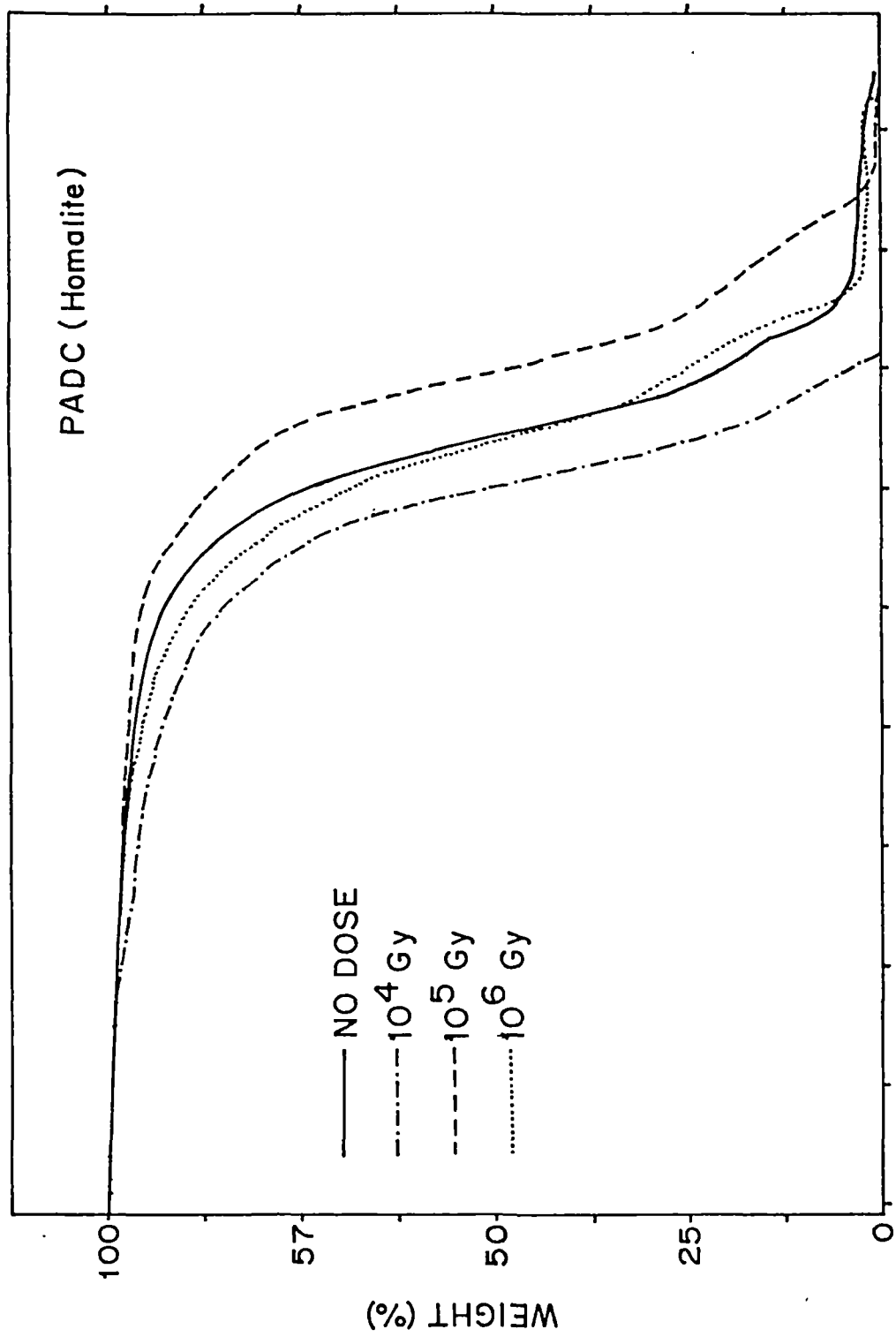

Fig. 5.1.17. TGA thermogram of gamma irradiated PADC (Homalite).

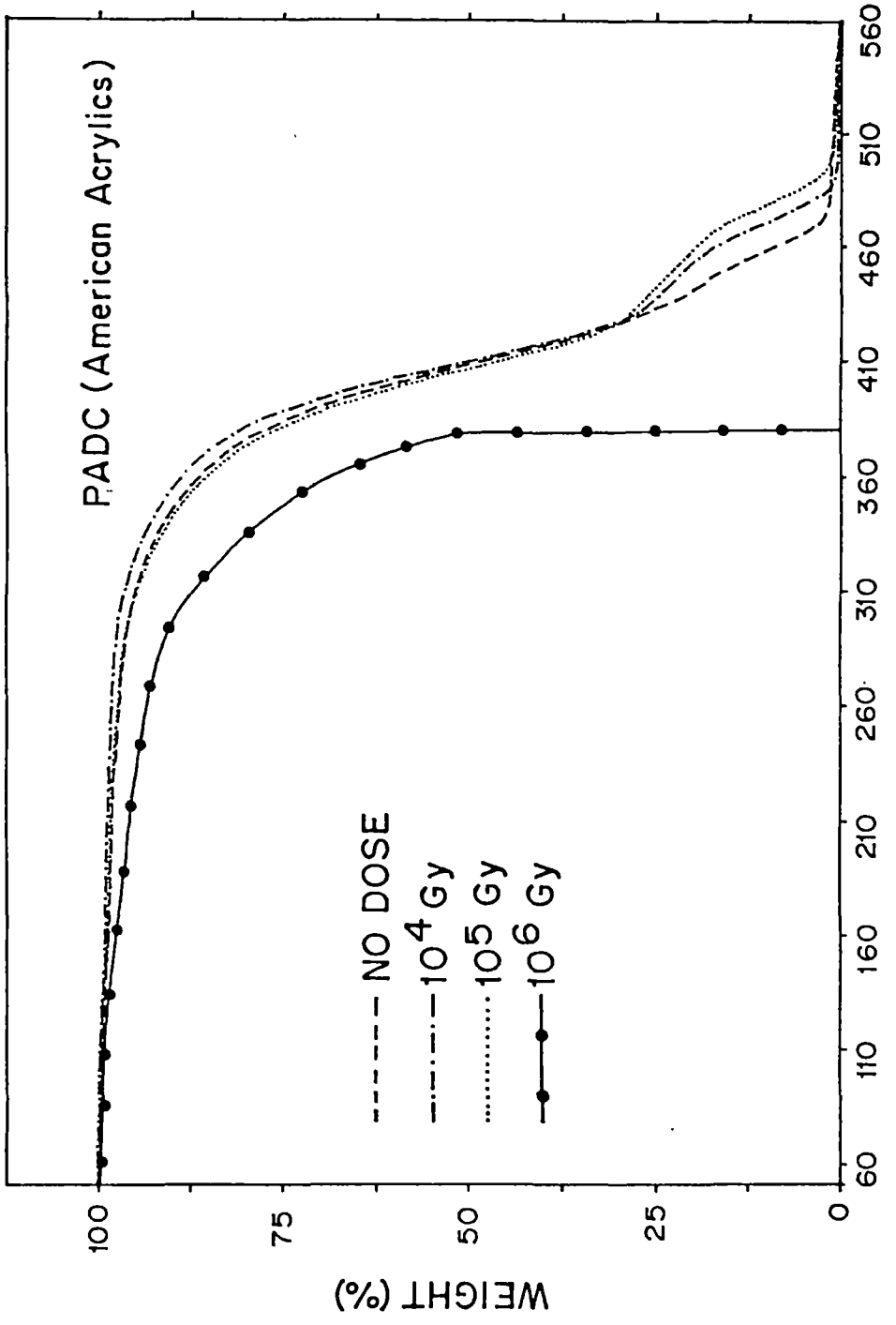

Fig. 5.1.18. TGA thermogram of gamma irradiated PADC (American Acrylics).

PART-2

In this part, details about the effects of gamma radiation on Makrofol-E, Lexan and Polycarbonate polymeric detectors are discussed.

5.2.1. PHYSICALLY OBSERVABLE CHANGES :- It was observed that upto a dose of 10^5 Gy, there were no visible changes in these detectors. But at 10^6 Gy of gamma dose the colourless films became light yellow.

5.2.2. TRACK STUDIES : Bulk-etch rates are determined for these detectors at 55°C, 60°C, 65°C and 70°C. Since there were no significant changes in the etch-rates at different gamma doses, we restricted the track study at three different doses (no dose, 10^3 Gy and 10^6 Gy). Moreover, all these detectors do not register alpha particles, so track-etch rate studies could not carried out for these detectors by using Durrani's relation[5].

Bulk-etch rate (V_G) at different etching temperatures for both pre-and post-gamma irradiation of these detectors exposed to different doses (No dose, 10^3 Gy and 10^6 Gy) are listed in Table 5.2.1, Table 5.2.2 and Table 5.2.3 respectively. The results show that there is no appreciable change in V_G. Bulk-etch rate remains invariant till the dose of 10^6 Gy. This is probably due to the fact that the magnitude of neither cross-linking nor scission of the polymeric chain has no

TABLE - 5. 2.1. BULK- ETCH RATE (V_G) IN μm/h FOR MAKROFOL-E FOR PRE- AND POST- GAMMA EXPOSURE

Temperature	No Dose	10^3 Gy		10^6 Gy	
		Pre	Post	Pre	Post
55°C	0.26 ± .04	0.26±.04	0.28±.04	0.35±.04	0.36±.04
60°C	0.73 ± .06	0.72± .06	0.78±.06	0.90±.06	1.03±.06
65°C	1.39 ± .07	1.41±.07	1.55±.07	1.84±.07	1.86±.07
70°C	1.98 ±.14	2.01± .14	2.03±.14	2.54±.14	2.54±.14

TABLE - 5. 2.2. BULK- ETCH RATE (V_G) IN μm/h FOR LEXAN FOR PRE- AND POST- GAMMA EXPOSURE

Temperature	No Dose	10^3 Gy		10^6 Gy	
		Pre	Post	Pre	Post
55°C	0.45 ± .02	0.47±.02	0.47±.02	0.55±.02	0.58±.02
60°C	0.64 ± .03	0.59± .03	0.64±.03	0.73±.03	0.85±.03
65°C	0.96 ± .03	0.96±.03	1.00±.03	1.19±.03	1.23±.03
70°C	1.37 ±0.03	1.38± .03	1.40±.03	1.63±.03	1.63±.03

TABLE - 5. 2. 3. BULK- ETCH RATE (V_G) IN μm/h FOR POLYCARBONATE FOR PRE- AND POST- GAMMA EXPOSURE

Temperature	No Dose	10^3 Gy		10^6 Gy	
		Pre	Post	Pre	Post
55°C	0.34 ±.02	0.34±.02	0.34±.02	0.48±.02	0.47±.02
60°C	0.62 ±.03	0.62± .03	0.63±.03	0.74±.03	0.73±.03
65°C	0.98 ±.03	1.00±.03	1.00±.03	1.37±.03	1.38±.03
70°C	1.42 ±.06	1.41± .06	1.41±.06	1.83±.06	1.76±.06

observable influence on the etch rate. It is known that gamma interaction with polymers results in either bond scissioning or cross-linking of the polymeric chain [11]. If the bond scission takes place, then the average molecular weight decreases, resulting in higher dissolution rate for the bulk material. On the other hand, cross-linking enhances the molecular weight, resulting in the decrease in the bulk-etch rate. None of these detectors show significant increase or decrease of the etch-rate (V_G). So we can assume that upto a dose of 10^6 Gy, gamma irradiation does not produce any observable effect on these detectors in terms of etching rate. Similar results were observed by Frank and Benton [12]. They found that upto the gamma dose of 1.0 X 10^8 rad (1.0 X 10^6 Gy), there were no significant changes in V_G for Lexan track detector.

For better understanding of radiation damage along the tracks, we also studied the track length measurements for fission fragments in these detectors at three different doses for pre-gamma exposure set which have been listed in Tables 5.2.4, 5.2.5 and 5.2.6. Maximum etchable track lengths as well as the complete etching time for fission fragment tracks are found out. Figs.5.2.1, 5.2.2 and 5.2.3 show the track lengths measured for different etching times for Makrofol-E, Lexan and polycarbonate detectors respectively. From the results it is evident that track length is not altered by gamma radiation of different doses below 10^6Gy. At the dose of 10^6 Gy, only slight increase in track length is observed. The maximum etchable track length

TABLE - 5. 2.4. TRACK-LENGTH IN μm FOR MAKROFOL-E AT DIFFERENT ETCHING TIME at 60°C

Etching time (hours)	No Dose	10^3 Gy	10^6 Gy
0.50	5.71 ± 2.24	5.65± 2.24	7.30± 2.24
0.75	8.44± 2.24	8.68± 2.24	11.22± 2.24
1 00	11.87± 2.24	10.80± 2 24	14.06± 2.24
1.25	14.88± 2.24	14.96± 2.24	16.93± 2.24
1.50	14.85± 2.24	14 89± 2.24	17.29± 2.24
1.75	14.73± 2.24	14 96± 2.24	16.14± 2.24
2.00	12.70± 2.24	12 77± 2 24	14.06± 2.24

TABLE -5. 2.5. TRACK- LENGTH IN μm FOR LEXAN AT DIFFERENT ETCHING TIME at 60°C

Etching time (hours)	No Dose	10^3 Gy	10^6 Gy
0.50	5.50 ± 2.24	5.80 ± 2.24	5.85 ± 2.24
0.75	8 50 ± 2 24	8.90 ± 2.24	9.03 ± 2.24
1.00	10.94 ± 2.24	11.15 ± 2.24	12.99 ± 2.24
1.25	13.93 ± 2.24	13.73 ± 2.24	15.99 ± 2.24
1.50	13.86 ± 2.24	13.93 ± 2 24	15.84 ± 2.24
1.75	13.74 ± 2.24	13.69 ± 2.24	15.71 ± 2.24
2.00	11.66 ± 2 24	11.59 ± 2 24	13.35 ± 2.24

TABLE - 5. 2.6. TRACK-LENGTH IN μm FOR POLYCARBONATE AT DIFFERENT ETCHING TIME at 60°C

Etching time (hours)	*No Dose*	*10^3 Gy*	*10^6 Gy*
0.75	5.67 ± 2.24	5.60 ± 2.24	5.64 ± 2.24
1.00	7.56 ± 2.24	7.42 ± 2.24	7.92 ± 2.24
1.25	8.16 ± 2.24	7.95 ± 2.24	9.77 ± 2.24
1.50	8.30 ± 2.24	8.34 ± 2.24	9.78 ± 2.24
1.75	8.01 ± 2.24	7.99 ± 2.24	9.35 ± 2.24
2.00	7.59 ± 2.24	7.70 ± 2.24	8.30 ± 2.24
2.25	6.10 ± 2.24	6.34 ± 2.24	8.05 ± 2.24

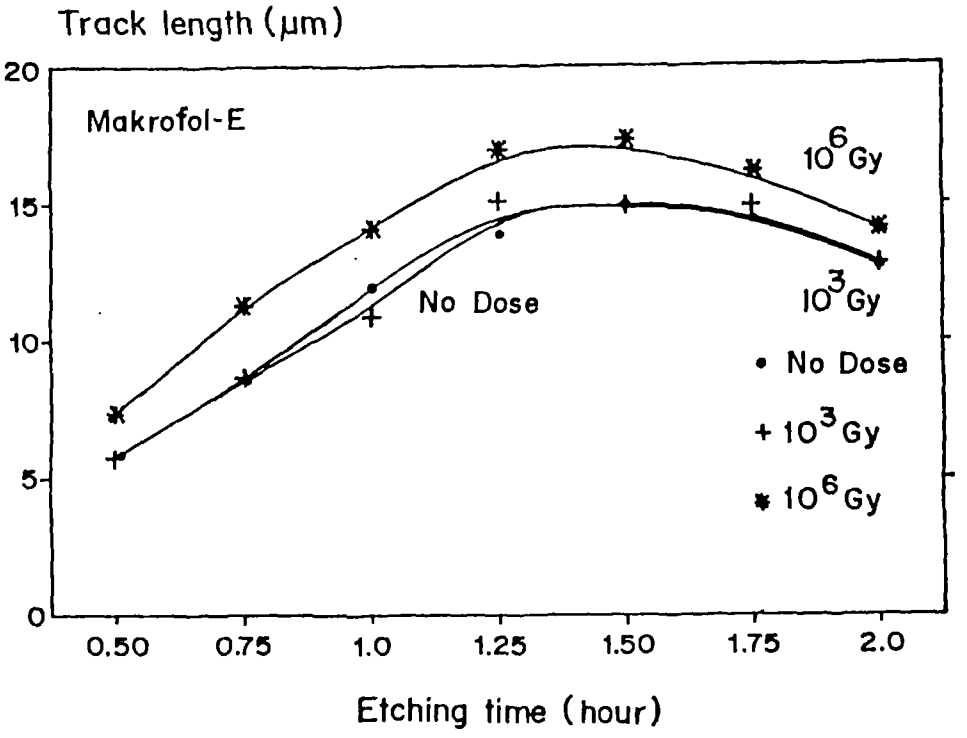

Fig. 5.2.1. Track length measured at different etching time in Makrofol-E detector.

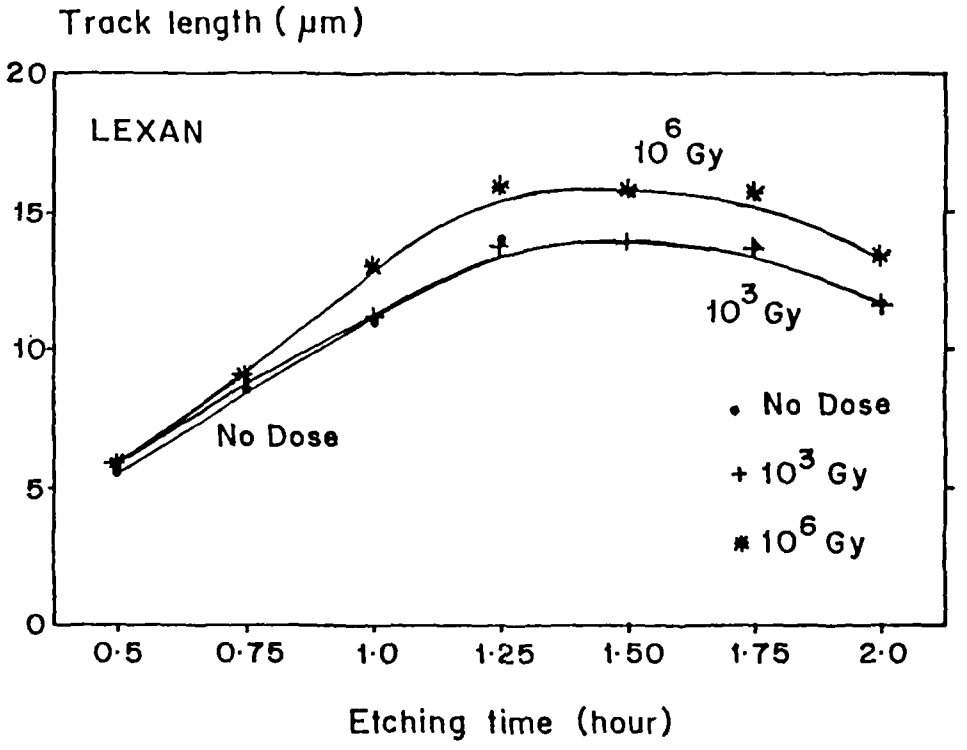

Fig. 5.2.2. Track length measured at different etching time in Lexan detector.

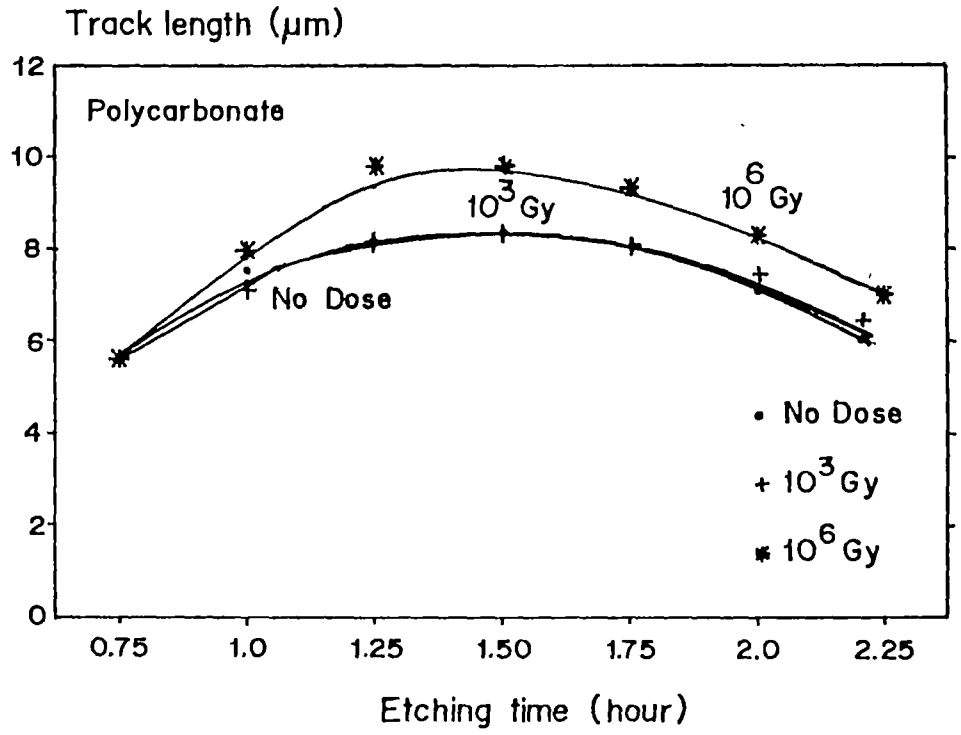

Fig. 5.2.3. Track length measured at different etching time for Polycarbonate detector.

for Makrofol-E ranges between 14-15 μm. At 10^6 Gy it becomes 17.3 μm i.e. an increase of about 15 - 20 %. The complete etching time is approximately 85 min. for the three doses for Makrofol-E detector. For Polycarbonate, we see that the complete etching time is about 105 min. and maximum etchable track length ranges between upto 8 – 9.5 μm. Lexan also behaves in a similar way. Here the complete etching time is about 78 min. and maximum etchable track length ranges between 13.9-15.9 μm.

Activation energies for bulk-etching of these detectors have been determined and are given in Table 5.2.7. The change in the activation energy is insignificant. Since bulk-etch rate has not altered to an appreciable extent by gamma doses, obviously significant change in the activation energy was not expected.

5.2.3. SPECTRAL STUDIES : Spectral studies were carried out by using three different techniques namely IR, UV-VIS and ESR spectroscopy. Spectral analysis of these detectors are discussed below.

UV - VIS spectra of Makrofol-E is shown Fig.5.2.4. The spectra of some particular doses like 10^3 Gy, 10^2 Gy, and 10^1 Gy have not been shown in the Fig.5.2.4 as the spectra at these doses overlap with the spectrum at the dose of 10^4 Gy. Moreover, the spectra are shown in the range 200 - 500 nm. This is because no significant changes were observed beyond 500 nm. In order to study the variation of transmittance with dose, transmittance have been measured at different

TABLE - 5. 2. 7. ACTIVATION ENERGY IN $kJmol^{-1}$ FOR BULK-ETCHING OF LEXAN, MAKROFOL-E AND POLYCARBONATE FOR PRE- AND POST-GAMMA EXPOSURE

Detector	No Dose	10^3 Gy		10^6 Gy	
		Pre	Post	Pre	Post
Lexan	61.2± 2.8	65.0 ± 2.6	58.7 ± 2.8	61.5 ± .2.5	58.6 ± 2.8
Makrofol-E	92.6± 6.8	94.9 ± 6.8	90.8 ± 6.8	92.3 ± 6.8	93.7 ± 6.8
Polycarbonate	82.4 ± 4.5	76.8 ±.4.5	77.4 ± 4.5	82.1 ± 4.5	76.3 ± 4.1

TABLE - 5. 2.8. TRANSMITTANCE (%) VERSUS WAVE LENGTH OF GAMMA IRRADIATED MAKROFOL-E DETECTOR

Wavelength	No Dose	10^1 Gy	10^2 Gy	10^3 Gy	10^4 Gy	10^5 Gy	10^6 Gy
380 nm	71.50	71.24	71.02	70.00	69.03	67.05	36.01
350 nm	69.50	69.03	69.00	68.00	67.03	63.01	15.03
335 nm	67.00	67.02	66.05	64.00	63.07	45.00	3.03
330 nm	66.75	66.05	65.13	61.57	61.67	42.31	1.08
320 nm	62.79	62.60	61.86	57.78	57.36	34.82	0.35
310 nm	57.75	57.60	57.36	52.99	52.99	29.59	0.20
300 nm	52.61	52.55	52.54	47.54	48.02	25.37	0.10

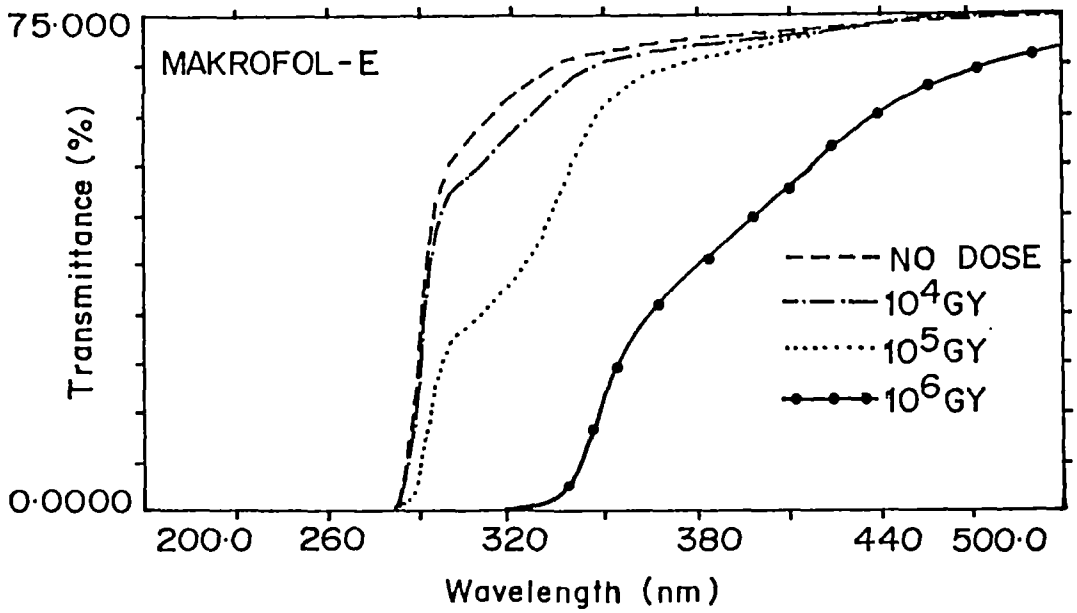

Fig. 5.2.4. **UV-VIS transmittance spectra of Makrofol-E detector exposed to different gamma doses.**

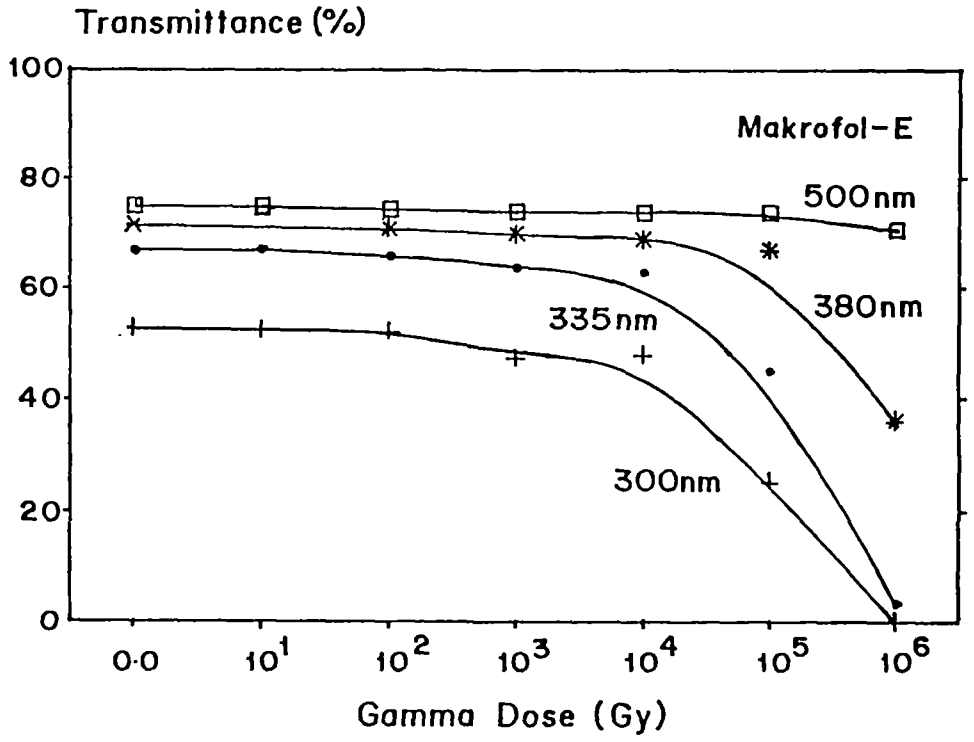

Fig. 5.2.5. **Dose dependence variation in transmittance of Makrofol-E detector at different wave lengths.**

wave lengths for detectors exposed to different gamma doses and are listed in Table.5.2.8. Though UV-VIS study does not give any information about bond cleavage or bond formation, but it is evident from these results that above the dose of 10^4 Gy, transmittance decreases with increasing gamma dose. The decrease is significant in the region 280 - 500 nm. For dosimetric applications of this study transmittance(%) data are plotted against gamma doses at different wave-lengths and are shown in Fig.5.2.5.

UV-VIS study of Lexan also shows a similar trend. From Fig.5.2.6 , one can understand that upto a dose of 10^4 Gy, there are no changes in the transmittance pattern. Only from 10^5 Gy dose it starts changing. Though there are no absorption peaks observed, it has been noted that the transmittance shifts towards higher wave length because of gamma exposure. The changes are significant in the region 300 – 500 nm. For dosimetric applications lower gamma doses ($< 10^4$ Gy) may not be as useful as higher doses. Fig.5.2.7 shows the dose dependent transmittance curves spectra at different wave lengths. Transmittance measured at different doses and at different wavelengths have been summarised in Table 5.2.9. It may be seen here that there is no observable influence on transmittance at 620 nm for different gamma doses. However, at lower wave lengths (370 & 410 nm) the transmittance decreases rapidly for gamma doses of 10^5 - 10^6 Gy.

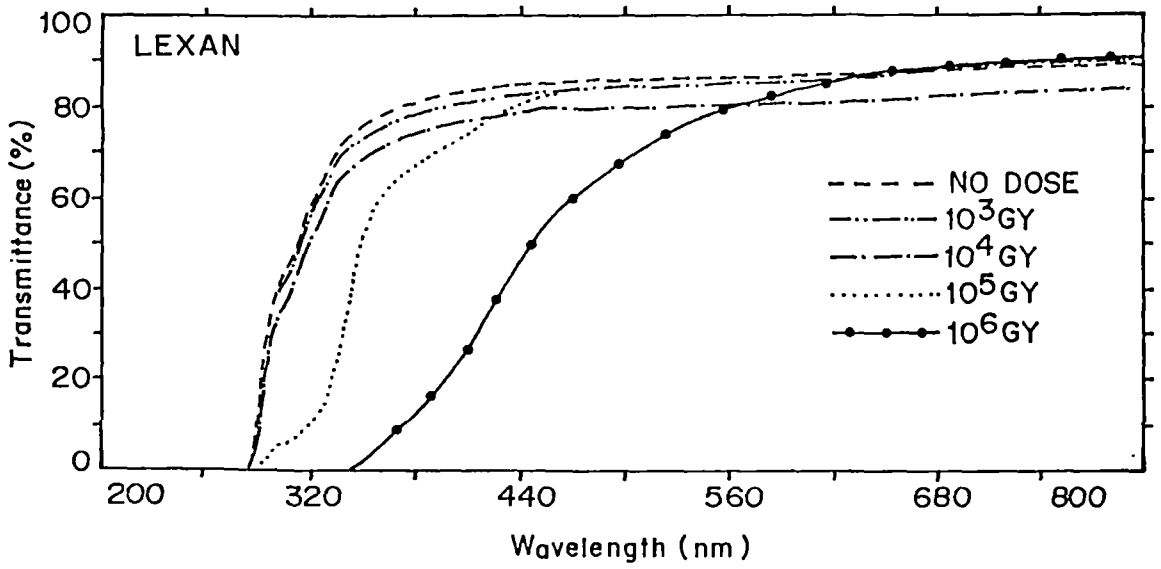

Fig. 5.2.6. UV-VIS transmittance spectra of Lexan detector exposed to different gamma doses.

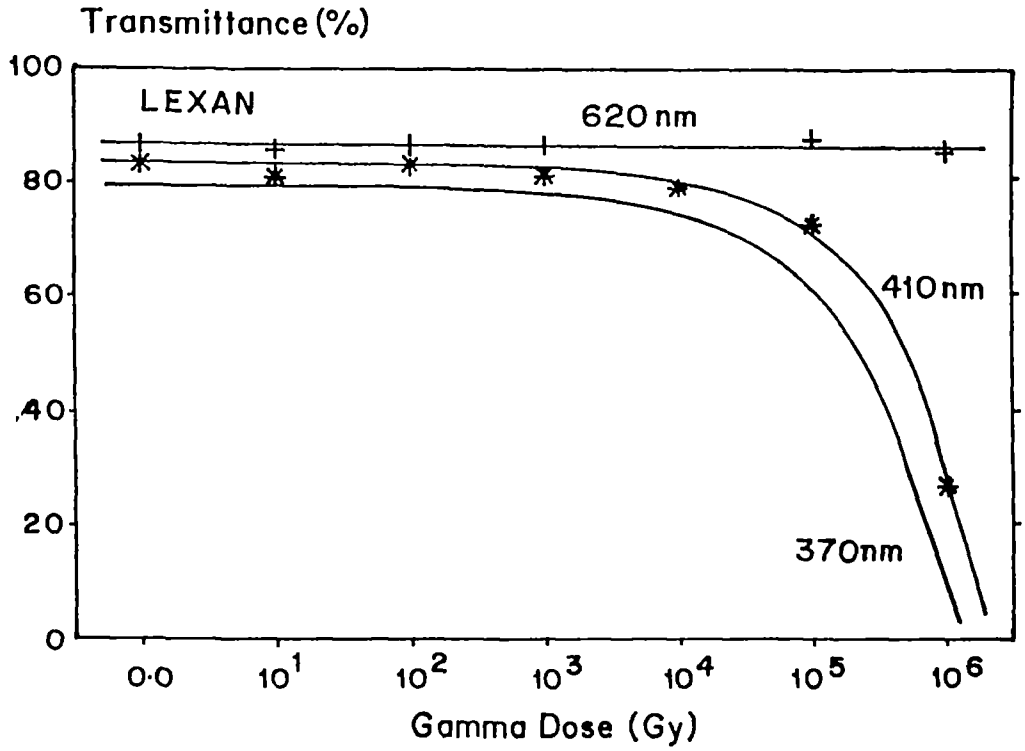

Fig. 5.2.7. Dose dependence variation in transmittance of Lexan detector at different wave lengths.

The transmittance spectra of Polycarbonate detectors exposed to different gamma doses are shown in Fig.5.2.8. It can be seen that there is no change in the transmittance upto the doses of 10^4 Gy. It then starts decreasing with dose. This decrease can be observed only between 390 nm to 520 nm. The difference in transmittance between 10^6 Gy and other lower doses became largest at around 410 nm. It is also quite interesting to observe that above 10^4 Gy of gamma dose , with the increase of doses, slope of the transmittance spectra starts decreasing and at 10^6 Gy, almost flatten out. So from these studies it can be concluded that gamma-ray dosimetric studies using UV-VIS light transmittance is more effective in the wavelength region between 370–480 nm. Fig.5.2.9 gives change in transmittance(%) with increasing dose. From this observation, it may also be concluded that transmittance at 420 nm is strongly related to the amount of gamma exposure and so it can be used as a simple method in gamma ray dosimetric measurements. Table 5.2.10 lists the values of transmittance measured at different wave lengths for different gamma doses.

IR study of these gamma irradiated polymers is not very informative. It is observed in all the cases that the concentration of some of the existing groups or bonds decreased at high doses of gamma irradiation. Neither total cleavage of bonds nor any new bonds are formed. One of the typical IR spectra of gamma irradiated Makrofol-E detector is shown in Fig.5.2.10.

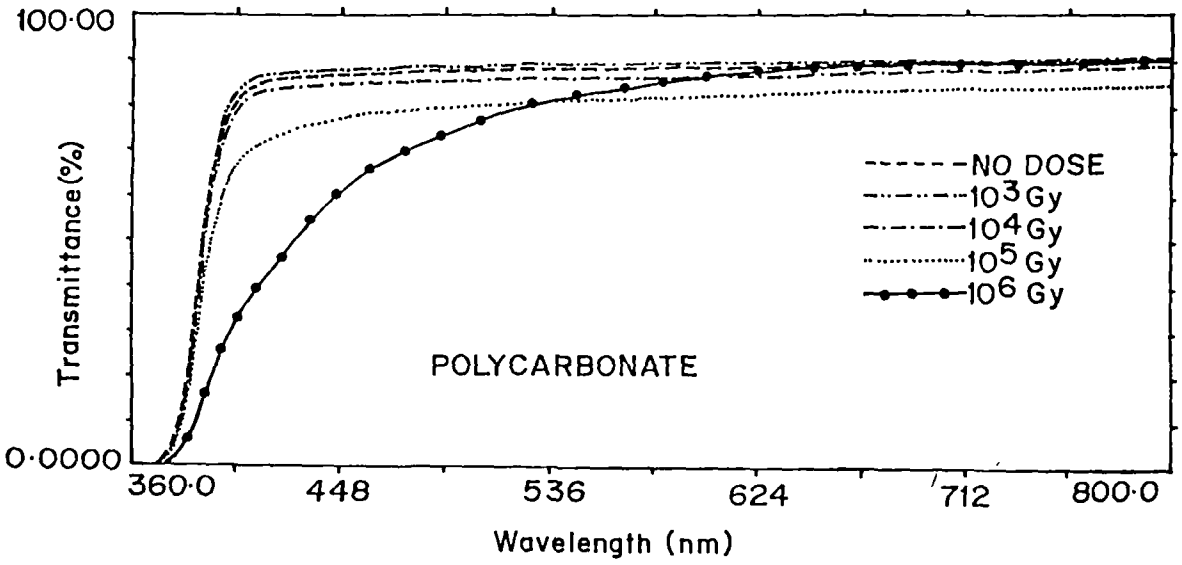

Fig. 5.2.8. UV-VIS transmittance spectra of Polycarbonate detector exposed to different gamma doses.

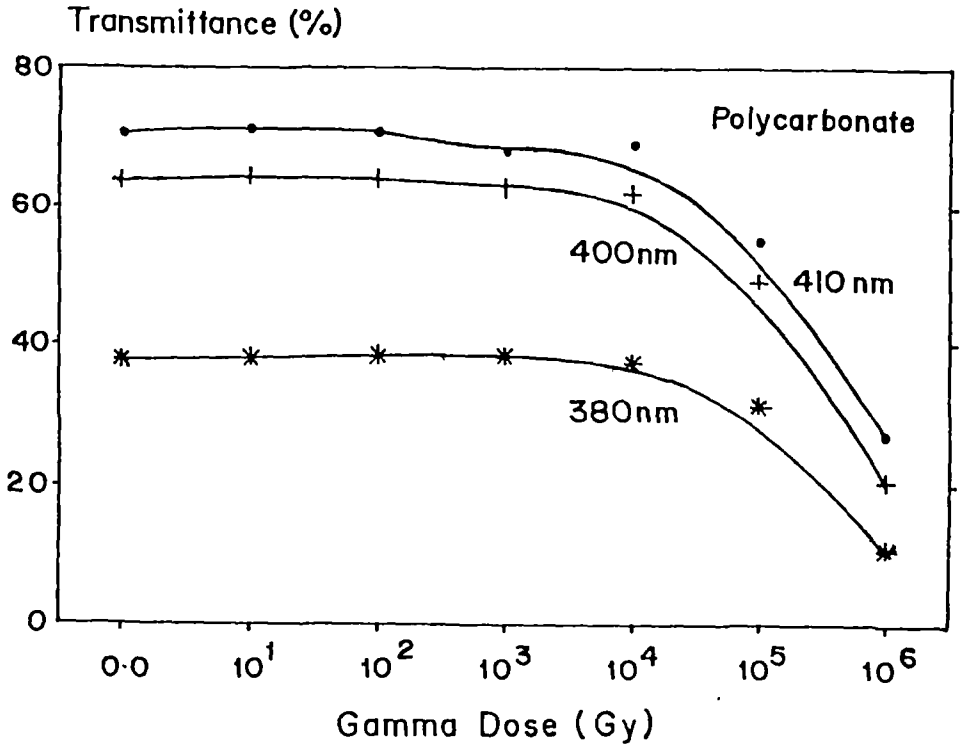

Fig. 5.2.9. Dose dependence variation in transmittance of Polycarbonate detector at different wave lengths.

TABLE - 5. 2.9. TRANSMITTANCE (%) VERSUS WAVE LENGTH OF GAMMA IRRADIATED LEXAN DETECTOR

Wavelength	No Dose	10^1 Gy	10^2 Gy	10^3 Gy	10^4 Gy	10^5 Gy	10^6 Gy
370 nm	79.62	77.96	79.64	79.64	72.52	63.99	9.35
380 nm	80.86	78.39	80.97	80.94	74.02	66.98	12.96
390 nm	81.86	79.56	82.01	81.97	75.21	69.44	16.87
400 nm	82.62	80.38	82.76	82.67	76.12	71.76	21.35
400 nm	75.24	74.42	66.04	72.56	71.23	16.84	0.056
410 nm	83.25	81.16	83.41	83.35	76.86	74.08	26.69
620 nm	86.82	85.89	87.03	87.02	80.82	87.77	85.18

TABLE - 5. 2.10. TRANSMITTANCE (%) VERSUS WAVE LENGTH OF GAMMA IRRADIATED POLYCARBONATE DETECTOR

Wavelength	No Dose	10^1 Gy	10^2 Gy	10^3 Gy	10^4 Gy	10^5 Gy	10^6 Gy
410 nm	70.50	71.50	71.07	68.03	68.95	55.09	27.03
400 nm	63.64	64.60	64.22	63.13	62.22	49.31	20.60
390 nm	37.66	38.01	38.28	38.22	37.38	31.30	10.77
380 nm	7.71	7.12	7.07	7.85	7.04	10.13	2.26

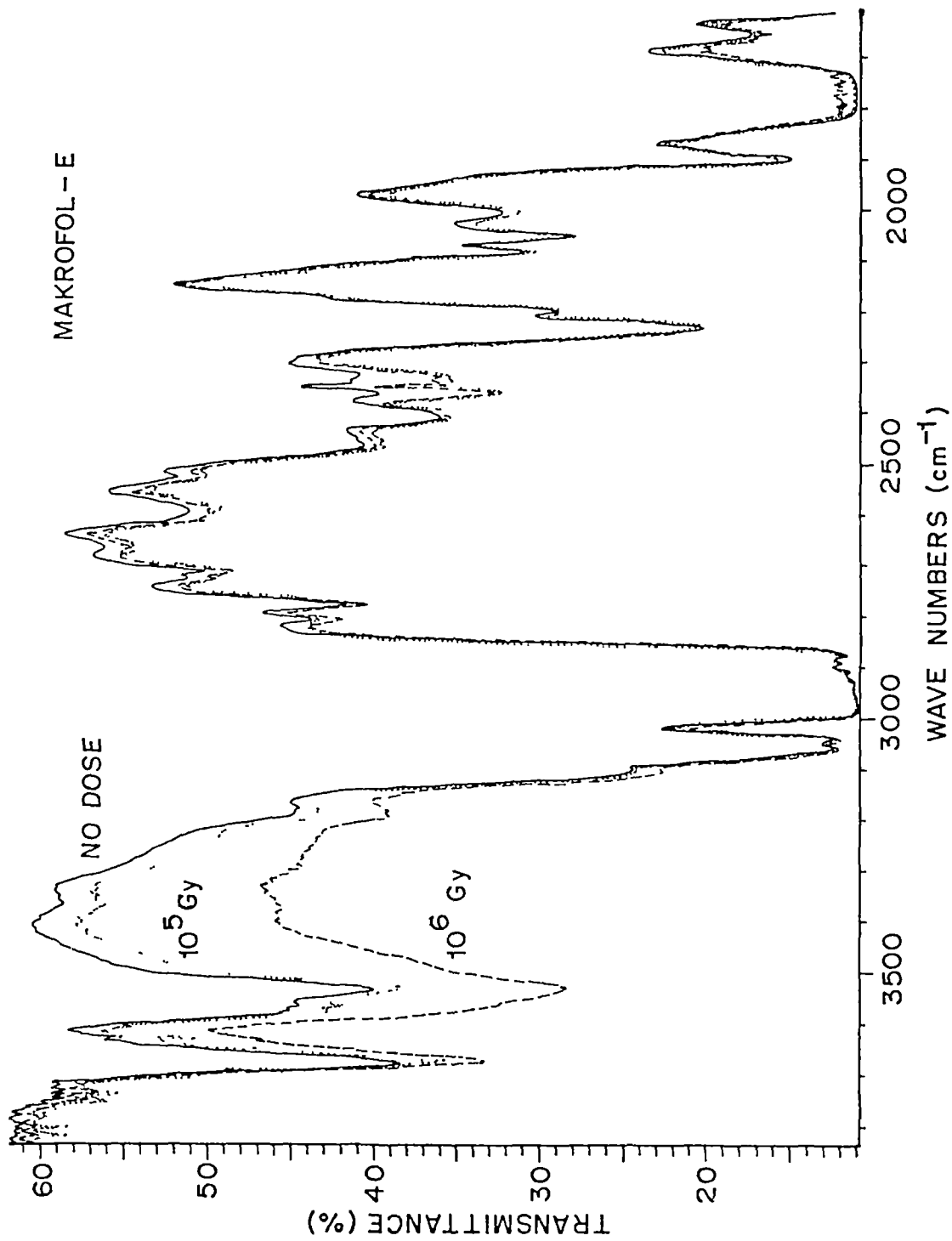

Fig. 5.2.10. IR spectra of gamma irradiated Makrofol-E detector.

ESR study of these detectors reveals some interesting information about the chemical modifications. It is observed that for all the three polymers, no radicals are observed till the dose of 10^5 Gy. But at the dose of 10^6 Gy, one could get a signal for the radical formation as shown in Fig.5.2.11. It is quite significant to observe that in all three cases the radical does not show any hyperfine splitting. Moreover, the radical signal gives the same g-value of 2.003 Gauss. This clearly signifies the presence of similar type of radicals in these polymeric films. Similar ESR signal in Makrofol was also observed by Chambaudet et.al. [13]. Edmonds and Durrani [14] also observed the same type of radical for gamma irradiated Lexan. They ascribed this signal to the presence of "carbon like" radicals, where the unpaired electron is delocalized over a number of carbon cycles or conjugated linear chains. But the carbon like radicals which take part in the delocalization must be created by some bond scission and if so, what happens to the other radicals? The other radicals should have also given its own signal. No explanation to this was offered by the earlier authors.

Since all the detectors discussed here having the same chemical structure and since the radical signals are also identical, so we can assume that some sort of similar chemical change might have taken place. Since there is no increase in the etch-rate values of these detectors at the dose of 10^6 Gy, clearly gives the indication that the back bone structure of these polymers remain unchanged by gamma

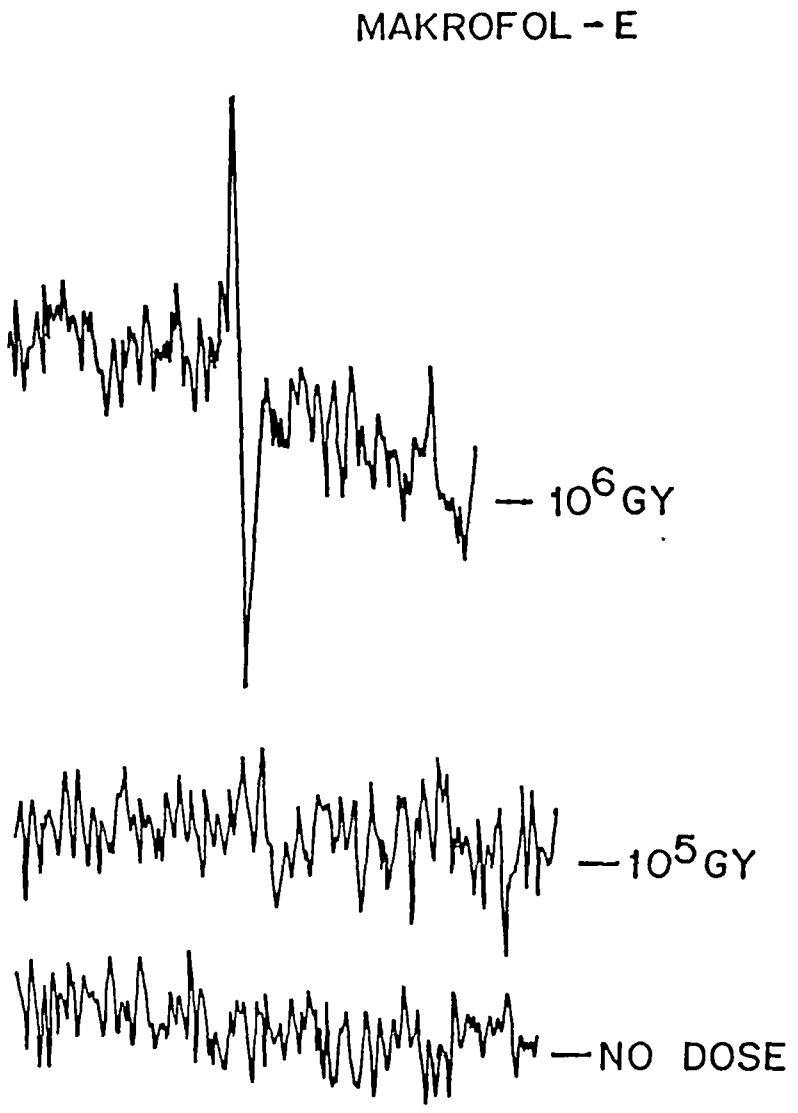

Fig. 5.2.11. ESR spectra of gamma irradiated Makrofol-E detector shows the radical signal at the dose of 10^6 Gy.

radiation. Had there been any scissioning of the main chain of the polymer, that would have reflected in the etch-rate values. In that case we should have got higher etch-rate values. So the radical which is observed may be due to the scission of some side chains like C–H bond of the phenyl ring. After scission, the Hydrogen radical that is formed due to bond cleavage probably combines with some other hydrogen radical and forms hydrogen gas. The radical on carbon atom delocalizes over the benzene ring system [13,14]. That is why only singlet radical signal for carbon is observed. Moreover the development of colour in the sample at the dose of 10^6 Gy is probably due to the presence of radicals in the irradiated polymeric film matrix.

5.2.4. THERMOGRAVIMETRIC ANALYSIS :Thermogravimetric analysis of Makrofol-E shows single step decomposition. In all cases, no change in the decomposition pattern is observed till the temperature of 430°C. The weight loss starts around 430°C and finishes around 580°C. Of course at 580°C, the total decomposition of the material is not completed. About 25% of the total weight still remains. There is no change in the thermal stability or decomposition pattern is observed in this detector because of gamma irradiation.

For Lexan also, it is a single step decomposition. In all cases the detectors are stable upto the temperature of 440°C. Then there is weight loss till the temperature of 580°C. There is no appreciable change in weight loss because of gamma exposure. Only at 10^6 Gy of

gamma dose, little change is observed. At around 580°C, till the dose of 10^5 Gy, 70% weight loss is observed. But at higher doses (10^6 Gy) 75% weight loss took place. So we can say that gamma radiation decreases the thermal stability of Lexan at high dose (10^6 Gy) particularly in the temperature range of 580°C–680°C.

Decomposition pattern of polycarbonate with temperature is quite striking. As shown in Fig.5.2.12, it is quite clear that upto a dose of 10^5 Gy, it is a single step decomposition. But when the dose becomes 10^6 Gy, two step decomposition is observed. In all cases, the decomposition starts around 480°C and finishes around 570°C. Above 570°C, no weight loss is observed till the dose of 10^5 Gy. Total weight loss in the range between 480°C – 570°C is around 70%. But in case of 10^6 Gy, weight loss starts around 420°C and finishes around 570°C. Again the second step of weight loss starts at 570°C and it continues upto 700°C. At 700°C, 7% of the total weight remains. This clearly indicates that upto the dose of 10^5 Gy, the detector is stable after first decomposition i.e. above 570°C, but in case of gamma doses of 10^6 Gy, the detector looses its stability above 570°C and weight loss continues upto the temperature of 700°C.

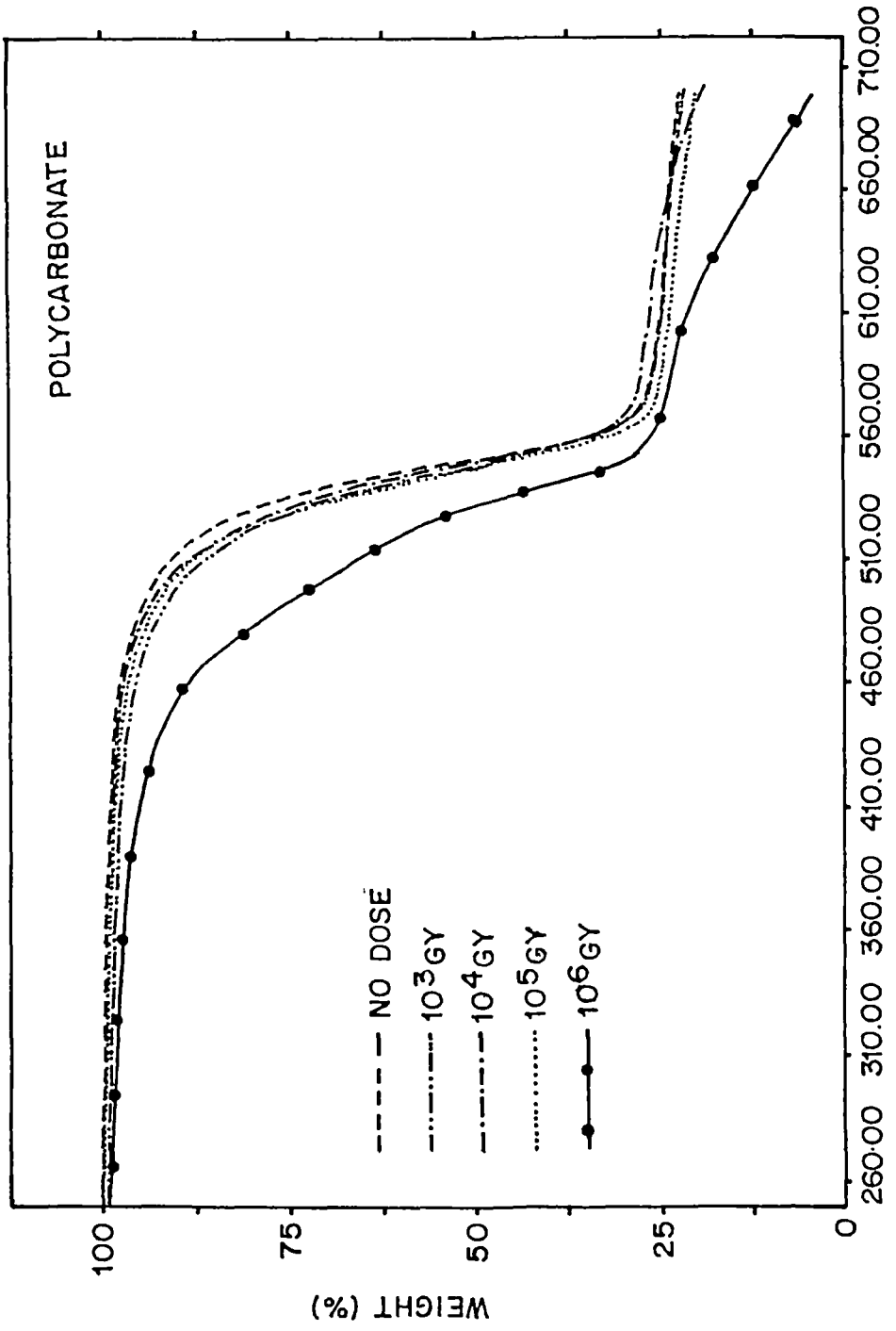

Fig. 5.2.12. TGA thermogram of gamma irradiated Polycarbonate polymeric detector.

PART-3

This part consists of results and discussion pertaining to the modifications in Triafol-TN and Triafol-BN caused by gamma radiation.

5.3.1. PHYSICALLY OBSERVABLE CHANGES:- There were no visible changes observed in these polymers upto the dose of 10^5 Gy of gamma radiation. But at 10^6 Gy, the Triafol-TN detector became so brittle that it turned into powder after irradiation. Hence no measurements could be performed for Triafol-TN exposed to 10^6 Gy. It has also been observed that the Triafol-BN detector turned brittle at a dose of 10^6 Gy. Though the Triafol-BN detector became brittle at the same dose, but it did not turn into powder and hence different measurements could be performed.

5.3.2. TRACK STUDIES :- The bulk-etch rates (V_G) are determined by the track diameter technique. The bulk-etch rates at different etching temperatures (55°C, 60°C, 65°C and 70°C) have been determined and are listed in Table 5.3.1 and Table 5.3.2 for both pre-gamma and post-gamma irradiation of Triafol-TN. The etching parameters of Triafol-TN as a function of different doses of gamma rays are measured and compared with the pristine material. Fig.5.3.1 shows the variation of V_G at 55°C and 70°C for Triafol-TN exposed to different doses of gamma rays. It is evident from the data that V_G remains almost constant in the range from no dose to 10^5 Gy. This is

TABLE - 5. 3.1 BULK- ETCH RATE (V_G) IN μm/h FOR TRIAFOL-TN FOR PRE- GAMMA EXPOSURE

Temperature	No Dose	10^1 Gy	10^2 Gy	10^3 Gy	10^4 Gy	10^5 Gy
55°C	1.75 ± .07	1.74 ± .07	1.77 ± .07	1.89 ± .07	1.80 ±.07	1.95 ±.07
60°C	2.35 ± .12	2.39± .12	2.42± .12	2.41± .12	2.40± .12	2.42± .12
65°C	2.76 ± .09	2.83± ..09	2.84± .09	2.84± .09	2.88± .09	2.86± .09
70°C	3.42 ± .13	3.61± .13	3.62± .13	3.75± .13	3.77± .13	3.83± .13

TABLE - 5. 3.2 BULK- ETCH RATE (V_G) IN μm/h FOR TRIAFOL-TN FOR POST-GAMMA EXPOSURE

Temperature	No Dose	10^1 Gy	10^2 Gy	10^3 Gy	10^4 Gy	10^5 Gy
55°C	1.75 ± .07	1.76 ± .07	1.77 ± .07	1.80 ± .07	1.79 ±.07	1.86 ±.07
60°C	2.35 ± .12	2.23± .12	2.40± .12	2.41± .12	2.39± .12	2.39± .12
65°C	2.76 ± .09	2.79± ..09	2.79± .09	2.80± .09	2.81± .09	2.82± .09
70°C	3.42 ± .13	3.62± .13	3.63± .13	3.71± .13	3.72± .13	3.79± .13

probably due to the fact that neither sufficient cross-linking nor scission of the polymeric chains has taken place which could influence the etch rates. The bulk-etch rates of this detector have been found to be comparable for both pre- and post-gamma exposure as summarised in Table 5.3.1 and Table 5.3.2. Hence, it is evident that the sequence of exposure to gamma radiation causes no significant effect on the bulk–etch rate in the case of Triafol-TN polymeric detectors. Bulk-etch rate (V_G) data of Triafol-BN provide very interesting results as shown in Fig.5.3.2. It is found that there are no change in V_G upto a gamma dose of 10^5 Gy . At a dose of 10^6 Gy, V_G increases abruptly for all etching temperatures. This unusual increase may be due to the scission of the molecular chain caused by gamma radiation. It is also observed that etch-rate remains invariant for both pre - and post -irradiated samples. Table 5.3.3 and Table 5.3.4 list the etch-rate values at different doses and at different temperatures for both the pre and post - gamma exposed Triafol-BN. These results show that the tracks created by the fission fragments are enhanced by high doses (10^6 Gy) of gamma radiation.

The activation energies for bulk-etching of these two polymeric solids have been determined by plotting Log V_G against the reciprocal of etching temperature (in absolute unit) for different doses. The data have been presented in Table 5.3.5 and Table 5.3.6. The straight lines which are parallel to each other (Fig.5.3.3 & Fig.5.3.4) reveal

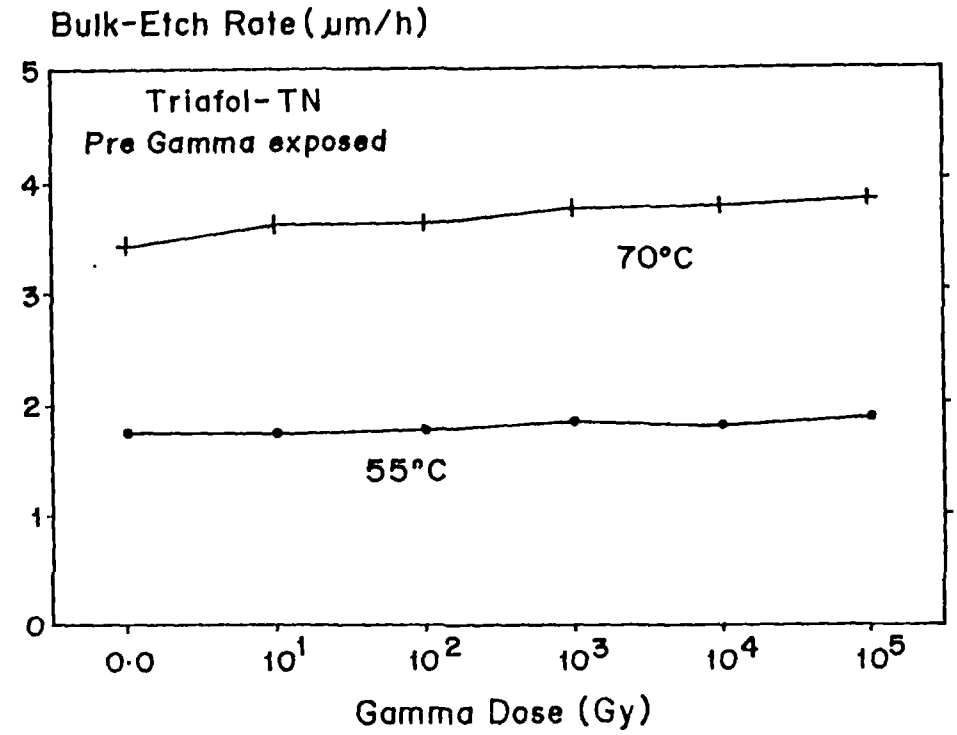

Fig. 5.3.1. Bulk-etch rate of pre - gamma irradiated Triafol-TN detector.

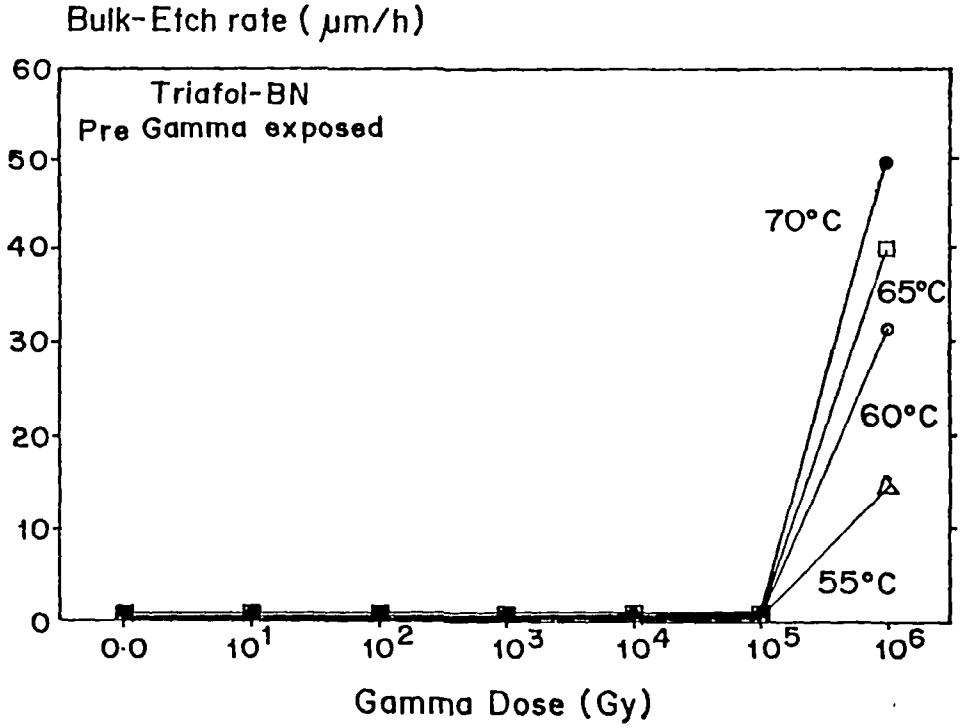

Fig. 5.3.2. Bulk-etch rate of pre-gamma irradiated Triafol-BN detector at different gamma doses and at different etching temperatures.

TABLE - 5. 3.3 BULK- ETCH RATE (V_G) IN μm/h FOR TRIAFOL-BN FOR PRE GAMMA EXPOSURE

Temperature	No Dose	10^1 Gy	10^2 Gy	10^3 Gy	10^4 Gy	10^5 Gy	10^6 Gy
55°C	0.38±.04	0.39±.04	0.38±.04	0.39±.04	0.39±.04	0.50±.04	14.66±1.6
60°C	0.64 ±05	0.65±.05	0.65±.05	0.65±.05	0.65±.05	0.68±.05	31.38±2.9
65°C	0.70±.06	0.73±.06	0.73±.06	0.72±.06	0.72±.06	0.75±.06	40.61±4.2
70°C	0.82±.06	0.82±.06	0.83±.06	0.84±.06	0.84±.06	1.10±.06	49.10±4.2

TABLE - 5. 3.4 BULK- ETCH RATE (V_G) IN μm/h FOR TRIAFOL-BN FOR POST- GAMMA EXPOSURE

Temperature	No Dose	10^1 Gy	10^2 Gy	10^3 Gy	10^4 Gy	10^5 Gy	10^6 Gy
55°C	0.38±.04	0.39±.04	0.39±.04	0.39±.04	0.39±.04	0.51±.04	15.60±1.6
60°C	0.64±.05	0.63±.05	0.61±.05	0.63±.05	0.65±.05	0.66±.05	29.29±2.9
65°C	0.70±.06	0.69±.06	0.69±.06	0.69±.06	0.70±.06	0.72±.06	39.88±4.2
70°C	0.82±.06	0.83±.06	0.83±.06	0.84±.06	0.84±.06	1.01±.06	50.49±4.2

TABLE - 5.3.5. ACTIVATION ENERGY IN ($kJmol^{-1}$) FOR BULK-ETCHING OF TRIAFOL -TN DETECTOR

Detectors	No Dose	10^1 Gy	10^2 Gy	10^3 Gy	10^4 Gy	10^5Gy
Pre-gamma set	40.09 ± 3.74	43.14 ± 3.74	42.28 ± 3.74	41.97 ± 3.74	43.67 ± 3.74	42.21 ± 3.74
Post - gamma set	40.09 ± 3.74	42.97 ± 3.74	42.21 ± 3.74	43.35 ± 3.74	43.03 ± 3.74	41.77 ± 3.74

TABLE - 5.3.6. ACTIVATION ENERGY IN ($kJmol^{-1}$) FOR BULK-ETCHING OF TRIAFOL -BN DETECTOR

Detector	No Dose	10^1 Gy	10^2 Gy	10^3 Gy	10^4 Gy	10^5Gy	10^6Gy
Pre Gamma	53.08 ± 5.46	53.08 ± 5.46	52.32 ± 5.46	51.17 ± 5.46	51.17 ± 5.46	59.98 ± 5.46	54.81 ±7.19
Post Gamma	53.08 ± 5.46	51.17 ± 5.46	51.17 ± 5.46	49.83 ± 5.46	51.17 ± 5.46	53.08 ± 5.46	51.74 ± 7.19

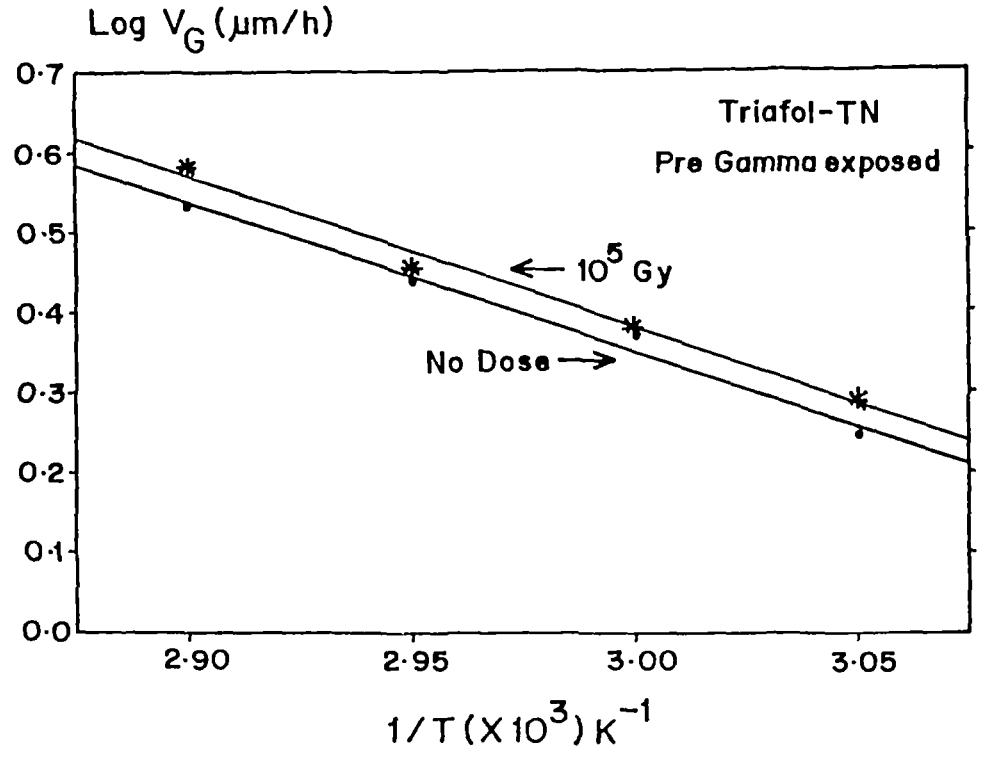

Fig. 5.3.3. Plot of Log V_G versus 1/T for Triafol-TN detector shows the parallel straight lines reveals the constancy of Activation Energy.

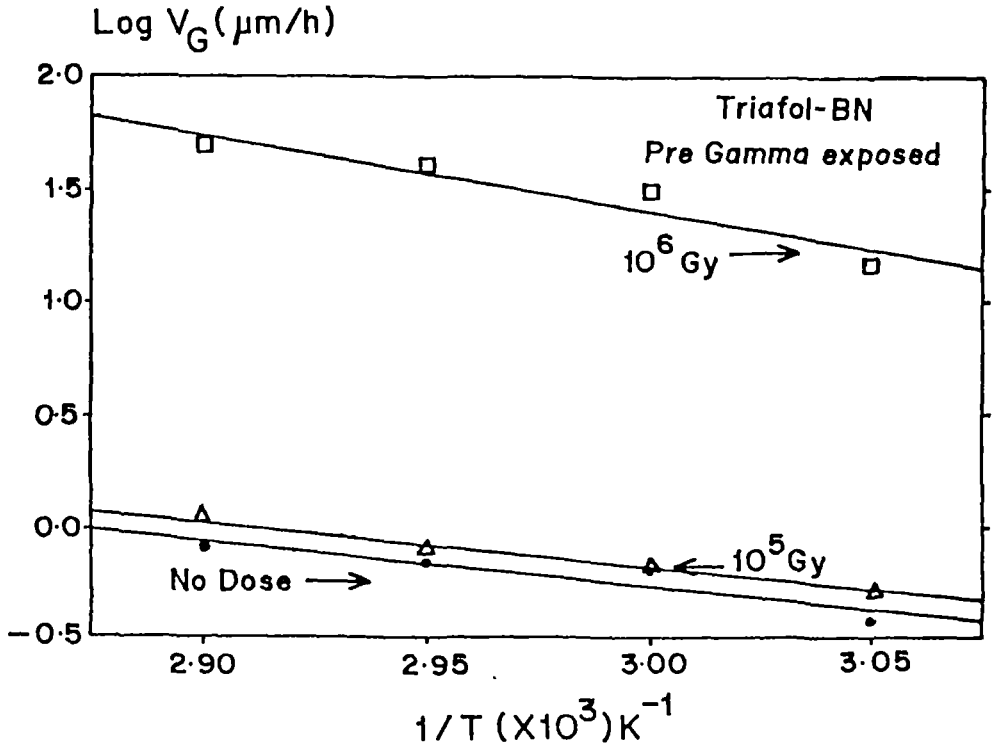

Fig. 5.3.4. Plot of Log V_G versus 1/T for Triafol-BN detector shows the parallel straight lines reveals the constancy of Activation Energy.

that the activation energy for bulk-etching remains unaltered under different doses of gamma radiation. It is interesting to observe that even though the etch-rate increases at 10^6 Gy, the activation energy remains the same and is found to be around 53 kJ/mole for Triafol-BN detector. Since, from the Arrhenius relation it is obvious that with increasing V_G, activation energy should decrease. This can be explained as follows : the rate constant A in Arrhenius relation changes with gamma doses but activation energy remains constant. Hence the increased rate of etching reaction due to radiation induced damage of polymer does not contribute to any observable decrease in activation energy.

5.3.3. SPECTRAL STUDIES :- Spectral studies were done using three different techniques to identify any structural characteristic changes due to gamma irradiation. Since the track studies of Triafol-BN clearly show some sort of bond scission at 10^6 Gy of gamma dose, we tried to analyse the chemical transformations or rearrangements which occurred in this particular detector at different doses. IR, ESR and UV-VIS techniques were used for this analysis.

UV-VIS study of Triafol-TN does not give any information about the chemical changes. It is understood that there is no significant change in the pattern of the transmittance, which means that no structural changes have taken place. This observation supports our

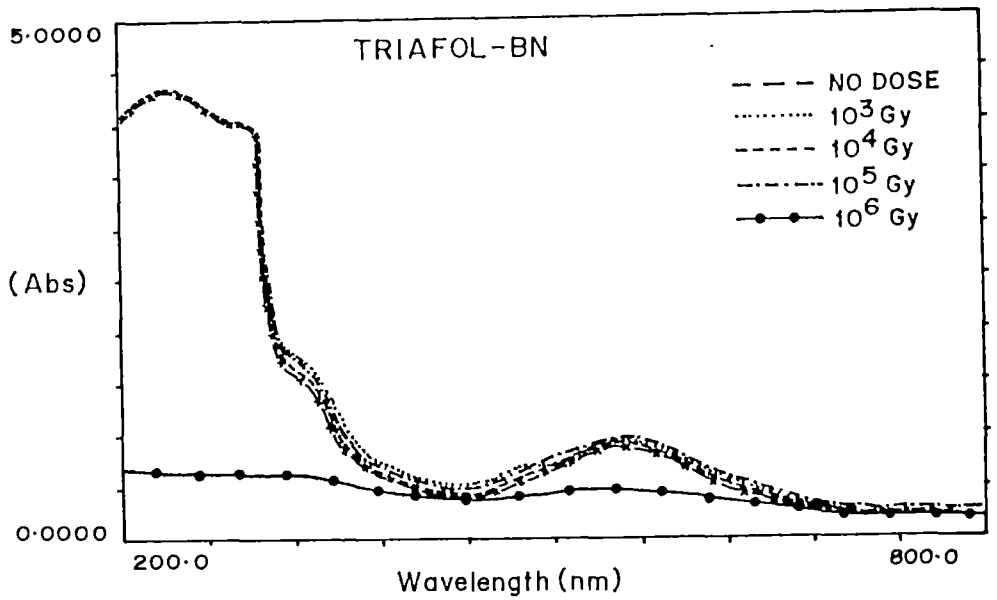

Fig. 5.3.5. UV - VIS absorption spectra of gamma irradiated Triafol-BN detector.

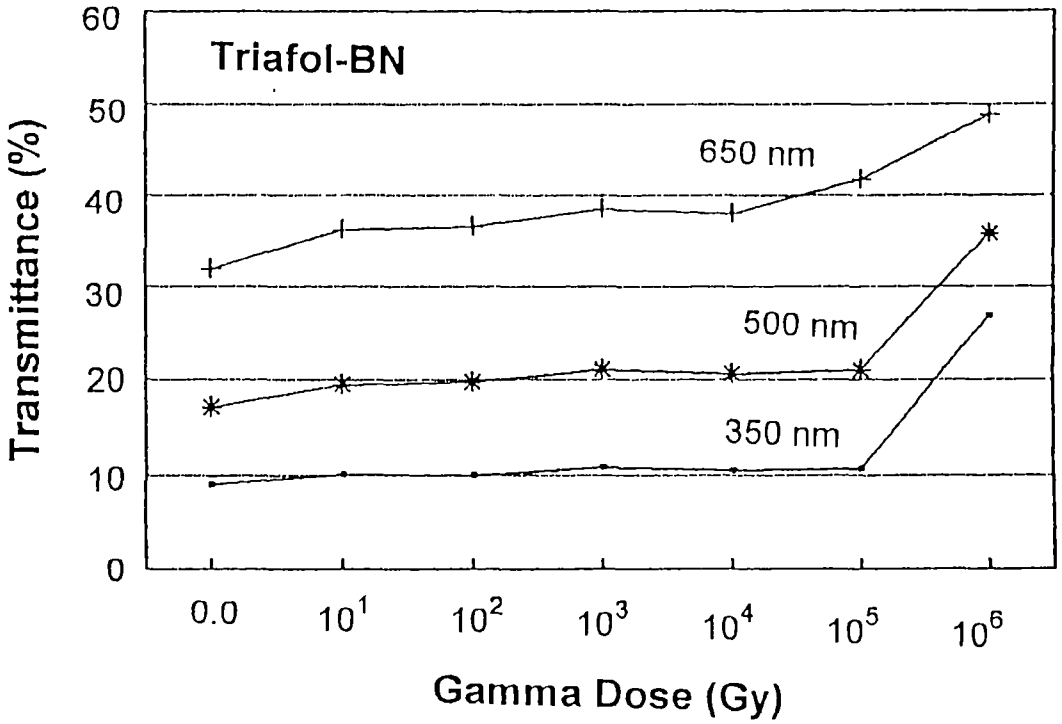

Fig. 5.3.6. Dose dependence variation in transmittance of gamma irradiated Triafol-BN detector.

results obtained from the track study. Any structural change, due to radiation damage, either cleavage or cross - linking would have shown corresponding signals in the UV-VIS spectra. UV-VIS study of Triafol-BN shows very significant changes. It can be seen in Fig.5.3.5 that below the dose of 10^5 Gy, there is no change in the absorption pattern. But at the dose of 10^6 Gy, the absorption pattern totally changes. The change is significant in the region 200–650 nm. It may be observed in Fig.5.3.5 that the absorption peak corresponding to 540 nm is disappeared. This signifies that the purple dye present in the film destroyed to some extent. That is why the colour of the detector becomes faded. The shoulder at 310 nm is probably because of the antioxidant present in the film [15] . At 10^6 Gy dose, the disappearance of the shoulder indicates that the antioxidant is removed by radiation. That is why the oxidation was favoured and the detector became brittle.

For dosimetric applications, UV–VIS study is very useful. For this, the transmittance(%) is measured against gamma dose at different wave lengths. Fig.5.3.6 gives the dependence of transmittance on gamma dose for Triafol-BN. Table 5.3.7 and Table 5.3.8 gives the transmittance(%) measured for different doses and at different wave lengths. It is clear from Fig.5.3.6 that for dosimetric applications, the doses of gamma radiation upto 10^5 Gy are not very useful. So systematic study from 10^5 Gy dose onwards at different dose intervals will be very useful for this purpose.

TABLE -5. 3. 7. TRANSMITTANCE (%) VERSUS WAVE LENGTH OF TRIAFOL-TN AT DIFFERENT DOSES OF GAMMA RADIATION

Wavelength	No Dose	10^1 Gy	10^2 Gy	10^3 Gy	10^4 Gy	10^5 Gy
350 nm	24.99	28.44	26.06	24.93	20.86	21.26
400 nm	28.00	28.44	29.31	28.40	24.07	27.04
473 nm	37.30	42.72	38.84	38.45	32.31	36.46
598 nm	23.51	25.83	23.77	23.50	20.45	26.04
650 nm	24.95	27.18	25.00	25.01	21.98	29.00

TABLE-5.3.8. TRANSMITTANCE (%) VERSUS WAVE LENGTH OF TRIAFOL-BN AT DIFFERENT DOSES OF GAMMA RADIATION

Wavelength	No Dose	10^1 Gy	10^2 Gy	10^3 Gy	10^4 Gy	10^5 Gy	10^6 Gy
350 nm	9.03	10.13	10.07	10.88	10.60	10.75	26.75
400 nm	25.69	29.93	29.36	30.65	30.38	29.19	37.60
450 nm	31.63	36.57	37.37	37.41	37.03	37.39	41.27
500 nm	17.19	19.49	19.73	21.08	20.61	21.00	35.79
650 nm	31.87	36.16	36.55	38.53	37.93	41.80	48.83

IR spectra for materials exposed to different doses of gamma rays are compared with the spectrum obtained for pristine samples. No significant change in the vibrational frequencies has been observed, which implies that inter chain separation is not affected by gamma radiation. IR study does not give any information about the bond cleavage or cross linking as we expected. It is found that all the peak positions are unshifted. Only the absorbance or transmittance value of particular functional group changes. It can be seen for *Triafol-BN* that for some of the important region like, 1600-1800 cm^{-1} (ester carbonyl region), 2850 - 3000 cm^{-1} (C-H stretching region), the absorbance decreases at 10^6 Gy dose as shown in Fig.5.3.7. This is probably due to the result of decrease in concentration of the pre-existing bonds or groups. It is striking to observe that the peak position at around 2360 cm^{-1}, which is due to the presence of CO_2 also becomes very intense at 10^6 Gy. This can be possible if some of the ester or ether groups of the detector got destroyed by radiation and produce CO_2 which in turn remained trapped in the detector matrix. Mass spectrometric measurements will be very useful for studying the radiation induced fragmentation of polymeric chains.

ESR study shows no radical signal both in unexposed as well as in exposed samples. So it could not give any information about the structural transformation.

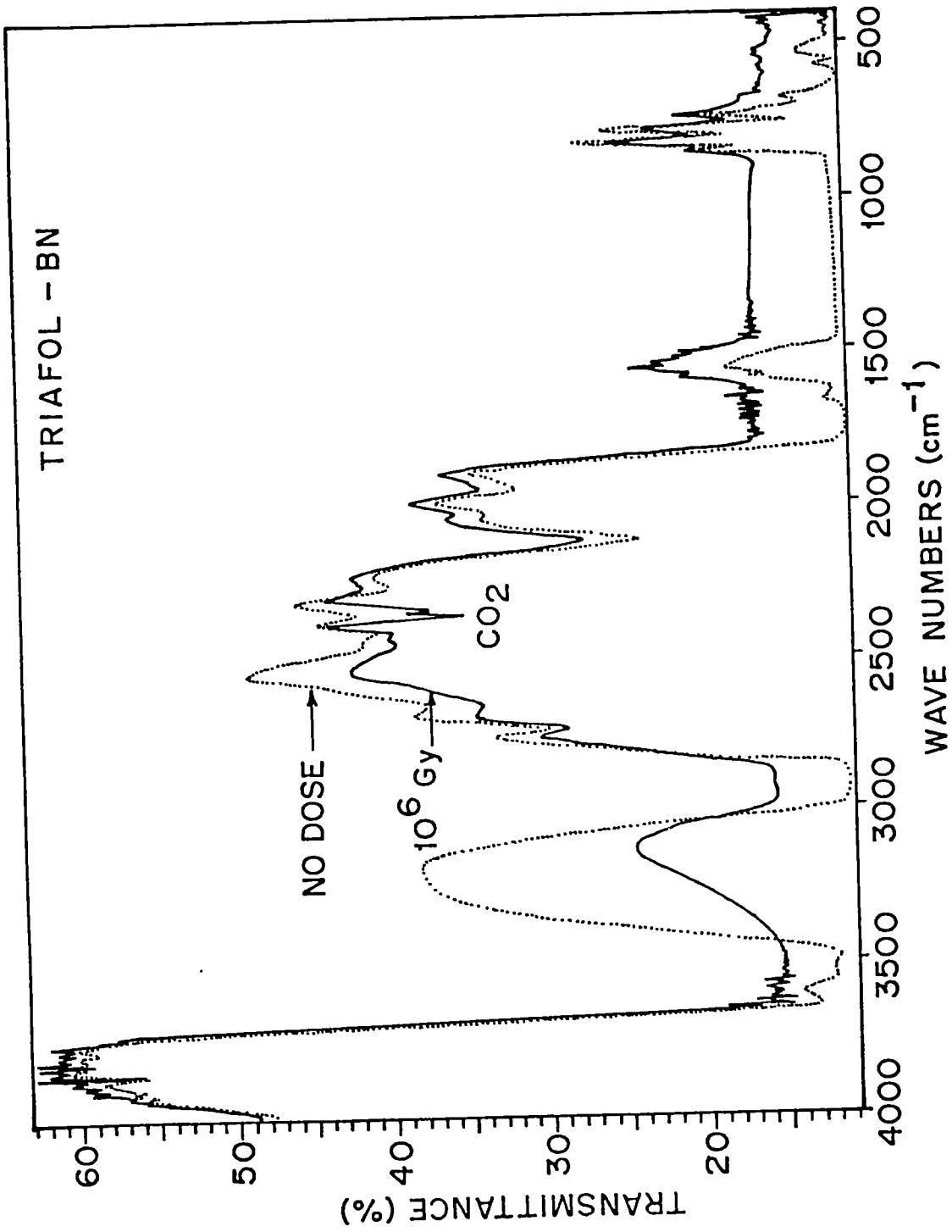

Fig. 5.3.7. IR spectra of gamma irradiated Triafol-BN detector.

5.3.4. THERMOGRAVIMETRIC ANALYSIS :- Thermogram of Triafol-TN exposed to different doses of gamma rays shows a similar trend. In all cases, it is observed that significant weight loss occurrs at around 330°C and continues till 447°C. The weight loss takes place in a single step. No step wise decomposition is observed. It is clear from the TGA response curve (Fig.5.3.8) that, the polymer is thermally stable upto 330°C in all cases. Above this temperature it decomposes and loses around 78% of the weight of the polymer . From this data, no conclusion about the thermal stability could be drawn. So different doses of gamma rays could not alter thermal stability of Triafol-TN detectors. These observations corroborate, the conclusions drawn from the track study and spectral studies, that gamma radiations do not produce change in the structure of Triafol-TN. It may be possible that some change occur in the thermal stability at higher doses that is above 10^5 Gy. Triafol-BN detector exposed to different doses of gamma radiation are heated from 40°C to around 640°C and consequently the weight losses were recorded. Fig.5.3.9 shows the total TGA thermogram. In case of no gamma dose the detector undergoes complete weight loss at around 580°C. But at higher doses (above 10^4Gy), about 7-9 % weight remains at that temperature. Upto the dose of 10^5 Gy, the detectors are thermally stable till 310°C and then the weight loss process start. But in the case of 10^6 Gy dose, the weight loss process starts at around 220°C. From the results obtained it can be concluded that because of high gamma exposure, at 10^6 Gy dose, the detectors stability decreases so the weight loss process starts at a lower temperature.

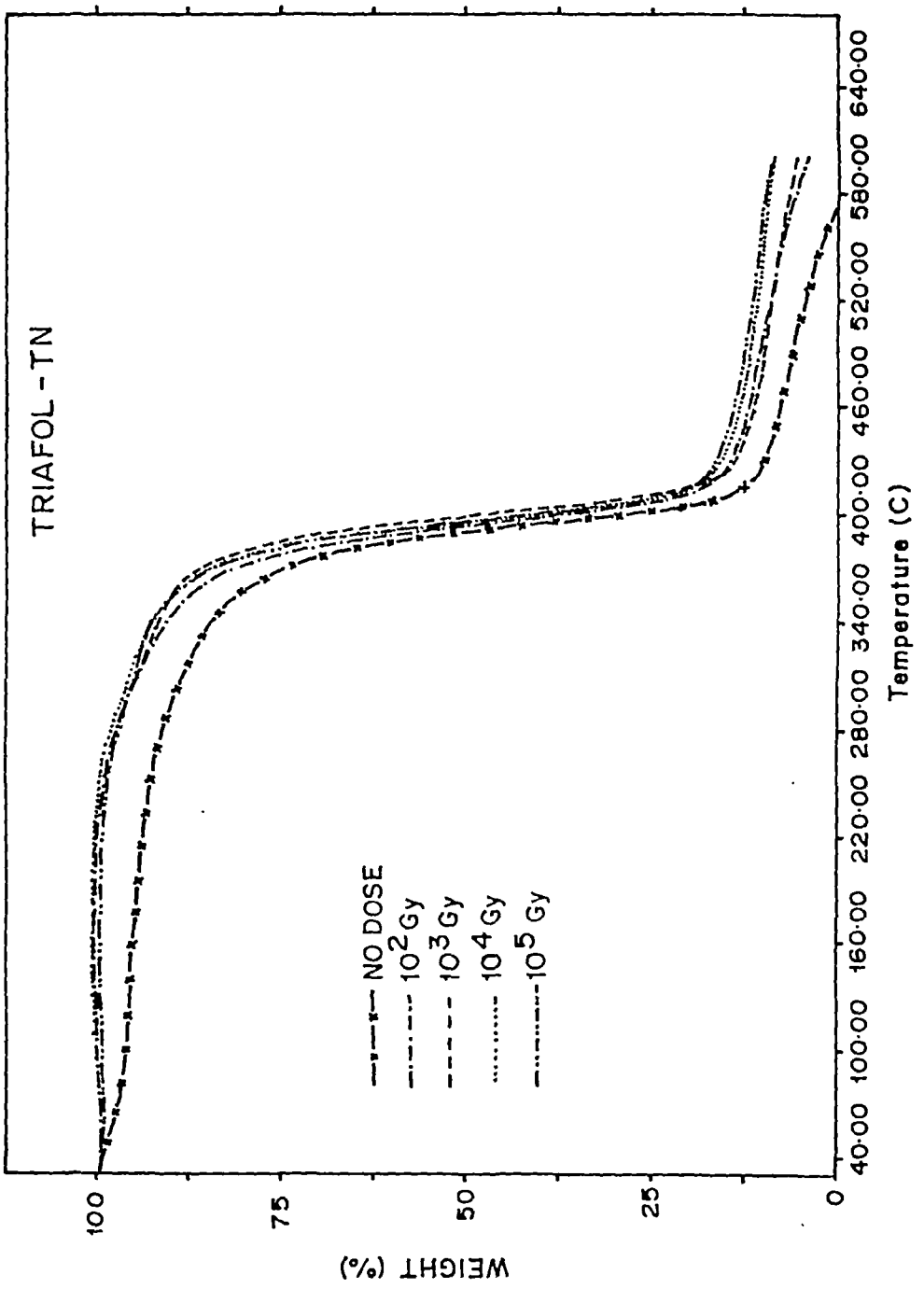

Fig. 5.3.8. TGA thermogram of gamma irradiated Triafol-TN detector.

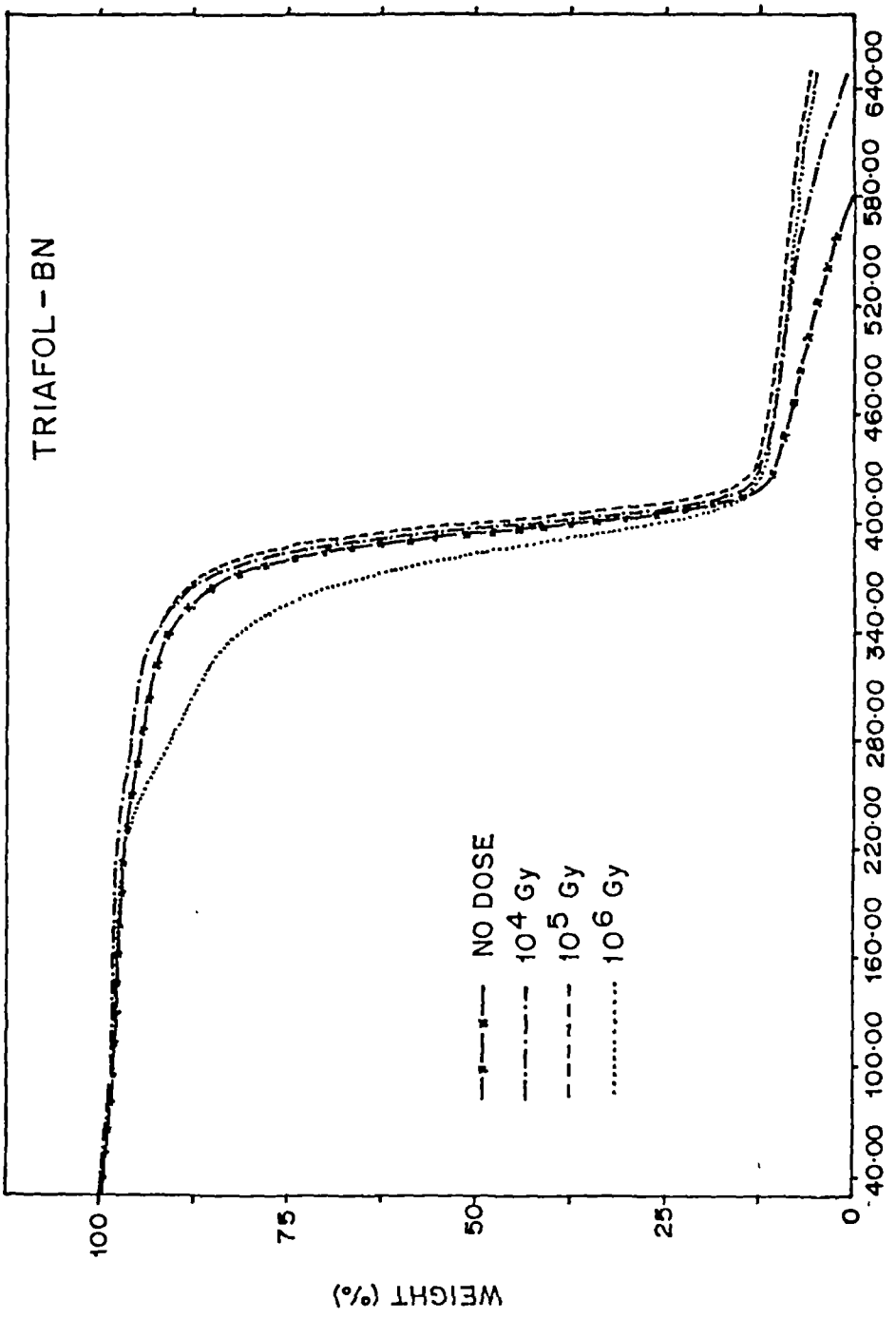

Fig. 5.3.9. TGA thermogram of gamma irradiated Triafol-BN detector.

REFERENCES

[1] Zamani M., Sampsonidis D. and Charalambous S. Dose rate effects on CR-39 SSNT Detector. Nuclear Tracks. 12 (1986), 125-128.

[2] Portwood T. and Henshaw D.L. The effect of gamma dose on the alpha response of CR-39. Nuclear Tracks. 12 (1986), 105-108.

[3] Singh S. and Singh B. The effect of gamma irradiations on etching characteristics of some Solid State Track Recorders. Nucl. Tracks Radiat. Meas. 15 (1988) , 199-202.

[4] Sharma S.L., Pal T., Rao V.V. and Enge W. Effect of gamma irradiation on bulk etch rate of CR-39. Nucl. Tracks Radiat. Meas. 18 (1991), 385-389.

[5] Shweikani R., Durrani S.A. and Tsuruta T. Effects of gamma irradiation on the bulk and track etching properties of Cellulose Nitrate (Daicel 6000) and CR-39 Plastics. Nucl. Tracks Radiat. Meas. 22 (1993), 153-156.

[6] Joseph A. and Varier K.M. Gamma ray dosimetric studies on CR-39 detector. Indian Journal of Pure & Applied Physics. 33 (1995), 406-409.

[7] Abu-Jarad F., Hala A.M., Farhat M. and Islam M. Effect of high gamma dose on the CR-39 properties. Radiat. Meas. 28 (1997) (in print)

[8] Fleischer R.L., Price P.B. and Walker R.M. Nuclear Tracks in Solids : Principles and Applications. University of California Press, Berkelay (1975).

[9] Khan H.A., Asharf M.A., Yameen S., Haroon M.R. and Hussain A. The effects of high gamma doses on the response of plastic track detectors. Nucl. Instr. Meth. 127 (1975), 105-108.

[10] Zamani M. and Charalambous S. The response of Cellulose Nitrate to gamma radiation. Nucl. Tracks. 4 (1981), 171-176.

[11] Durrani S.A. and Bull R.K. Solid State Nuclear Track Detection, Pergaman Press, Oxford (1987).

[12] Frank A.L. and Benton E.V. Dielectric plastics as high-exposure gamma-ray detectors. Radiation Effects. 2 (1970), 269-272.

[13] Chambaudet A. (L.A.176)., Bernas A.(E.R.CNRS 98) and Rochin J.(LA 75). On the formation of heavy ion latent tracks in polymeric detectors. Radiat. Effects. 34 (1975), 57-59.

[14] Edmonds E .A. and Durrani S.A. Relationship between thermoluminescence, Radiation-Induced Electron Spin Resonance and Track etchability of Lexan Polycarbonate. Nuclear Tracks. 3 (1979), 3-11.

[15] Mayaki S., Dasliva A. O. and Tidjani A. Effects of gamma irradiation on Cellulose Nitrate LR 115 Type 11. Radiat. Meas. 26 (1996), 657-661.


CHAPTER- 6

CHAPTER-6

CONCLUSION AND FUTURE PERSPECTIVES

6.1 CONCLUSION :- The present investigations have revealed that several physico-chemical changes occur in polymers due to gamma exposure. Chapter-5 contains the details about the modifications that takes place in seven different polymeric detectors by gamma radiation. Some important properties like bulk-etch rate, track-etch rate, transmittance of uv-vis, thermal stability etc. are greatly influenced by gamma radiation. There is also indication of some structural modifications through bond cleavage. The modifications or changes observed in irradiated polymers are summarized below :-

(1) The properties viz. track, optical, thermal resistance and chemical structure of the Triafol-TN and Triafol-BN are found to remain unchanged upto the dose of 10^5 Gy of gamma radiation. But at the dose of 10^6 Gy, both Triafol-TN and Triafol-BN polymers became brittle and fragile. Triafol-TN turned into powdered form at such high doses. This brittleness of the polymer is probably due to the destruction of anti-oxidant present in the polymeric film.

(2) The purple dye present in the polymeric film (Triafol-BN) got destroyed to an appreciable extent by a gamma dose of 10^6 Gy and therefore, the colour of the Triafol-BN films disappeared.

(3) The thermal stability for the Triafol-BN decreases at 10^6 Gy of gamma dose and it starts losing weight at lower temperature (220°C).

(4) There are also indications about CO_2 formation through the destruction of ester or ether groups in Triafol-BN polymeric film at 10^6 Gy gamma dose.

(5) This destruction in Triafol-BN leads to a decrease in average molecular weight of the polymer and consequently increases the bulk-etch rate.

(6) It has been observed that the bulk-etch rate increases with gamma doses for Triafol-BN detector, but the activation energy for bulk-etching does not change significantly.

(7) Bulk-etch rates of Makrofol-E, Lexan and Polycarbonate are not altered to an appreciable extent by exposing to high doses of gamma radiation (10^6 Gy). This may be due to the presence of two benzene rings in the monomer units of these polymers which provide resistance to radiation induced damage due to delocalization of the excitation energy.

(8) From the UV-VIS studies one may conclude that, for dosimetric applications of these polymers (Makrofol-E, Lexan and Polycarbonate) gamma doses of 10^4 Gy and above are suitable.

(9) Thermal resistance has not been modified by different doses of gamma radiation for Makrofol-E and Lexan polymers. But for

Polycarbanate, thermal resistance decreases at higher doses (10^6 Gy) and the weight loss starts at lower temperature (410°C).

(10) ESR study for Makrfol-E, Lexan and Polycarbonate give the information about the cleavage of C-H bond of Benzene ring. The radical which is formed on carbon atom delocalizes in the ring system. The hydrogen radical formed probably combines with other hydrogen radical to produce hydrogen gas.

(11) For PADC polymeric films upto the doses of 10^5 Gy, neither bond scissioning nor cross-linking has taken place. But at the dose of 10^6 Gy, etch-rate increases due to the consequence of bonds cleavage.

(12) At the dose of 10^6 Gy, it has been observed that the bonds joining polyallyl chains with diethyleneglycol in PADC (American Acrylics) have been possibly raptured due to passage of gamma rays and produce following radicals :

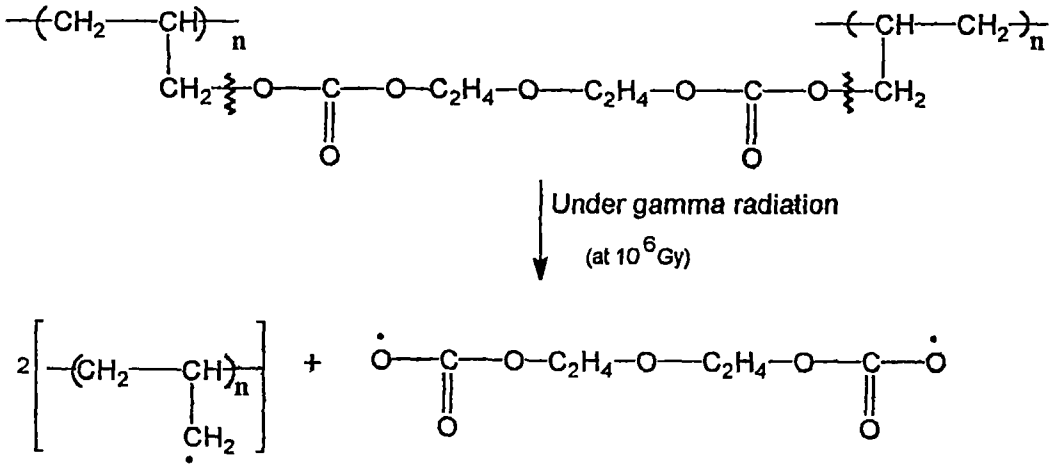

(13) In the case of PADC (American Acrylics) the etch rates remain invariant for both pre- and post-mode of gamma exposure, where as for PADC (Homalite), the post gamma exposure enhances etch-rates value as compared to pre-gamma exposure. This is presumably due to the deposition of additional energy for post-gamma exposure at the latent damage trails created by fission fragments in the material.

(14) It have been observed that the bulk-etch rate increases for both the PADC detectors with gamma doses, but the activation energy does not change significantly.

(15) UV-VIS study reveals that the dosimetric applications of PADC (American Acrylics), are suitable for gamma doses higher than 10^3 Gy.

(16) The appearance of colour (Yellow) in exposed PADC (American Acrylics) at high doses is due to the presence of radicals. These are formed and trapped in the detector matrix and are responsible for imparting colour to the transparent sample.

6.2 FUTURE PERSPECTIVES :- On the basis of the results of the present experiment, it is established that this area of research has a wider scope for further studies. Following activities may augment the present studies for a deeper understanding of the radiation induced modifications of the polymers :

(1) It will be useful to study the change in the track properties in PADC by gradual increase of gamma dose from 10^5 to 10^6 Gy, for its possible use as dosimeter.

(2) Studies at higher doses (above 10^6 Gy) will be significant in the case of Makrofol-E, Polycarbonate and Lexan, for understanding and quantifying the etching response of these materials under gamma exposure.

(3) Both for Triafol-TN and Triafol-BN polymers, it is necessary to study the effect of gradual increase in gamma dose in the range between 10^5 - 10^6 Gy on its bulk-etch properties.

(4) Low temperature irradiation followed by ESR study will be useful for trapping the radicals formed by chain scission.

(5) UV-VIS study can be used to find out the effect of different doses of gamma rays on the optical band gap and accordingly the size of carbon cluster formed by radiation damage.

(6) Several commonly used polymers (viz. PET, PI, PP, PVC, PVDF etc.) and newer materials such as SR-86, SR-90, LR-115 etc. should be studied for their response to gamma exposure.

(7) XRD studies can be done to observe the structural changes (amorphization, dilation, distortions) caused by gamma radiation in these polymers.

(8) Heavy ion induced modifications of these polymers may also be carried out. The SEM, TEM study will be useful for understanding the surface damage induced by heavy ions on these polymers.

(9) Some other studies like Conductivity, Thermoluminesence, Annealing and Hardness measurements are also important to evaluate radiation induced modifications in these polymers.

CURRICULUM VITAE

NAME DIPAK SINHA

DATE OF BIRTH 30th March, 1969.

EDUCATIONAL QUALIFICATIONS :

Examination Passed	Board/University	Year	Result
B.Sc.(Chemistry)	N.E.H.University	1990	1st Div.
M.Sc. (Chemistry)	N.E.H.University	1993	1st Div.

List of Publications :-

[1] Measurement of Indoor Radon in some Dwellings in Aizawl (India). K.K.Dwivedi, A.Srivastava, S.Ghosh, **D.Sinha**, C.Laldawngliana, R. Lalramengzami, A. Saxena. Indoor Environment. 1995, 4, 362 - 364.

[2] Measurement of potential alpha energy exposure (PAEE) of Radon and its progenies in dwellings in the North-Eastern region of India. A.Srivastava, R.Lalramengzami, C.Laldawngliana, **D.Sinha**, S.Ghosh, K.K.Dwivedi, A.Saxena and T.V. Ramachandran. Radiation Measurements. Vol.26, pp. 291 - 295, 1996.

[3] Energy-loss and Mean ranges of ^{86}Kr and ^{197}Au in Tantalum. K.K.Dwivedi, A.Srivastava, S.Ghosh, **D.Sinha**, A.Saxena and R. Brandt. Radiation Measurements, vol. 26, pp. 561 - 563, 1996.

[4] Range and energy loss of ^{58}Ni and ^{129}Xe ions in Hostaphan. A. Srivastava, C. Laldawngliana, **D. Sinha**, S. Ghosh, K.K. Dwivedi and R. Brandt. Indian journal of pure and applied physics. vol.34, pp. 371 - 375, june '96.

[5] Measurement of range and energy loss of energetic ^{58}Ni and ^{197}Au ions in Kapton. A. Srivastava, C. Laldawngliana, **D. Sinha**, S. Ghosh, K.K. Dwivedi and R. Brandt. Nuclear Science Journal. Vol. 33, pp. 85 - 93, April' 96.

[6] Effect of gamma rays on PADC detectors. **D. Sinha**, S. Ghosh, A. Srivastava, V.G. Dedgaonkar and K.K. Dwivedi. Radiation Measurements. Vol. 28, 1997 (in press).

[7] Mean ranges of ^{12}C in some plastic detectors. K.K. Dwivedi, **D. Sinha**, S. Singh, A. Srivastava, D. Avasti. Radiation Measurements. Vol. 28, 1997(in press).

[8] Mean ranges of ^{161}Dy in Zn-P and Hostaphan Detector. S. Ghosh, **D. Sinha**, A. Srivastava, A. Kulukshetra, K.K. Dwivedi and R. Brandt. Radiation Measurements. Vol. 28, 1997 (in press).

[9] Photon induced modifications of Triafol-BN and Triafol-TN polymeric detectors. **D. Sinha**, G.K. Sarkar, S. Ghosh, A. Kulukshetra, K.K. Dwivedi and D. Fink. communicated to Radiation Effects and Defects in Solids.

[10] Structural modifications and track registration response of some gamma irradiated polycarbonate detectors. **D. Sinha**, S. Ghosh, K.K. Dwivedi and D. Fink. Communicated to Radiation Measurements.

[11] Modifications of radiation detection response of PADC track detectors by Photons **D. Sinha** and K.K. Dwivedi. Communicated to Radiation Physics and Chemistry.